

(Atmospheric) Climate Dynamics

Fred Kucharski

This course consists of 12 lectures.

- Each lecture is 90 minutes long.
- At the end of each lesson, exercises will be given as homework and discussed in the beginning of the following lesson.
- Recommended textbooks:
James R. Holton: Dynamic Meteorology, Third edition, Academic Press.
Joseph Pedlosky: Geophysical Fluid Dynamics, Springer-Verlag.
Others are suggested in the individual lectures. Many others are good as well, so choose!
- Evaluation criteria: 1/3 for weekly assignments, 2/3 for final examination.
- Lecture notes will be available at
http://users.ictp.it/~kucharsk/lecture_notes_CD_section1.pdf, etc.
- If you find mistakes, corrections are highly appreciated!

Topics in the course

- Vorticity equation for synoptic-scale motion; potential vorticity conservation [1.5 h]
- Quasi-geostrophic motion; Thermo-Hydrodynamic equations in pressure coordinates [1.5 h]
- Rossby waves; free Rossby waves; forced Rossby waves [1.5 h]

- Baroclinic instability; two-layer model [1.5 h]
- Equatorial waves; Rossby-gravity waves; Kelvin waves [1.5 h]
- ENSO atmosphere and ocean feedback mechanisms; Gill model; Reduced Gravity Model [1.5h]
- Boundary Layer Processes; turbulent fluxes; Ekman pumping [1.5 h]
- The General Circulation; Hadley Cell; Ferrell Cell [1.5 h]
- Tropical zonal and meridional circulations; Walker circulation; Sverdrup balance [1.5h]
- Energetics of the General Circulation; Lorenz' energy cycle [1.5 h]
- Analysis of climate Variability; EOF analysis, PCA analysis [3 h]

1 Vorticity equation for synoptic-scale motion

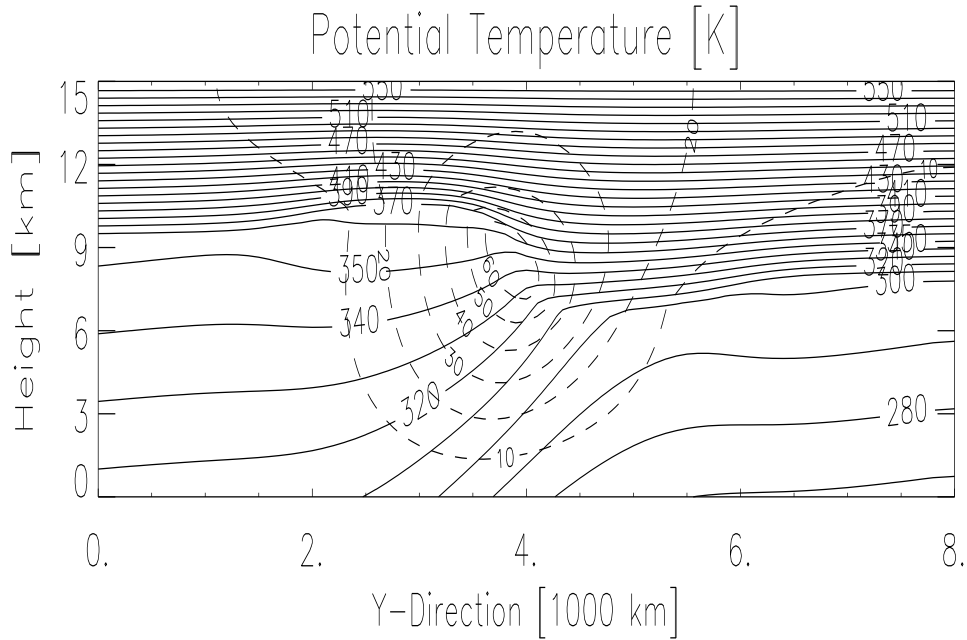


Figure 1: Idealised situation (meridional-vertical section) of the extratropical mean state. Potential temperature (solid lines, K) and zonal wind (dashed, m/s). As we will show later in the Climate Dynamics course the wind approximately fulfill the thermal wind equation $\partial u_g / \partial z \approx -g / (fT) \partial T / \partial y$.

Vorticity is an important concept for the analysis of all kind of atmospheric motions, but in particular for large-scale atmospheric motions. We use the approximate horizontal equations of motion (in the vertical the equation of motion degenerates to the hydrostatic equation) on a sphere, but neglecting all metric terms that occur in the total derivative. Furthermore, we use the abbreviations $dx = r \cos \phi d\lambda, dy = r d\phi, dz = dr$). Also recall the definition of the Coriolis parameter $f \equiv 2\Omega \sin \phi$, and note that we have already neglected the small term proportional to the vertical velocity Coriolis term.

$$\frac{\partial u}{\partial t} + u \frac{\partial u}{\partial x} + v \frac{\partial u}{\partial y} + w \frac{\partial u}{\partial z} - fv = -\frac{1}{\rho} \frac{\partial p}{\partial x} \quad (1)$$

$$\frac{\partial v}{\partial t} + u \frac{\partial v}{\partial x} + v \frac{\partial v}{\partial y} + w \frac{\partial v}{\partial z} + fu = -\frac{1}{\rho} \frac{\partial p}{\partial y} \quad (2)$$

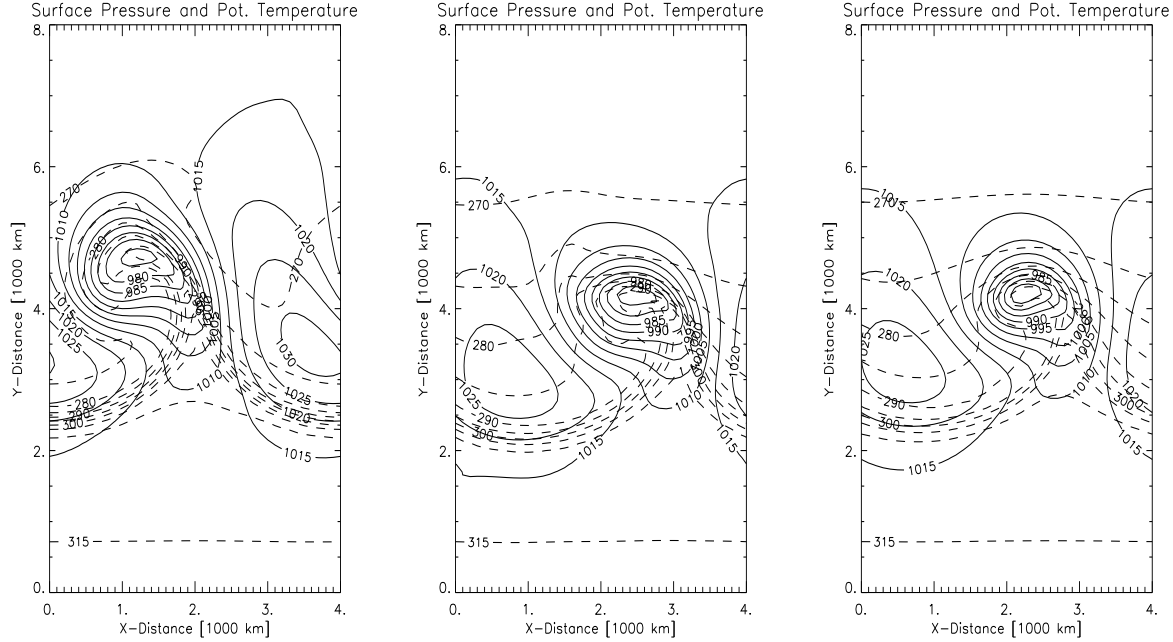


Figure 2: Typical surface pressure [hPa] and potential temperature [K] distributions in extratropical cyclones.

If we apply $\partial/\partial y$ to Eq. 1 and $\partial/\partial x$ to Eq. 2 and subtract the first from the second, we obtain using the definition $\xi = \partial v/\partial x - \partial u/\partial y$ (Exercise!)

$$\begin{aligned} \frac{\partial \xi}{\partial t} + u \frac{\partial \xi}{\partial x} + v \frac{\partial \xi}{\partial y} + w \frac{\partial \xi}{\partial z} + (\xi + f) \left(\frac{\partial u}{\partial x} + \frac{\partial v}{\partial y} \right) \\ + \left(\frac{\partial w}{\partial x} \frac{\partial v}{\partial z} - \frac{\partial w}{\partial y} \frac{\partial u}{\partial z} \right) + v \frac{df}{dy} = \frac{1}{\rho^2} \left(\frac{\partial \rho}{\partial x} \frac{\partial p}{\partial y} - \frac{\partial \rho}{\partial y} \frac{\partial p}{\partial x} \right) \end{aligned} \quad (3)$$

The coriolis parameter only depends on y , so we may write:

$$\begin{aligned} \frac{d}{dt}(\xi + f) = - (\xi + f) \left(\frac{\partial u}{\partial x} + \frac{\partial v}{\partial y} \right) \\ - \left(\frac{\partial w}{\partial x} \frac{\partial v}{\partial z} - \frac{\partial w}{\partial y} \frac{\partial u}{\partial z} \right) + \frac{1}{\rho^2} \left(\frac{\partial \rho}{\partial x} \frac{\partial p}{\partial y} - \frac{\partial \rho}{\partial y} \frac{\partial p}{\partial x} \right). \end{aligned} \quad (4)$$

This is the vorticity equation usually used to analyse synoptic-scale motions (the direction is perpendicular to the earth's surface). It states the the rate of change of

absolute vorticity following the motion is given by the sum of three terms, called the divergence term, the tilting or twisting term, and the solenoidal term, respectively.

The first term on the right-hand side may be interpreted as expression of the angular momentum conservation. Imagine a ice scater who rotates and while rotating moves his arms closer to his body: His rotation accelarates. But since we are dealing with large scales, in Eq. 4 the absolute vorticity, $\eta = \xi + f$, has to be considered. The interpretation of the second term is that vertical vorticity may be generated by the tilting of horizontal vorticity components by a non-uniform vertical motion field. The meaning of the third term is the soleniodal term. It can be expressed as (exercise!):

$$\frac{1}{\rho^2} \left(\frac{\partial \rho}{\partial x} \frac{\partial p}{\partial y} - \frac{\partial \rho}{\partial y} \frac{\partial p}{\partial x} \right) = \frac{1}{\rho^2} (\nabla \rho \times \nabla p) \cdot \mathbf{k} , \quad (5)$$

where $\alpha = 1/\rho$ is the specific volume and \mathbf{k} is the unit vector in vertical direction. In order to create vorticity through the solenoidal term, lines of constant density have to intersect with lines of constant pressure. A land-sea breeze is a typical example where vorticity in created in such a way.

1.1 Scale analysis of the vorticity equation

In order to understand which terms and therefore mechanisms are the dominant ones in the vorticity equation (4) in this section a 'scale-analysis' will be performed. The scale analysis uses the dimensions of the synoptic scales we are interested in, but also observed magnitudes of flow velocites and other quantities. It is not a rigorous proceddure (you use part of the answer as input), but it helps to identify dominant mechanisms.

The scales are given in the following table:

Table 1: Scale parameters for synoptic-scale flow.

$U \sim 10 \text{ m s}^{-1}$	horizontal velocity scale
$W \sim 1 \text{ cm s}^{-1}$	vertical velocity scale
$L \sim 10^6 \text{ m}$	length scale
$H \sim 10^4 \text{ m}$	vertical scale
$\delta p \sim 10 \text{ hPa}$	horizontal pressure scale
$\rho \sim 1 \text{ kg m}^{-3}$	mean density
$\delta \rho / \rho \sim 10^{-2}$	fractional density fluctuation
$L/U \sim 10^5 \text{ s}$	time scale
$f_0 \sim 10^{-4} \text{ s}^{-1}$	Coriolis parameter
$\beta = df/dy \sim 10^{-11} \text{ m}^{-1} \text{ s}^{-1}$	'beta' parameter

This gives

$$\xi = \frac{\partial v}{\partial x} - \frac{\partial u}{\partial y} \sim \frac{U}{L} \sim 10^{-5} \text{ s}^{-1} , \quad (6)$$

and

$$\xi/f_0 \sim U/(f_0L) \equiv Ro \sim 10^{-1} \quad , \quad (7)$$

the ratio of relative to planetary vorticity is equal to the *Rossby number*, which is small for synoptic flow. Therefore, ξ may be neglected compared to f in the divergence term in the vorticity equation

$$(\xi + f) \left(\frac{\partial u}{\partial x} + \frac{\partial v}{\partial y} \right) \approx f \left(\frac{\partial u}{\partial x} + \frac{\partial v}{\partial y} \right) \quad (8)$$

The magnitudes of the various terms in equation 4 can now be estimated as follows:

$$\begin{aligned} \frac{\partial \xi}{\partial t}, u \frac{\partial \xi}{\partial x}, v \frac{\partial \xi}{\partial y} &\sim \frac{U^2}{L^2} \sim 10^{-10} s^{-2} \\ w \frac{\partial \xi}{\partial z} &\sim \frac{WU}{HL} \sim 10^{-11} s^{-2} \\ v \frac{df}{dy} &\sim U\beta \sim 10^{-10} s^{-2} \\ f \left(\frac{\partial u}{\partial x} + \frac{\partial v}{\partial y} \right) &\sim \frac{f_0 U}{L} \sim 10^{-9} s^{-2} \\ \left(\frac{\partial w}{\partial x} \frac{\partial v}{\partial z} - \frac{\partial w}{\partial y} \frac{\partial u}{\partial z} \right) &\sim \frac{WU}{HL} \sim 10^{-11} s^{-2} \\ \frac{1}{\rho^2} \left(\frac{\partial \rho}{\partial x} \frac{\partial p}{\partial y} - \frac{\partial \rho}{\partial y} \frac{\partial p}{\partial x} \right) &\sim \frac{\delta \rho \delta p}{\rho^2 L^2} \sim 10^{-11} s^{-2} \end{aligned}$$

The estimation of the divergence is an overestimation. Indeed it will be shown later in this course the the divergent part of the flow (which is also the non-geostrophic part) is an order of magnitude smaller than the rotational part (geostrophic). We have therefore

$$\left(\frac{\partial u}{\partial x} + \frac{\partial v}{\partial y} \right) \sim 10^{-6} s^{-1} \quad , \quad (9)$$

which means that the divergence is typically one order of magnitude smaller than the vorticity of synoptic-scale motion. Therefore,

$$f \left(\frac{\partial u}{\partial x} + \frac{\partial v}{\partial y} \right) \sim 10^{-10} s^{-2} \quad . \quad (10)$$

Therefore in the vorticity equation (4), we have the first order balance

$$\frac{d_h(\xi + f)}{dt} = -f \left(\frac{\partial u}{\partial x} + \frac{\partial v}{\partial y} \right) \quad , \quad (11)$$

where

$$\frac{d_h}{dt} \equiv \frac{\partial}{\partial t} + u \frac{\partial}{\partial x} + v \frac{\partial}{\partial y} \quad . \quad (12)$$

The synoptic-scale vorticity equation 11 states that the rate of change of absolute vorticity following the horizontal motion is approximately given by the generation (destruction) of vorticity owing to horizontal convergence (divergence). Indeed, this is considered to be the main mechanism of cyclone (and anticyclone) developments, connecting cyclonic motion to low pressure and anticyclonic motion to high pressure (only for large-scale motions!).

1.2 The Barotropic (Rossby) Potential Vorticity Equation

As barotropic model of the Atmosphere we assume that there is incompressibility and the flow may be confined by the height of two given boundaries, $h(x, y, z, t) = H_t - H_b$ (see also lecture on equatorial waves). The incompressibility condition may be expressed as

$$\frac{\partial u}{\partial x} + \frac{\partial v}{\partial y} = -\frac{\partial w}{\partial z} \quad . \quad (13)$$

We also assume that the horizontal velocities are independent of height. With this we can integrate the vorticity equation (11) vertically to obtain

$$h \frac{d_h(\xi + f)}{dt} = (f + \xi)[w(H_t) - w(H_b)] \quad . \quad (14)$$

Note that in equation (14), the relative vorticity ξ may be replaced, to a first approximation, by the geostrophic relative vorticity

$$\xi \approx \xi_g \equiv \nabla^2 gh / f_0 = \nabla^2 \Phi / f_0 \quad , \quad (15)$$

where we have assumed that the meridional scale, L , is small compared to the radius of the earth so that the geostrophic wind may be defined using a constant reference latitude of the Coriolis parameter $f \approx f_0 \equiv 2\Omega \sin \phi_0$. Also, in the operator (12) the horizontal velocities may be approximated by the geostrophic ones

$$\mathbf{v} \approx \mathbf{v}_g \equiv f_0^{-1} \mathbf{k} \times \nabla gh = f_0^{-1} \mathbf{k} \times \nabla \Phi \quad , \quad (16)$$

Equations 15 and 16 can be derived from the geostrophic equations and integration of the hydrostatic equation for an incompressible fluid (exercise!). Note that, for beauty, we have re-introduced the small ξ effect on the rhs of Eq. (14). Since $w(H_t) = dH_t/dt, w(H_b) = dH_b/dt$ we have,

$$\frac{1}{\xi + f} \frac{d_h(\xi + f)}{dt} = \frac{1}{h} \frac{d_h h}{dt} \quad . \quad (17)$$

Integrating left and right side leads to

$$\frac{d_h}{dt} [\ln(\xi + f)] = \frac{d_h}{dt} [\ln h] \quad , \quad (18)$$

which implies that

$$\frac{d_h}{dt} \frac{(\xi + f)}{h} = 0 \quad , \quad (19)$$

which is the potential vorticity conservation theorem for a barotropic fluid, first obtained by C. G. Rossby. The quantity conserved following the horizontal motion is the barotropic potential vorticity. It explains nicely some features of the observed stationary waves, e.g. induced by the Rocky mountains. If the flow is purely horizontal, i.e. rigid lid and lower boundary, then we obtain the *barotropic vorticity equation*

$$\frac{d_h(\xi + f)}{dt} = 0 \quad , \quad (20)$$

which states that the absolute vorticity is conserved following the horizontal motion. The flow in the mid-troposphere approximately fulfills this condition and equation (20) may be used to explain the movement of air particles in Rossby waves!

Note that using the approximations (15) and (16) the barotropic vorticity equation (20) can be re-written in terms of the streamfunction $\psi \equiv \Phi/f_0 = gh/f_0$ or equivalently also in terms of geopotential $\Phi = gh$ (exercise!)

$$\frac{d_h}{dt} \nabla^2 \psi + \beta \frac{\partial \psi}{\partial x} = 0 \quad . \quad (21)$$

Also the operator d_h/dt can be expressed in terms of streamfunction

$$\frac{d_h}{dt} = \frac{\partial}{\partial t} - \frac{\partial \psi}{\partial y} \frac{\partial}{\partial x} + \frac{\partial \psi}{\partial x} \frac{\partial}{\partial y} \quad (22)$$

Equations (21) and (22) can be used conveniently to compute Rossby wave solutions numerically (exercise in section 3!)

Exercises

1. Show that applying $\partial/\partial y$ to Eq. 1 and $\partial/\partial x$ to Eq. 2 leads to Eq. 3.
2. Show the validity of Eq. 5.
3. Show that the geostrophic formulations 15 and 16 can be derived from the usual geostrophic wind

$$\mathbf{v}_g \equiv \frac{1}{\rho f_0} \mathbf{k} \times \nabla p$$

and that with this the barotropic vorticity equation 20 can be written as Eq. 21 with 22.

4. An air parcel at 30 N moves northward conserving absolute vorticity. If its initial relative vorticity is $5 \times 10^{-5} s^{-1}$, what is its relative vorticity upon reaching 90 N?
5. An air column at 60 N with $\xi = 0$ initially stretches from the surface to a fixed tropopause at 10 km. If the air column moves until it is over a mountain barrier 2.5 km high at 45 N, what are its absolute vorticity and relative vorticity as it passes the mountain top, assuming that the flow satisfies the barotropic potential vorticity equation?

2 Quasi-geostrophic motion

2.1 The basic equations in isobaric Coordinates

The basic governing equations are (see Eqs. 1 and 2)

The horizontal momentum equations

$$\frac{d\mathbf{v}}{dt} + f\mathbf{k} \times \mathbf{v} = -\frac{1}{\rho}\nabla p \quad , \quad (23)$$

where $v = \mathbf{i}u + \mathbf{j}v$ and the nabla operator has just the horizontal components.

The vertical equation of motion degenerates for all large-scale motion (e.g. scales more than 100 km) into the hydrostatic equation:

$$\frac{\partial p}{\partial z} = -\rho g \quad . \quad (24)$$

Equation (24) states that there is a monotonic relation between pressure p and height z , which leads to the possibility of using p as a vertical coordinate. The basic equation for deriving all transformation from the height to the pressure coordinate system is: $\psi(x, y, p, t) = \psi(x, y, z, t)$, which leads, for example to

$$\frac{\partial \psi}{\partial x} \Big|_p = \frac{\partial \psi}{\partial x} \Big|_z + \frac{\partial \psi}{\partial z} \frac{\partial z}{\partial x} \Big|_p \quad . \quad (25)$$

Inserting $\psi = p$ and applying Eq. (25) also to the derivative in y direction gives the transformation for the horizontal pressure gradient force $\nabla_z p = \rho g \nabla_p z = \rho \nabla_p \Phi$. Thus the horizontal momentum equation reads

$$\frac{d\mathbf{v}}{dt} + f\mathbf{k} \times \mathbf{v} = -\nabla_p \Phi \quad . \quad (26)$$

This looks a little like the horizontal momentum equation of the shallow water model, but it is not! Applying $\psi(x, y, p, t) = \psi(x, y, z, t)$ to a vertical derivative and letting $\psi = p$ gives the hydrostatic equation in pressure coordinates

$$\frac{\partial \Phi}{\partial p} = -\frac{1}{\rho} = -\alpha = -\frac{RT}{p} \quad . \quad (27)$$

The total derivative d/dt is invariant and can be expressed as (as follows directly from $\psi = \psi(x, y, p, t)$)

$$\frac{d}{dt} = \frac{\partial}{\partial t} + \frac{\partial}{\partial x} \frac{dx}{dt} + \frac{\partial}{\partial y} \frac{dy}{dt} + \frac{\partial}{\partial p} \frac{dp}{dt} \quad (28)$$

$$= \frac{\partial}{\partial t} + u \frac{\partial}{\partial x} + v \frac{\partial}{\partial y} + \omega \frac{\partial}{\partial p} \quad (29)$$

$$= \frac{\partial}{\partial t} + \mathbf{v} \cdot \nabla_p + \omega \frac{\partial}{\partial p} \quad . \quad (30)$$

$\omega = dp/dt$ (called the 'omega' vertical velocity) is the pressure change following the motion. Note that when w is positive ω is typically negative.

The Continuity Equation

The easiest way to derive the continuity equation is through the principle of mass conservation. For an infinitesimal mass element we may write:

$$\delta m = \rho \delta V = \rho \delta x \delta y \delta z = -\delta x \delta y \frac{1}{g} \delta p \quad . \quad (31)$$

Note that the first part of equation (31) is just the definition of the density. In the second part the hydrostatic equation (24) has been used to replace the vertical perturbation by a pressure perturbation. Let's calculate the derivative of (31) following the motion (conservation of mass)

$$\frac{1}{\delta m} \frac{d}{dt} \delta m = \frac{g}{\delta x \delta y \delta p} \frac{d}{dt} \frac{\delta x \delta y \delta p}{g} = 0. \quad (32)$$

After applying the product rule of differentiation, and changing the order of differentiation we obtain

$$\frac{1}{\delta x} \delta \frac{d}{dt} x + \frac{1}{\delta y} \delta \frac{d}{dt} y + \frac{1}{\delta p} \delta \frac{d}{dt} p = \frac{\delta u}{\delta x} + \frac{\delta v}{\delta y} + \frac{\delta \omega}{\delta p} = 0 \quad . \quad (33)$$

Letting $\delta x, \delta y, \delta z \rightarrow 0$, it follows the continuity equation in pressure coordinates:

$$\left(\frac{\partial u}{\partial x} + \frac{\partial v}{\partial y} \right)_p + \frac{\partial \omega}{\partial p} = 0 \quad . \quad (34)$$

In pressure coordinates the full continuity equation takes the form of that of an incompressible fluid, i.e. the time derivative of density does not occur anymore explicitly.

The Thermodynamic Energy Equation

Recall Eqs. 108 or 110 for the Enthalpy, and after multiplying with T from our Earth System Thermodynamics course (for $ds = 0$), which was approximately valid for the atmosphere in which phase transitions from water vapor to liquid water are allowed (do you remember what the symbols L_{lv} and m_v stand for?):

$$c_p \frac{dT}{dt} - \frac{RT}{p} \frac{dp}{dt} = -L_{lv} \frac{dm_v}{dt} \quad . \quad (35)$$

If we further allow diabatic processes to occur (e.g. radiation), then we can simply add $T ds/dt$ on the rhs and abbreviate those terms as Q .

$$c_p \frac{dT}{dt} - \alpha \frac{dp}{dt} = Q \quad . \quad (36)$$

Q is thus the heat added by diabatic processes (i.e. condensation, radiation).

Using the total derivative in pressure coordinates and the definition of ω we have

$$\left(\frac{\partial T}{\partial t} + u \frac{\partial T}{\partial x} + v \frac{\partial T}{\partial y} \right)_p - S_p \omega = \frac{Q}{c_p} \quad , \quad (37)$$

where the stability factor

$$S_p = \frac{RT}{c_p p} - \frac{\partial T}{\partial p} = -\frac{T}{\theta} \frac{\partial \theta}{\partial p} \quad (38)$$

has been introduced. In Eq. (38) we have used the definition of the potential temperature (Exercise!)

$$\theta = T \left(\frac{p_0}{p} \right)^{\frac{R}{c_p}} . \quad (39)$$

p_0 is a constant reference pressure here. Using the dry adiabatic lapse rate $\Gamma_d = g/c_p$, we have also (exercise!)

$$S_p = (\Gamma_d - \Gamma)/(\rho g) \quad , \quad (40)$$

where the definition of the lapse rate $-dT/dz = \Gamma$ has been used.

The set of equations (26), (27), (34) and (37) is the basis for our analysis of synoptic-scale motion, but also the basis for many numerical models of the atmospheric circulation.

2.2 Some observed features of the extratropical mean flow

A primary goal of dynamic meteorology is to interpret the observed structure of large-scale atmospheric motions in terms of physical laws governing the motions. These laws, which express the conservation of momentum, mass, and energy completely determine the relationships among the pressure, temperature, and velocity fields. However, the pure laws provide an enormously complicated picture of the motions. For extratropical synoptic-scale motions, however, the horizontal velocities are approximately geostrophic. Such motions, which are often referred to as *quasi-geostrophic*, are simpler to analyze than, for example tropical disturbances. They are also the major systems of interest in traditional short-range weather forecasting and are thus a reasonable starting point for dynamical analysis. In this section we show that for extratropical synoptic-scale systems the twin requirement of hydrostatic and geostrophic balance constrain the baroclinic motions so that to a good approximation the structure and evolution of the three-dimensional velocity field are determined by the distribution of geopotential height on isobaric surfaces. The equations that express these relationships constitute the quasi-geostrophic system. Before developing this system of equations it is useful to summarize briefly the observed structure of mid-latitude synoptic systems and the mean circulations in which they are embedded.

Zonally averaged cross sections do provide some useful information on the gross structure of the planetary-scale circulation, in which synoptic-scale eddies are embedded. Fig. 3 and 4 show the zonal mean meridional-vertical sections of temperature (left) anomaly from zonal mean and zonal velocity (right) for northern (December-to-February; DJF) and southern winter (June-to-August; JJA), respectively. The vertical direction is measured in pressure (hPa). The average pole-to-equator temperature gradient in the Northern Hemisphere troposphere is much

larger in winter than in summer. In the southern hemisphere the difference between summer and winter temperature distributions is smaller, owing mainly to the large thermal inertia of oceans together with the greater fraction of the surface that is covered by oceans in the Southern Hemisphere. The zonal flow and the meridional temperature gradients satisfy to a large degree the thermal wind relation (Exercise!), the largest zonal wind speeds are located in upper levels in regions with the largest meridional temperature gradients

$$\frac{\partial u_g}{\partial p} = \frac{R}{f p} \left(\frac{\partial T}{\partial y} \right)_p \quad (41)$$

The core of maximum zonal wind speed (called *jet stream axis*) is located just below the *tropopause* (the boundary between troposphere and stratosphere). In both hemispheres the location is about 30-35 during winter and 40-45 during summer.

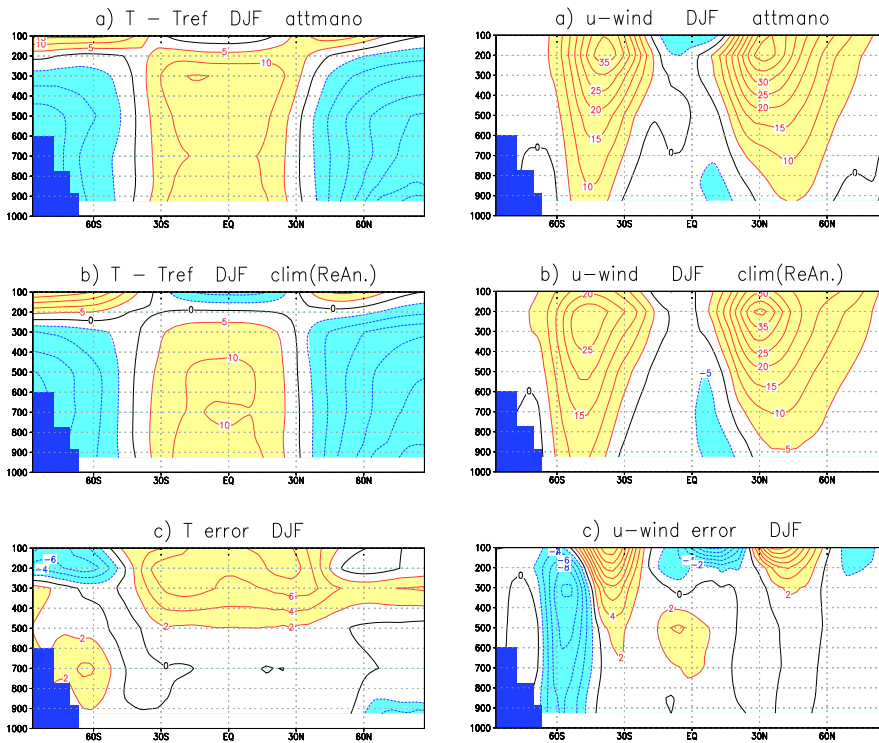


Figure 3: Northern winter meridional-height sections of temperature deviations from zonal mean (left) and zonal wind (right). Units are K for temperature and m/s for wind.

However, there are some important deviations from the zonal mean picture. Fig. 5 shows the zonal wind distribution at the 200 hPa level. As can be seen the largest wind speeds are concentrated just off the coast of Asia and North America, where also the largest meridional temperature gradients occur. Also, whereas the

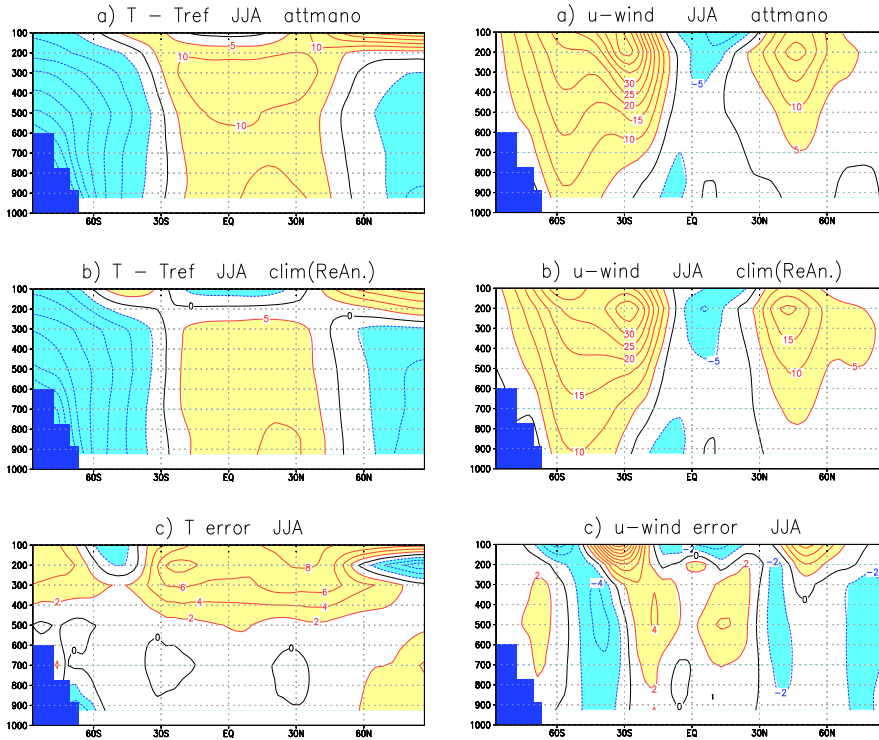


Figure 4: Southern winter meridional-height sections of temperature deviations from zonal mean (left) and zonal wind (right). Units are K for temperature and m/s for wind.

pacific jet is quite zonal, the Atlantic one is clearly tilted from the south-west to the north-east. It is in these regions where most extratropical cyclones and anticyclones develop. I will be shown in section 4 that the mechanisms where these systems draw energy from is the meridional temperature gradient due to an instability called *baroclinic instability*. The systems propagate downstream along the *storm tracks* that approximately follow the jet axis.

The large departure of the northern winter climatological jet stream from zonal symmetry can also be inferred from examination of Fig. 6, which shows the DJF mean 500 hPa geopotential contours (the z from $\Phi = gz$ in Eq. 26). Even after averaging the geopotential height contours for one season, very striking departures from zonal symmetry remain. These are clearly linked to the distribution of continents and Oceans (for example orographic *Rossby waves* due to approximate barotropic potential vorticity conservation [see section 1.2]).

The most prominent asymmetries are the throughs to the east of the American and Asian continents. Referring back to Fig. 5, we see that the intense jet at 35 N and 140 E is a result of the semipermanant trough in that region (that is the isolines of height show strong gradient in that region).

Thus, it is apparent that the mean flow in which synoptic systems are embedded

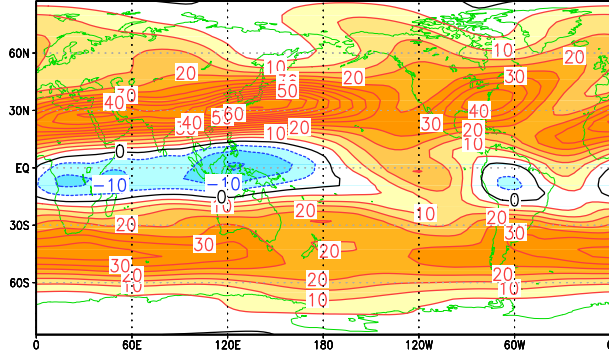


Figure 5: Northern winter (DJF) 200 hPa zonal wind. Units are m/s.

should really be regarded as a longitude-dependent time-averaged flow. In addition to its longitudinal dependence, the planetary-scale flow also varies from day to day owing to its interactions with transient synoptic-scale disturbances.

It is a common observation in fluid dynamics that jets in which strong velocity shears occur may be unstable with respect to small perturbations. By this is meant that any small disturbance introduced into the jets will tend to amplify, drawing energy from the jet as it grows. Most synoptic-scale systems in mid-latitude appear to develop as the result of an instability of the jet-stream flow. This instability, called *baroclinic instability*, depends on the meridional temperature gradient, particularly at the surface. Hence, through the thermal wind relationship, baroclinic instability depends on vertical wind shear.

2.3 The Quasi-geostrophic approximation

The main goal of this chapter is to show how the observed structure of midlatitude systems can be interpreted in terms of the constraints imposed on synoptic-scale motions by the dynamical equations. Specifically we show that for equations that are hydrostatic and nearly geostrophic the three-dimensional flow is determined approximately by the isobaric distribution of geopotential height $[\Phi(x, y, p, t)]$. For this analysis, it is convenient to use the isobaric coordinate system both because meteorological measurements are generally referred to constant-pressure surfaces and because the dynamical equations are somewhat simpler in isobaric coordinates than in height coordinates. Thus, use of the isobaric coordinate system simplifies the development of approximate prognostic and diagnostic equations.

2.3.1 Scale Analysis in Isobaric Coordinates

We consider the set of equations (26), (27), (34) and (37). In the following we will drop the notation $()_p$ to indicate derivatives at constant pressure, which is valid in this section for all horizontal and time derivatives. The stability parameter is positive [$S_p \approx 5 \times 10^{-4} \text{ K Pa}^{-1}$ in the mid-troposphere]. This set of equations,

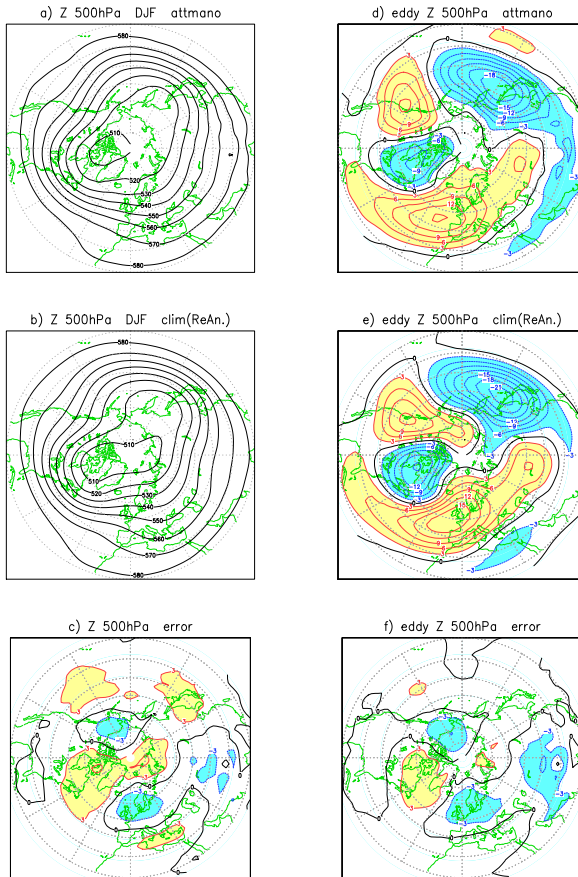


Figure 6: Northern winter (DJF) 500 hPa zonal geopotential height. Units are decametre.

although simplified by use of the hydrostatic approximation and by neglect of some small terms that appear in the complete spherical coordinate form, still contains terms that are of secondary significance for mid-latitude synoptic-scale systems. They can be further simplified by the observation that the horizontal flow is nearly geostrophic and that the ratio of the magnitudes of vertical to horizontal velocities is of the order of 10^{-3} .

We first separate the horizontal velocity into geostrophic and ageostrophic parts by letting

$$\mathbf{v} = \mathbf{v}_g + \mathbf{v}_a \quad , \quad (42)$$

where the geostrophic wind is defined as

$$\mathbf{v}_g \equiv f_0^{-1} \mathbf{k} \times \nabla \Phi \quad , \quad (43)$$

and \mathbf{v}_a is just the difference between the total horizontal wind and the geostrophic wind. Here we have assumed that the meridional scale, L , is small compared to the

radius of the earth so that the geostrophic wind may be defined using a constant reference latitude of the Coriolis parameter ($f \approx f_0$ as in equation 15). Note that the definition (43) implies that the geostrophic wind is non-divergent.

For the systems of interest $|\mathbf{v}_g| \gg |\mathbf{v}_a|$. More precisely,

$$\frac{|\mathbf{v}_a|}{|\mathbf{v}_g|} \sim O(Ro) \approx 10^{-1} \quad . \quad (44)$$

The *Rossby number* Ro has been introduced in Eq. (7).

The momentum can then be approximated to $O(Ro)$ by its geostrophic value, and the rate of change of momentum or temperature following the horizontal motion can be approximated to the same order by the rate of change following the geostrophic wind. Thus, in the total derivative (30), \mathbf{v} can be replaced by \mathbf{v}_g and the vertical advection, which arises from ageostrophic flow, can be neglected. The rate of change of momentum following the total motion is then approximately equal to the rate of change of the geostrophic momentum following the geostrophic wind:

$$\frac{d\mathbf{v}}{dt} \approx \frac{d_g \mathbf{v}_g}{dt} \quad , \quad (45)$$

where

$$\frac{d_g}{dt} = \frac{\partial}{\partial t} + \mathbf{v}_g \cdot \nabla = \frac{\partial}{\partial t} + u_g \frac{\partial}{\partial x} + v_g \frac{\partial}{\partial y} \quad . \quad (46)$$

Note, however, that the vertical advection in the thermodynamic equation, 37, has been combined already with the adiabatic expansion term to provide the stability term $S_p \omega$.

Although a constant f_0 can be used in defining \mathbf{v}_g , it is still necessary to retain the dynamical effect of the variation of the Coriolis parameter with latitude in the Coriolis force term in the momentum equation. This variation can be approximated by expanding the latitudinal dependence of f in a Taylor series about a reference latitude ϕ_0 and retaining only the first two terms to yield

$$f = 2|\Omega| \sin \phi \approx f_0 + \beta y \quad , \quad (47)$$

that is the $\sin \phi$ -dependence is approximated linearly for a given latitude ϕ_0 by a Taylor series expansion (therefore $\beta = 2|\Omega| \cos \phi_0 / a$; a being the mean radius of the earth). This approximation is usually referred to as *mid-latitude beta-plane* approximation. For synoptic-scale motions the ratio of the first two terms in the expression of f has the order of magnitude

$$\frac{\beta L}{f_0} \approx \frac{\cos \phi_0 L}{\sin \phi_0 a} \sim O(Ro) \ll 1 \quad . \quad (48)$$

This justifies letting the coriolis parameter have a constant value f_0 in the geostrophic approximation and approximating its variation in the coriolis force term by (47).

From Eq. (26) the acceleration following the motion is equal to the difference between the Coriolis force and the pressure gradient force. This difference depends on the departure of the actual wind from the geostrophic wind. We can write, using (42), (47) and (43)

$$\begin{aligned} f\mathbf{k} \times \mathbf{v} + \nabla\Phi &= (f_0 + \beta y)\mathbf{k} \times (\mathbf{v}_g + \mathbf{v}_a) - f_0\mathbf{k} \times \mathbf{v}_g \\ &\approx f_0\mathbf{k} \times \mathbf{v}_a + \beta y\mathbf{k} \times \mathbf{v}_g \quad . \end{aligned} \quad (49)$$

The approximate horizontal momentum equation thus has the form

$$\frac{d_g \mathbf{v}_g}{dt} = -f_0\mathbf{k} \times \mathbf{v}_a - \beta y\mathbf{k} \times \mathbf{v}_g \quad . \quad (50)$$

Since the geostrophic wind (43) is non-divergent, the continuity equation (34) may be written as

$$\nabla \cdot \mathbf{v}_a + \frac{\partial \omega}{\partial p} = 0 \quad , \quad (51)$$

which shows that ω is only defined by the ageostrophic part of the wind field (i.e. it is the ageostrophic wind that drives vertical motions that are relevant for energy conversions!!!).

In the thermodynamic energy equation (37) the horizontal advection can be approximated by its geostrophic value. However, as mentioned above, the vertical advection is not neglected, but forms part of the adiabatic heating and cooling term. This term must be retained because the static stability is usually large enough on the synoptic scale that the adiabatic heating or cooling owing to vertical motion is of the same order as the horizontal temperature advection despite the smallness of the vertical velocity. It can be somewhat simplified, though, by dividing the total temperature field T_{tot} , into a basic state (standard atmosphere) portion that depends only on pressure, $T_0(p)$, plus a deviation from the basic state, $T(x, y, p, t)$

$$T_{tot} = T_0(p) + T(x, y, p, t) \quad . \quad (52)$$

Since $|dT_0/dp| \gg |\partial T/\partial p|$ only the basic state portion of the temperature field need to be included in the static stability term and the quasi-geostrophic thermodynamic energy equation may be expressed in the form

$$\frac{\partial T}{\partial t} + \mathbf{v}_g \cdot \nabla T - \left(\frac{\sigma p}{R}\right) \omega = \frac{Q}{cp} \quad , \quad (53)$$

where $\sigma \equiv -RT_0 p^{-1} d \ln \theta_0 / dp$ and θ_0 is the potential temperature corresponding to a basic state temperature T_0 ($\sigma \approx 2 \times 10^{-6} \text{ m}^2 \text{ Pa}^{-2} \text{ s}^{-2}$ in the midtroposphere).

Equations (50), (43), (27), (51) and (53) constitute the quasi-geostrophic equations. If Q is known these form a complete set in the dependent variables $\Phi, T, \mathbf{v}_g, \mathbf{v}_a$ and ω .

2.4 The Quasi-Geostrophic Vorticity Equation

Just as the horizontal momentum can be approximated to $O(Ro)$ by its geostrophic value, the vertical component of the vorticity can also be approximated geostrophically. Using Eq. (43) the geostrophic vorticity $\xi_g = \mathbf{k} \cdot \nabla \times \mathbf{v}_g$ can be expressed in terms of the Laplacian of the geopotential

$$\xi_g = \frac{\partial v_g}{\partial x} - \frac{\partial u_g}{\partial y} = \frac{1}{f_0} \nabla^2 \Phi \quad . \quad (54)$$

Equation (54) can be used to determine $\xi_g(x, y)$ at any given time from a known field $\Phi(x, y)$. Alternatively, (54) can be solved by inverting the Laplacian operator to determine Φ from a known distribution of ξ provided that suitable conditions on Φ are specified on the boundaries of the region in question. This *invertibility* is one reason why vorticity is such a useful forecast diagnostic; if the evolution of vorticity can be predicted, then inversion of Eq. (54) yields the evolution of the geopotential field, from which it is possible to determine the geostrophic wind. Since the Laplacian of a field tends to be a maximum where the function itself is a minimum, positive vorticity implies low values of geopotential and vice versa (see Fig. 6). We will use the invertibility to solve a problem numerically in section 3.

The quasi-geostrophic vorticity equation can be obtained from the x and y components of the quasi-geostrophic momentum equation (50) and yields (exercise!)

$$\frac{d_g \xi_g}{dt} = -f_0 \left(\frac{\partial u_a}{\partial x} + \frac{\partial v_a}{\partial y} \right) - \beta v_g \quad , \quad (55)$$

which should be compared with Eq. (11). Thus the quasi-geostrophic vorticity equation takes the form of the barotropic vorticity equation! Using (51), Equation (55) can be re-written as

$$\frac{\partial \xi_g}{\partial t} = -\mathbf{v}_g \cdot \nabla (\xi_g + f) + f_0 \frac{\partial \omega}{\partial p} \quad , \quad (56)$$

which states that the local rate of change of geostrophic vorticity is given by the sum of the advection of the absolute vorticity by the geostrophic wind plus the concentration or dilution of vorticity by stretching or shrinking of fluid columns (the divergence effect). The vorticity tendency owing to vorticity advection [the first term on the right in Eq. (56)] may be rewritten as

$$-\mathbf{v}_g \cdot \nabla (\xi_g + f) = -\mathbf{v}_g \cdot \nabla \xi_g - \beta v_g \quad . \quad (57)$$

The two terms on the right represent the geostrophic advections of relative vorticity and the planetary vorticity, respectively. For disturbances in the westerlies, these two effects tend to have opposite signs. In the upstream of a 500 hPa trough, the geostrophic wind is directed from the negative vorticity maximum at the ridge toward the positive vorticity maximum at the trough so that $-\mathbf{v}_g \cdot \nabla \xi_g < 0$. But at the same time, since $v_g < 0$ in that region, the geostrophic wind has its y component directed down the gradient of planetary vorticity so that $-\beta v_g > 0$. Hence, in

this region the advection of relative vorticity tends to decrease the local relative vorticity, whereas the advection of planetary vorticity tends to increase the local relative vorticity. Similar arguments (but with reversed signs) apply to a region downstream a trough. Therefore, advection of relative vorticity tends to move the vorticity and trough (and ridge) pattern eastward (downstream). But advection of planetary vorticity tends to move the troughs and ridges westward against the advecting wind field.

The net effect of advection on the evolution of the vorticity pattern depends upon which type of advection dominates. Given a geopotential height wavy field, the vorticity increases with the square of the wave number, so that the first term on the right of Eq. (57) is larger for large wave numbers (i.e. short waves; typically $L_x < 3000$ km), while for long waves ($L_x > 10000$ km) the planetary vorticity advection tends to dominate. Therefore, as a general rule, short wavelength synoptic-scale systems should move eastward with the advecting zonal flow while long planetary waves should tend to be stationary or move against the zonal advection. This will be discussed in more details when we derive the dispersion relation for Rossby waves.

Vorticity advection does not alone determine the evolution of meteorological systems. The orographic effects, for example seems to have vanished from Eq. (56). But they are still present, because orography will lead to vertical motions that make the second term on the right important.

Exercises

1. Show that

$$\frac{RT}{c_p p} - \frac{\partial T}{\partial p} = -\frac{T}{\theta} \frac{\partial \theta}{\partial p} = (\Gamma_d - \Gamma)/(\rho g)$$

using the definition of potential temperature, and dry adiabatic and actual lapse rates.

2. Show that from (50) follows the quasi-geostrophic vorticity equation (55). [Hint: apply $\partial/\partial x$ to the second component of Eq. (50) and subtract $\partial/\partial y$ applied to the first component of Eq. (50)].
3. Derive the thermal wind equation for u-component of the zonal wind (Eq. 41) and also for the v-component in pressure coordinates using the geostrophic relation 43.
4. Suppose that on the 500 hPa surface the relative vorticity at a certain location at 45° N latitude is increasing at a rate of $3 \times 10^{-6} s^{-1}$ per 3 h. The wind is from southwest at 20 m/s. and the relative vorticity decreases toward the northeast at a rate of $4 \times 10^{-6} s^{-1}$ per 100 km. Use the quasi-geostrophic vorticity equation to estimate the horizontal divergence at this location on a β plane.
5. Given the following expression for the geopotential field:

$$\Phi(x, y, p, t) = \Phi_0(p) + f_0[-Uy + k^{-1}V \cos(\pi p/p_0) \sin k(x - ct)] \quad , \quad (58)$$

where U, V, c, k, p_0 are constants, use the quasi-geostrophic vorticity equation (56) to obtain an estimate for ω . Assume that $df/dy = \beta$ is a constant (not zero) and that ω vanishes for $p = p_0$.

3 Rossby Waves

3.1 Free Barotropic Rossby Waves

The dispersion relation for free barotropic Rossby waves can be derived by linearizing the barotropic vorticity equation in the form (21). This equation states that the absolute (geostrophic) vorticity is conserved following the horizontal (geostrophic) motion. As usual, we assume that the fields can be expressed as small perturbations from a basic state $\psi = \bar{\psi} + \psi'$. We linearize using a basic state that has only flow in zonal direction $\bar{\psi} = -\bar{u}y + \text{const}$. This mean state fulfills Eq. (21). With this mean state $\nabla^2\psi = \nabla^2\psi'$. Thus, by linearizing, in the first term the total derivative operator can be replaced by the mean operator and it follows

$$\left(\frac{\partial}{\partial t} + \bar{u}\frac{\partial}{\partial x}\right)\nabla^2\psi' + \beta\frac{\partial\psi'}{\partial x} = 0 \quad . \quad (59)$$

As usual, we seek for solutions of the type

$$\psi' = Ae^{i(kx+ly-\nu t)} \quad . \quad (60)$$

Inserting (60) into (59) yields the dispersion relation

$$(-\nu + k\bar{u})(-k^2 - l^2) + k\beta = 0 \quad , \quad (61)$$

which we can solve immediately for ν

$$\nu = \bar{u}k - \beta k/K^2 \quad , \quad (62)$$

where $K^2 \equiv k^2 + l^2$ is the total horizontal wave number squared. Recalling that $c_x = \nu/k$, we find that the zonal phase speed relative to the mean wind is

$$c_x - \bar{u} = -\beta/K^2 \quad . \quad (63)$$

Thus, the Rossby wave zonal phase propagation is always westward relative to the mean zonal flow. Furthermore, the Rossby wave phase speed depends inversely on the square of the horizontal wave number. Therefore, Rossby waves are dispersive waves whose phase speeds increase rapidly with increasing wavelength. This result is consistent with the discussion in section 2.4, in which we showed that the advection of planetary vorticity, which tends to make the disturbances *retrogress*, increasingly dominates over relative vorticity advection as the wavelength of a disturbance increases. Equation (63) provides a quantitative measure of this effect in cases where the disturbance is small enough in amplitude.

From Eq. (63) we may calculate the stationary free Rossby wave wavelength

$$K^2 = \beta/\bar{u} \equiv K_s^2 \quad . \quad (64)$$

This means that stationary free Rossby waves only exist if there is a positive mean flow \bar{u} . This condition is important for Rossby waves that may be generated by tropical convection.

The group velocity of Rossby waves may be calculated as (exercise!):

$$c_{gx} \equiv \frac{\partial \nu}{\partial k} = \bar{u} + \beta \frac{k^2 - l^2}{K^4} \quad (65)$$

$$c_{gy} \equiv \frac{\partial \nu}{\partial l} = 2 \frac{\beta k l}{K^4} \quad (66)$$

Therefore, the energy propagation of stationary Rossby waves is always eastward (Fig. 7; exercise!).

These waves can also be derived from the original, compressible equations, but the analysis is much more complicated. There are some minor modifications in the phase velocities if the full equations are considered, but the main results remain valid.

3.2 Forced Topographic Rossby waves

Forced stationary Rossby waves are of primary importance for understanding the planetary-scale circulation pattern. Such modes may be forced by longitudinal dependent latent heating, or by flow over topography. Of particular importance for the Northern Hemisphere extratropical circulation are stationary Rossby modes forced by flow over the Rockies and the Himalayas.

As the simplest possible dynamical model of topographic Rossby waves we use the barotropic vorticity equation for a homogeneous fluid of variable depth (e.g. Eqs. 14 or 17). We assume that the upper boundary is at fixed height H and the lower boundary is at the variable height $h_T(x, y)$. We also use the quasi-geostrophic scaling $|\xi| \ll f_0$. Then, from 14 and 17 we have

$$H \frac{d_h(\xi + f)}{dt} = -f_0 \frac{dh_T}{dt} \quad , \quad (67)$$

where it has been also assumed that $h \equiv H - h_t \approx H$ on the left side (i.e. the mountain height is much smaller than the troposphere height). After linearizing (as we did to derive Eq. 59)

$$\left(\frac{\partial}{\partial t} + \bar{u} \frac{\partial}{\partial x} \right) \nabla^2 \psi' + \beta \frac{\partial \psi'}{\partial x} = -\frac{f_0}{H} \bar{u} \frac{\partial h_T}{\partial x} \quad . \quad (68)$$

Lets consider the solutions of Eq. (68) for the special case of a sinusoidal lower boundary. We specify the topography to have the form

$$h_T(x, y) = h_0 \sin(kx + \phi) \cos ly \quad , \quad (69)$$

where ϕ is an arbitrary phase (therefore equivalent to $A \cos kx + B \sin kx$). If we insert the streamfunction perturbation

$$\psi' = \psi_0 \sin(kx + \phi) \cos ly \quad , \quad (70)$$

then Eq. (68) has the steady-state solution (i.e. dropping the partial time derivative) [exercise!]

$$\psi_0 = f_0 h_0 / [H(K^2 - K_s^2)] \quad . \quad (71)$$

The streamfunction is either exactly in phase (ridges over the mountains) or exactly out of phase (troughs over the mountains) with the topography depending on the sign $K^2 - K_s^2$. For long waves, ($K < K_s$), the topographic vorticity source in Eq. (68) is primarily balanced by meridional advection of planetary vorticity (the β effect). For short waves ($K > K_s$) the source is balanced primarily by the zonal advection of relative vorticity.

The topographic wave solution (71) has the unrealistic characteristic that when the wave number exactly equals the critical wave number K_s the amplitude goes to infinity. This is the resonant response case when the wave number reaches the stationary wave number of free Rossby waves.

Fig. 7 gives another example for a stationary Rossby wave, caused by ENSO forcing.

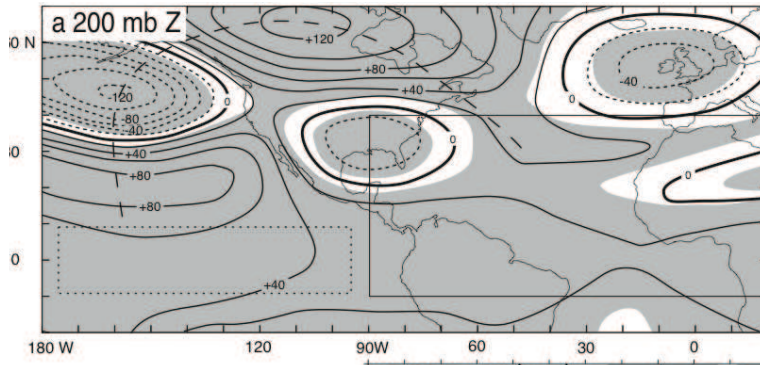


Figure 7: Stationary Rossby wave induced by ENSO.

Exercises

1. Derive the group velocities for Rossby waves (65) and (66) and show that for stationary Rossby waves fulfilling Eq. (64), the c_{gx} component is always positive.
2. Show that (71) is the solution of (68) with (69).
3. Using the linearized form of the potential vorticity equation (11) and the β -plane approximation, derive the Rossby wave speed for a homogeneous incompressible ocean of depth h . Assume a motionless basic state and small perturbations that depend only on x and t ,

$$u = u'(x, t), \quad v = v'(x, t), \quad h = H + h'(x, t) \quad , \quad (72)$$

where H is the mean depth of the ocean. With the aid of the continuity equation for a homogeneous layer

$$\frac{\partial h'}{\partial t} + H \frac{\partial u'}{\partial x} = 0 \quad (73)$$

and the geostrophic wind relationship $v' = gf_0^{-1} \partial h' / \partial x$. Show that the perturbation vorticity equation can be written in the form

$$\frac{\partial}{\partial t} \left(\frac{\partial^2}{\partial x^2} - \frac{f_0^2}{gH} \right) h' + \beta \frac{\partial h'}{\partial x} = 0 \quad (74)$$

and that $h' = h_0 e^{ik(x-ct)}$ is a solution provided that

$$c = -\beta(k^2 + f_0^2/gH)^{-1} \quad . \quad (75)$$

If the ocean is 4 km deep, what is the Rossby wave speed at latitude 45° N for a wave of 10000 km zonal wavelength?

4. Rossby-type waves can be generated in a rotating cylindrical vessel if the depth of the fluid is dependent on the radial coordinate. To determine the Rossby wave speed formula for this equivalent β effect, we assume that the flow is confined between rigid lids in an annular region whose distance from the axis of rotation is large enough so that the curvature terms in the equations can be neglected. We then can refer the motion to cartesian coordinates with x directed azimuthally and y directed toward the axis of rotation. If the system is rotating at angular velocity Ω and the depth is linearly dependent on y ,

$$H(y) = H_0 - \gamma y \quad , \quad (76)$$

show that the perturbation (shallow water) continuity equation ($dH/dt = -H\nabla \cdot \mathbf{v}$) can be written as

$$H_0 \left(\frac{\partial u'}{\partial x} + \frac{\partial v'}{\partial y} \right) - \gamma v' = 0 \quad (77)$$

and that the perturbation quasi-geostrophic vorticity equation is thus

$$\frac{\partial}{\partial t} \nabla^2 \psi' + \beta \frac{\partial \psi'}{\partial x} = 0 \quad , \quad (78)$$

where ψ' is the perturbation geostrophic streamfunction and $\beta = 2\Omega\gamma/H_0$. What is the Rossby wave speed in this situation for waves of wavelength 100 cm in both the x and y directions if $\Omega = 1s^{-1}$, $H_0 = 20$ cm, and $\gamma = 0.05$? (Hint: Assume that the velocity field is geostrophic except in the divergence term.)

5. Solve the nonlinear potential vorticity conservation equation (19) using (22) and including a Ekman pumping term $r_e \xi$, $r_e = 1/day$ numerically for a channel with the centre at $45^\circ N$ of $L_y = 3 \cdot 10^6$ m meridional width and a zonally periodic domains of a length of $L_x = 2 \cdot 10^7$ m using a spatial discretization of $\Delta x = \Delta y = d = 1 \cdot 10^5$ m and a Δt of 1 h. Assume that the top is fixed at a height $H = 1.2 \cdot 10^4$ m, so that the total height of the fluid is given by $h = H - h_t$. Let a sinusoidal mountain be if the shape

$$h_t(x, y) = h_0 \sin(N2\pi x/L_x) \cos(\pi y/L_y) \quad ,$$

where $h_0 = 1 \cdot 10^3$ m, and let N (the number of the mountain waves in the channel) be a) N=2 and b) N=8. The initial condition zonal flow, which, expressed in streamfunction means

$$\psi(x, y, 0) = -10(y - L_y) \quad .$$

Compare the solutions for a) and b) (after 7 days) and especially compare the position of the eddy streamfunction crests relative to the mountain crests for both cases and interpret the results. Hint: Equation (19), with the condition of a fixed upper height H and given lower topography, including Ekman pumping terms can be written as

$$\frac{\partial}{\partial t} \xi = F(x, y, t) - r_e \xi = - \left[\frac{\partial}{\partial x} (u\xi) + \frac{\partial}{\partial y} (v\xi) \right] - \beta v + \frac{f_0}{h} \left[\frac{\partial}{\partial x} (uh) + \frac{\partial}{\partial y} (vh) \right] - r_e \xi \quad . \quad (79)$$

and

$$u = - \frac{\partial \psi}{\partial y} \quad (80)$$

$$v = \frac{\partial \psi}{\partial x} \quad (81)$$

$$\xi = \nabla^2 \psi \quad , \quad (82)$$

given that the quasi-geostrophic approximations (15) and (16) are valid. Note that Eq. (79) can be written in its formulation because the geostrophic wind (Eq. 80) is divergence free and the height does not depend explicitly on time.

Discretize the terms in Eq. (79) as (using an implicit discretization of the Ekman damping)

$$\xi(t + \Delta t) = \xi(t) + \Delta t F_{i,j}(t) - \Delta t r_e \xi(t + \Delta t) \quad (83)$$

with

$$\begin{aligned} F_{i,j}(t) &= - \frac{1}{2d} [(u_{i+1,j} \xi_{i+1,j} - u_{i-1,j} \xi_{i-1,j}) + (v_{i,j+1} \xi_{i,j+1} - v_{i,j-1} \xi_{i,j-1})] - \beta v_{i,j} \\ &+ \frac{f_0}{h_{i+1,j}} \frac{1}{2d} \\ &[(u_{i+1,j} h_{i+1,j} - u_{i-1,j} h_{i-1,j}) + (v_{i,j+1} h_{i,j+1} - v_{i,j-1} h_{i,j-1})] \quad (84) \end{aligned}$$

where the right side is evaluated at the time t , where the fields are already known. This leads to

$$\xi(t + \Delta t) = (\xi(t) + \Delta t F_{i,j}) / (1 + \Delta t r_e) \quad (85)$$

Knowing the vorticity, the streamfunction can be determined by Eq. (82), which can be discretized as (see MMG lectures)

$$(\psi_{i+1,j} + \psi_{i-1,j} + \psi_{i,j+1} + \psi_{i,j-1} - 4\psi_{i,j}) / d^2 = \xi_{i,j} \quad (86)$$

If we can solve this equation for $\psi_{i,j}$, we can derive the velocity fields by using Eqs. (80), (81) in discretized form

$$u_{i,j} = -(\psi_{i,j+1} - \psi_{i,j-1}) / (2d) \quad (87)$$

$$v_{i,j} = (\psi_{i,j+1} - \psi_{i,j-1}) / (2d) \quad (88)$$

$$(89)$$

A scheme how to solve the initial value problem is:

- (a) Given the initial condition $\psi_{i,j}$, (86) can be solved to determine $\xi_{i,j}$, (87) and (88) can be used to determine the velocities
- (b) Evaluate $F_{i,j}$ using Eq. (84).
- (c) $\xi_{t+\Delta t}$ can be determined by integrating (85).
- (d) Knowing $\xi_{t+\Delta t}$, (86) can be inverted to calculate $\psi_{t+\Delta t}$
- (e) Go back to (a).

Integrate this scheme for 7 days to reach a steady-state solution and plot the eddy streamfunction and topography.

4 Baroclinic Instability

4.1 A two-layer Model

Even for a highly idealized mean flow profile the mathematical treatment of baroclinic instability in a continuously stratified atmosphere is rather complicated. Thus, we focus on the simplest model that can incorporate baroclinic processes. The atmosphere is represented by two discrete layers bounded by surfaces numbered 0, 2, and 4 (generally taken to be the 0-, 500-, and 1000-hPa surfaces, respectively). The quasi-geostrophic vorticity equation for the midlatitude β plane is applied at levels denoted 1 and 3 and the thermodynamic energy equation is applied at level 2. Before writing the specific equations of the two-layer model, it is convenient to define a *geostrophic streamfunction*, $\psi \equiv \Phi/f_0$ (see definitions leading to Eq. 21). Then the geostrophic wind (Eq. 43) and the geostrophic vorticity (Eq. 54) can be expressed as

$$\mathbf{v} = \mathbf{k} \times \nabla\psi, \quad \xi = \nabla^2\psi \quad (90)$$

The quasi-hydrostatic vorticity equation (56) and the hydrostatic thermodynamic equation (53) can be written with help of (27) in terms of ψ and ω as (assuming no diabatic processes)

$$\frac{\partial}{\partial t} \nabla^2\psi + \mathbf{v} \cdot \nabla(\nabla^2\psi) + \beta \frac{\partial\psi}{\partial x} = f_0 \frac{\partial\omega}{\partial p} \quad (91)$$

$$\frac{\partial}{\partial t} \left(\frac{\partial\psi}{\partial p} \right) = -\mathbf{v} \cdot \nabla \left(\frac{\partial\psi}{\partial p} \right) - \frac{\sigma}{f_0} \omega \quad (92)$$

We now apply the vorticity equation (91) at the two levels designated as 1 and 3, which are in the middle of the two layers. To do this we must estimate the divergence term $\partial\omega/\partial p$ at these levels using finite difference approximations to the vertical derivatives

$$\left(\frac{\partial\omega}{\partial p} \right)_1 \approx \frac{\omega_2 - \omega_0}{\delta p}, \quad \left(\frac{\partial\omega}{\partial p} \right)_3 \approx \frac{\omega_4 - \omega_2}{\delta p}, \quad (93)$$

where δp is the pressure interval between levels 0-2 and 2-4 and subscript notation is used to designate the vertical level for each dependent variable. The resulting vorticity equations are

$$\frac{\partial}{\partial t} \nabla^2\psi_1 + \mathbf{v}_1 \cdot \nabla(\nabla^2\psi_1) + \beta \frac{\partial\psi_1}{\partial x} = f_0 \frac{\omega_2}{\delta p} \quad (94)$$

$$\frac{\partial}{\partial t} \nabla^2\psi_3 + \mathbf{v}_3 \cdot \nabla(\nabla^2\psi_3) + \beta \frac{\partial\psi_3}{\partial x} = -f_0 \frac{\omega_2}{\delta p} \quad (95)$$

where we have used the fact that $\omega_0 = 0$ and assumed that $\omega_4 = 0$, which is approximately true for a level lower boundary surface. We next write the thermodynamic energy equation (92) at level 2. Here we must evaluate $\partial\psi/\partial p$ using the difference formula

$$(\partial\psi/\partial p) \approx (\psi_3 - \psi_1)/\delta p \quad .$$

The result is

$$\frac{\partial}{\partial t}(\psi_1 - \psi_3) = -\mathbf{v}_2 \cdot \nabla(\psi_1 - \psi_3) + \frac{\sigma \delta p}{f_0} \omega_2 \quad . \quad (96)$$

The first term on the right-hand side in Eq. (96) is the advection of the 250-750 hPa thickness by the wind at 500 hPa. However, ψ_2 , the 500 hPa streamfunction, is not a predicted field in this model. Therefore, ψ_2 must be obtained by linearly interpolating between the 250- and 750-hPa levels

$$\psi_2 = (\psi_1 + \psi_3)/2 \quad . \quad (97)$$

If this interpolation formula is used, (94)-(96) become a closed set of prediction equations in the variables ψ_1, ψ_3 , and ω_2 .

4.2 Linear Perturbation Analysis

To keep the analysis as simple as possible we assume that the streamfunctions ψ_1 and ψ_3 consists of basic state parts that depend linearly on y alone, plus perturbations that depend only on x and t (similar to section 3). Thus, we let

$$\begin{aligned} \psi_1 &= -U_1 y + \psi'_1(x, t) \\ \psi_3 &= -U_3 y + \psi'_3(x, t) \\ \omega_2 &= \omega'_2(x, t) \quad . \end{aligned} \quad (98)$$

The zonal velocities at levels 1 and 3 are then constants with the values U_1 and U_3 , respectively. Hence, the perturbation field has meridional and vertical velocity components only. Inserting (98) into (94)-(96) and linearizing yields the perturbation equations (see section 3)

$$\left(\frac{\partial}{\partial t} + U_1 \frac{\partial}{\partial x} \right) \frac{\partial^2 \psi'_1}{\partial x^2} + \beta \frac{\partial \psi'_1}{\partial x} = f_0 \frac{\omega'_2}{\delta p} \quad (99)$$

$$\left(\frac{\partial}{\partial t} + U_3 \frac{\partial}{\partial x} \right) \frac{\partial^2 \psi'_3}{\partial x^2} + \beta \frac{\partial \psi'_3}{\partial x} = -f_0 \frac{\omega'_2}{\delta p} \quad (100)$$

$$\left(\frac{\partial}{\partial t} + U_m \frac{\partial}{\partial x} \right) (\psi'_1 - \psi'_3) - U_T \frac{\partial}{\partial x} (\psi'_1 + \psi'_3) = \frac{\sigma \delta p}{f_0} \omega'_2 \quad , \quad (101)$$

where we have linearly interpolated to express \mathbf{v}_2 in terms of ψ_1 and ψ_3 and have defined

$$U_m \equiv (U_1 + U_3)/2, \quad U_T \equiv (U_1 - U_3)/2 \quad .$$

Thus, U_m and U_T are, respectively, the vertically averaged mean zonal wind and the mean thermal wind for the interval $\delta p/2$. The dynamical properties of this system are more clearly expressed if (99)-(101) are combined to eliminate ω'_2 . We first note that (99) and (100) can be rewritten as

$$\left(\frac{\partial}{\partial t} + (U_m + U_T) \frac{\partial}{\partial x} \right) \frac{\partial^2 \psi'_1}{\partial x^2} + \beta \frac{\partial \psi'_1}{\partial x} = f_0 \frac{\omega'_2}{\delta p} \quad (102)$$

$$\left(\frac{\partial}{\partial t} + (U_m - U_T) \frac{\partial}{\partial x} \right) \frac{\partial^2 \psi'_3}{\partial x^2} + \beta \frac{\partial \psi'_3}{\partial x} = -f_0 \frac{\omega'_2}{\delta p} \quad . \quad (103)$$

We now define the barotropic and baroclinic perturbations as

$$\psi_m \equiv (\psi'_1 + \psi'_3)/2, \quad \psi_T \equiv (\psi'_1 - \psi'_3)/2 \quad (104)$$

Adding (102) and (103) and using the definitions in (104) yields

$$\left[\frac{\partial}{\partial t} + U_m \frac{\partial}{\partial x} \right] \frac{\partial^2 \psi_m}{\partial x^2} + \beta \frac{\partial \psi_m}{\partial x} + U_T \frac{\partial}{\partial x} \left(\frac{\partial^2 \psi_T}{\partial x^2} \right) = 0 \quad , \quad (105)$$

while subtracting (103) from (102) and combining with (101) to eliminate ω'_2 yields

$$\left[\frac{\partial}{\partial t} + U_m \frac{\partial}{\partial x} \right] \left(\frac{\partial^2 \psi_T}{\partial x^2} - 2\lambda^2 \psi_T \right) + \beta \frac{\partial \psi_T}{\partial x} + U_T \frac{\partial}{\partial x} \left(\frac{\partial^2 \psi_m}{\partial x^2} + 2\lambda^2 \psi_m \right) = 0 \quad , \quad (106)$$

where $\lambda^2 \equiv f_0^2/[\sigma(\delta p)^2]$. Equations (105) and (106) govern the evolution of the barotropic (vertically averaged) and baroclinic (thermal) perturbation vorticities, respectively. As usual we assume that wavelike solutions exist of the form

$$\psi_m = A e^{ik(x-ct)}, \quad \psi_T = B e^{ik(x-ct)} \quad . \quad (107)$$

Substituting these assumed solutions into (105) and (106) and dividing through by the common exponential factor, we obtain a pair of simultaneous linear algebraic equations for the coefficients of A, B

$$ik[(c - U_m)k^2 + \beta]A - ik^3 U_T B = 0 \quad (108)$$

$$ik[(c - U_m)(k^2 + 2\lambda^2) + \beta]B - ik U_T (k^2 - 2\lambda^2)A = 0 \quad . \quad (109)$$

From the Mathematical Methods course we know that a homogeneous set of equations has only nontrivial solutions if the determinant of the coefficients for A and B is zero. Thus the phase speed c must satisfy the condition

$$\begin{vmatrix} (c - U_m)k^2 + \beta & -k^2 U_T \\ -U_T(k^2 - 2\lambda^2) & (c - U_m)(k^2 + 2\lambda^2) + \beta \end{vmatrix} = 0 \quad , \quad (110)$$

which gives a quadratic dispersion equation in c

$$(c - U_m)^2 k^2 (k^2 + 2\lambda^2) + 2(c - U_m)\beta(k^2 + \lambda^2) + [\beta^2 + U_T^2 k^2 (2\lambda^2 - k^2)] = 0 \quad , \quad (111)$$

The solution for c is

$$c = U_m - \frac{\beta(k^2 + \lambda^2)}{k^2(k^2 + 2\lambda^2)} \pm \delta^{1/2} \quad , \quad (112)$$

where

$$\delta \equiv \frac{\beta^2 \lambda^4}{k^4 (k^2 + 2\lambda^2)^2} - \frac{U_T^2 (2\lambda^2 - k^2)}{(k^2 + 2\lambda^2)} \quad . \quad (113)$$

We have shown that (107) is a solution for the system (105) and (106) only if the phase speed satisfies (112). Although (112) appears to be rather complicated, it is immediately apparent that if $\delta < 0$ the phase speed will have an imaginary part and

the perturbations will amplify exponentially. Before discussing the general physical conditions required for exponential growth it is useful to consider two special cases.

As the first special case we let $U_T = 0$ so that the basic state thermal wind vanishes and the mean flow is barotropic. There can be no instability if the thermal wind vanishes (i. e. without horizontal mean-state temperature gradients). The *available potential energy* stored in the mean state temperature gradients is responsible for baroclinic growth! The phase speeds in this case are

$$c_1 = U_m - \beta k^{-2} \quad (114)$$

and

$$c_2 = U_m - \beta(k^2 + 2\lambda^2)^{-1} \quad (115)$$

These are real quantities that correspond to the free (normal mode) oscillations for the two-level model with a barotropic basic state current. The phase speed c_1 is simply the dispersion relationship for a barotropic Rossby wave with no y dependence (see Eq. [63]). Substituting the expression (114) in place of c in (108) and (109) we see that in this case $B = 0$, so that the perturbation is barotropic in structure. The expression (115), on the other hand, may be interpreted as the phase speed of an internal baroclinic Rossby wave. Note that c_2 is a dispersion relationship analogous to the Rossby wave speed for a homogeneous ocean with a free surface, which was given in problem 3 of section 3. But, in the two-level model, the factor $2\lambda^2$ appears in the denominator in place of the f_0/gH for the oceanic case. In each of these cases there is vertical motion associated with the Rossby wave so that static stability modified the phase speed.

Comparing (114) and (115) we see that the phase speed of the baroclinic mode is generally much less than that of the barotropic mode, since for average midlatitude tropospheric conditions $\lambda^2 \approx 2 \times 10^{-12} \text{ m}^{-2}$, which is comparable in magnitude to k for zonal wavelength of $\sim 4500 \text{ km}$.

Returning to the general case where all terms are retained in (112), the stability criterion is most easily understood by computing the *neutral curve*, which connects all values of U_T and k for which $\delta = 0$ so that the flow is *marginally stable*. From Eq. (112), the condition $\delta = 0$ implies that

$$\frac{\beta^2 \lambda^4}{k^4(2\lambda^2 + k^2)} = U_T^2(2\lambda^2 - k^2) \quad (116)$$

or

$$k^4/(4\lambda^4) = 1/2\{1 \pm [1 - \beta^2/(4\lambda^4 U_T^2)]^{1/2}\} \quad (117)$$

Fig. 4.2 shows nondimensional quantity $k^2/2\lambda^2$, which is a measure of the zonal wavelength, plotted against the nondimensional parameter $2\lambda^2 U_T/\beta$, which is proportional to the thermal wind, according to Eq. (117).

As indicated in the figure, the neutral curve separates the unstable region of the U_T, k plane from the stable region. It is clear that the inclusion of the β effect serves to stabilize the flow, for unstable roots exist only for $|U_T| > \beta/(2\lambda^2)$. In addition to a

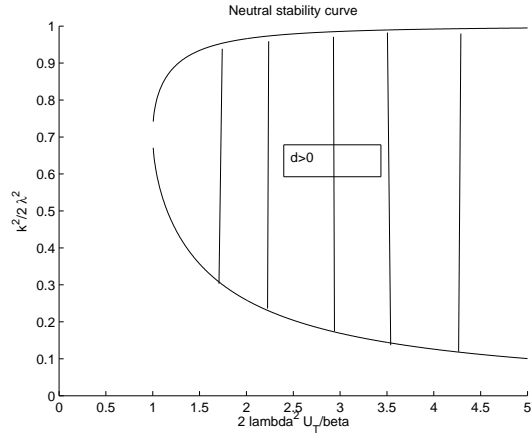


Figure 8: Neutral stability curve for the two-level baroclinic model

minimum value of U_T required for unstable growth depends strongly on k . Thus, the β effect strongly stabilizes the long-wave end of the wave spectrum ($k \rightarrow 0$). Again, the flow is always stable for waves shorter than the critical wavelength $L_c = \sqrt{2}\pi/\lambda$ (why?). The long-wave stabilization associated with the β effect is caused by the rapid westward propagation of long waves, which occurs only when the β effect is included in the model.

Differentiating Eq. (116) with respect to k and setting $dU_T/dk = 0$, we find the minimum value of U_T for which unstable waves exist occurs when $k^2 = \sqrt{2}\lambda^2$. This wave number corresponds to the wave of maximum instability. Wave numbers for observed disturbances should be close to the wave number of maximum instability, for if U_T were gradually raised from zero the flow would first become unstable for perturbations of wave number $k = 2^{1/4}\lambda$. Those perturbations would then amplify and in the process remove energy from the mean thermal wind, thereby decreasing U_T and stabilizing the flow. Under normal conditions of static stability the wavelength of maximum instability is about 4000 km, which is close to the average wavelength for midlatitude synoptic systems.

Exercises

1. Suppose that a baroclinic fluid is confined between two rigid horizontal lids in a rotating tank in which $\beta = 0$ but friction is presented in the form of linear drag proportional to the velocity (i.e., $\mathbf{Fr} = -\mu\mathbf{v}$). Show that the two-level model perturbation vorticity equations in cartesian coordinates can be written as

$$\left(\frac{\partial}{\partial t} + U_1 \frac{\partial}{\partial x} + \mu \right) \frac{\partial^2 \psi'_1}{\partial x^2} - f_0 \frac{\omega'_2}{\delta p} = 0$$

$$\left(\frac{\partial}{\partial t} + U_3 \frac{\partial}{\partial x} + \mu \right) \frac{\partial^2 \psi'_3}{\partial x^2} + f_0 \frac{\omega'_2}{\delta p} = 0 \quad ,$$

where perturbations are assumed in the form given in Eq. (98). The thermodynamic equation remains (101). Assuming solutions of the form (107), show that the phase speed satisfies a relationship similar to (112), with β replaced everywhere by $i\mu k$ and that as a result the condition for baroclinic instability becomes

$$U_T > \mu(2\lambda^2 - k^2)^{-1/2} \quad .$$

5 Equatorial Wave Theory

Lecture based on 'An Introduction to Dynamic Meteorology' by J. R. Holton, *Academic Press, INC.*, 3rd edition, 511 pp.

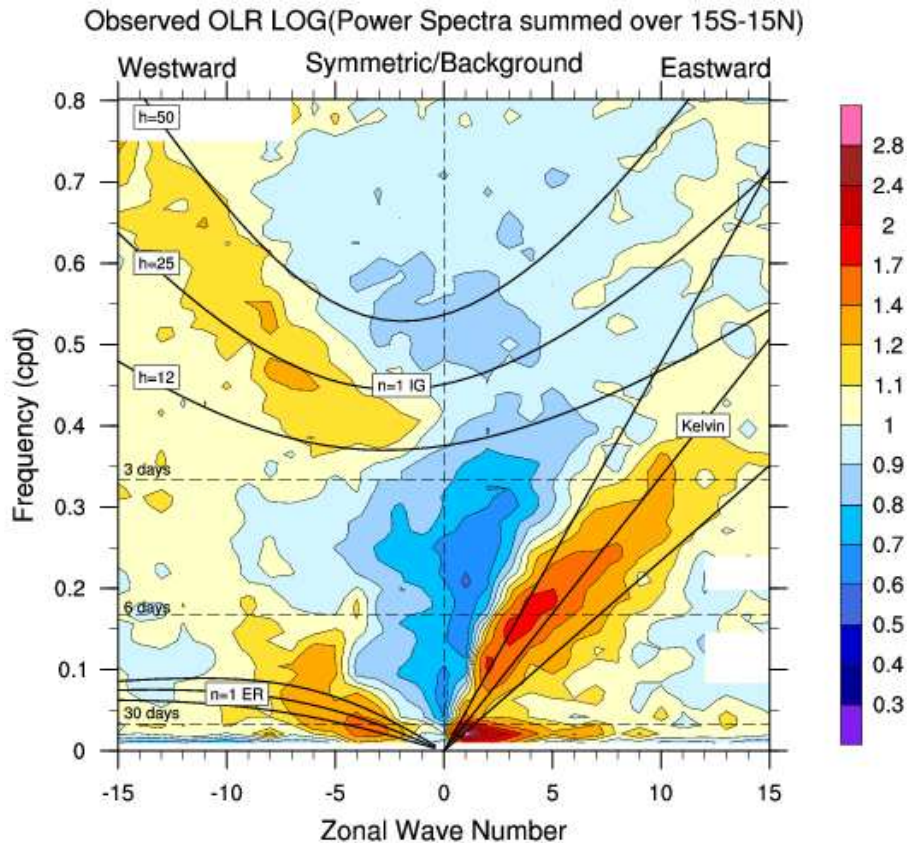


Figure 9: Dispersion diagram for tropical Outgoing longwave radiation. Source: www.cgd.ucar.edu, NOAA.

Equatorial waves are an important class of eastward and westward propagating disturbances that are trapped about the equator (that is, they decay away from the equatorial region). In a dispersion diagram for observed equatorial quantities, these wave can be identified as regions of increased energy density (Fig. 9).

Diabatic heating by organized tropical convection may excite equatorial wave motions (see Fig. 10). Through such waves the dynamical effects of convective storms can be communicated over large longitudinal distances in the tropics. Such waves can produce remote responses to localized heat sources. Furthermore, by influencing the pattern of low-level moisture convergence they can partly control the spatial and temporal distribution of convective heating. In order to introduce equatorial waves in the simplest possible context, we here use a shallow-water model

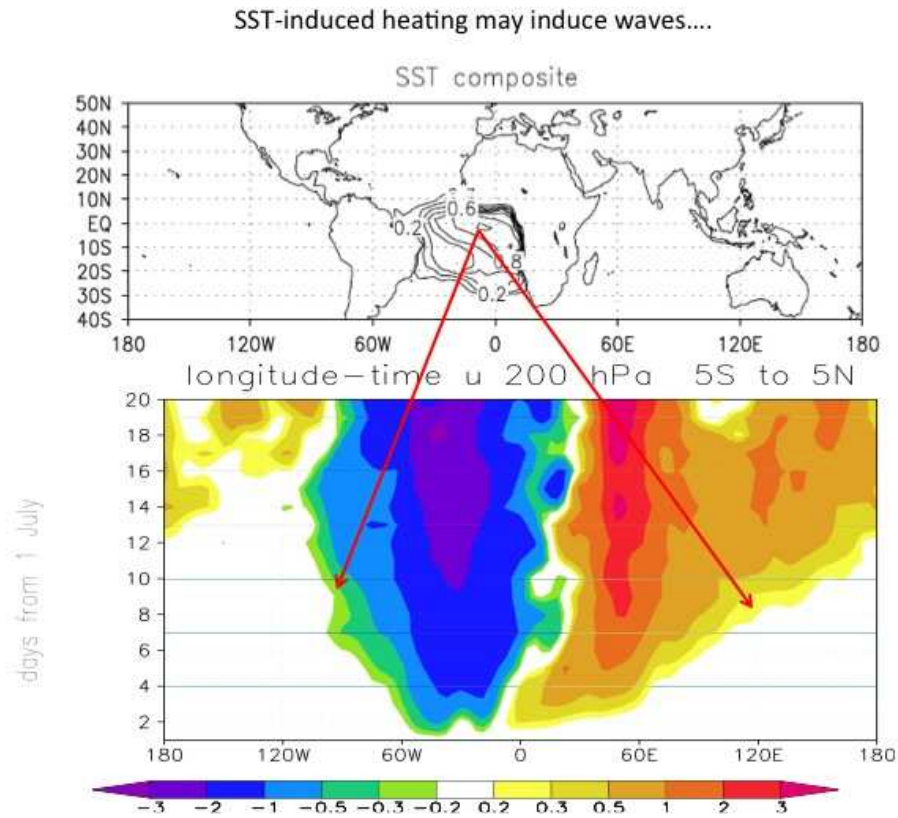


Figure 10: Equatorial Kelvin and Rossby waves triggered by an SST-induced heating. Source: Kucharski et al. 2008: A Gill-Matsuno-type mechanism explains the tropical Atlantic influence on African and Indian monsoon rainfall. *Q. J. R. Meteorol. Soc.* (2009), 135, 569-579, DOI: 10.1002/qj.406

and concentrate on the *horizontal* structure.

5.1 The shallow water equations

The shallow water equations are a drastic simplification to the real atmospheric flow. However, despite its simplicity it gives often a good insight into many atmospheric wave phenomena. The basic assumptions in the shallow water model are

- (i) The flow is incompressible $\rho = \text{const.}$
- (ii) The flow is shallow enough so that the horizontal velocity components are independent of height.
- (iii) The flow is hydrostatic. Accelerations in the vertical direction may be neglected.

Let us consider the horizontal momentum equations 1 and the hydrostatic equation 24

$$\frac{\partial u}{\partial t} + (\mathbf{v} \cdot \nabla)u = -\frac{1}{\rho} \frac{\partial p}{\partial x} + fv \quad (118)$$

$$\frac{\partial v}{\partial t} + (\mathbf{v} \cdot \nabla)v = -\frac{1}{\rho} \frac{\partial p}{\partial y} - fu \quad (119)$$

$$\frac{1}{\rho} \frac{\partial p}{\partial z} = -g, \quad (120)$$

Further consider the continuity equation

$$\frac{\partial \rho}{\partial t} + \nabla \cdot (\rho \mathbf{v}) = 0. \quad (121)$$

Integrating the hydrostatic equation from a height z to the top of the fluid leads to (assuming the pressure is vanishing there)

$$\int_z^{h(x,y,t)} \frac{\partial p}{\partial z} dz = - \int_z^{h(x,y,t)} \rho g dz, \quad \text{or} \quad (122)$$

$$-p(x, y, z, t) = -\rho g[h(x, y, t) - z]. \quad (123)$$

Thus the horizontal pressure gradient force in the equations of motion 118, 119 may be expressed as

$$-\frac{1}{\rho} \frac{\partial p}{\partial x} = -g \frac{\partial h}{\partial x} = -\frac{\partial \Phi}{\partial x} \quad (124)$$

$$-\frac{1}{\rho} \frac{\partial p}{\partial y} = -g \frac{\partial h}{\partial y} = -\frac{\partial \Phi}{\partial y}, \quad (125)$$

where we have defined $\Phi(x, y, t) = gh(x, y, t)$. Thus, keeping in mind that there the horizontal velocities do not depend on the vertical direction and ignoring the coriolis term proportional to the vertical velocity, the horizontal equations of motion may be written as

$$\frac{\partial u}{\partial t} + (\mathbf{u} \cdot \nabla)u = -\frac{\partial \Phi}{\partial x} + fv \quad (126)$$

$$\frac{\partial v}{\partial t} + (\mathbf{u} \cdot \nabla)v = -\frac{\partial \Phi}{\partial y} - fu, \quad (127)$$

The number of dependent variables in Eqs. 126 and 127 is reduced to 3, (u, v, Φ) . Thus, if we have another equation only containing (u, v, Φ) , then the system may be complete. This is achieved by simplification of the continuity equation 121 and vertical integration. First, we note that because of $\rho = \text{const}$, Eq. 121 reduces to

$$\frac{\partial w}{\partial z} = -\nabla \cdot \mathbf{u}. \quad (128)$$

If we integrate this equation vertically from 0 to $h(x, y, t)$ we have

$$\int_0^h \frac{\partial w}{\partial z} dz = - \int_0^h \nabla \cdot \mathbf{u} dz \quad (129)$$

$$w(h) := \frac{dh}{dt} = \frac{\partial h}{\partial t} + \mathbf{u} \cdot \nabla h = -(\nabla \cdot \mathbf{u})h \quad (130)$$

Eq. 130 may as well be written as

$$\frac{\partial \Phi}{\partial t} + \mathbf{u} \cdot \nabla \Phi = -\Phi \nabla \cdot \mathbf{u} . \quad (131)$$

Eqs. 126, 127 and 131 build a complete set of differential equations for (u, v, Φ) , and are called the *shallow water equations*.

5.2 Linearization for an Equatorial β -plane

Now we linearize the set of equations 126, 127 and 131 about a motionless mean state with height h_e on an equatorial β -plane. Generally speaking, the β -plane assumption states that $f = 2|\omega| \sin \phi \approx f_0 + \beta y$, that is the $\sin \phi$ -dependence is approximated linearly for a given latitude ϕ_0 by a Taylor series expansion (therefore $\beta = 2|\omega| \cos \phi_0 / a$; a being the mean radius of the earth). If we set the base point at the equator we have $f_0 = 0$, therefore $f \approx \beta y$.

$$\frac{\partial u'}{\partial t} = -\frac{\partial \Phi'}{\partial x} + \beta y v' \quad (132)$$

$$\frac{\partial v'}{\partial t} = -\frac{\partial \Phi'}{\partial y} - \beta y u' \quad (133)$$

$$\frac{\partial \Phi'}{\partial t} = -gh_e \left(\frac{\partial u'}{\partial x} + \frac{\partial v'}{\partial y} \right) , \quad (134)$$

where the primed variables denote the perturbations from the basic state. This is our basic set of linearized equations (with variable coefficients!) to study equatorial wave dynamics. By adjusting the scale height h_e as well the ocean case may be included.

Discuss Inertia-Gravity waves for extratropical situation and approximation $f = f_0 = \text{const}$, and assume $u'(x, t), v'(x, t), \Phi'(x, t)$.

5.2.1 Equatorial Rossby and Rossby-Gravity Modes

In order to find solutions to the linearized system 132, 133 and 134, we assume that the y -dependence can be separated

$$\begin{pmatrix} u' \\ v' \\ \Phi' \end{pmatrix} = \begin{bmatrix} \hat{u}(y) \\ \hat{v}(y) \\ \hat{\Phi}(y) \end{bmatrix} e^{i(kx - \nu t)} . \quad (135)$$

Substitution of Eq. 135 into 132-134 then yields a set of ordinary differential equations in y for the meridional structure functions $\hat{u}, \hat{v}, \hat{\Phi}$:

$$-i\nu\hat{u} = -ik\hat{\Phi} + \beta y\hat{v} \quad (136)$$

$$-i\nu\hat{v} = -\frac{\partial\hat{\Phi}}{\partial y} - \beta y\hat{u} \quad (137)$$

$$-i\nu\hat{\Phi} = -gh_e \left(ik\hat{u} + \frac{\partial\hat{v}}{\partial y} \right). \quad (138)$$

If Eq. 136 is solved for $\hat{u} = k/\nu\hat{\Phi} + i\beta y\hat{v}/\nu$ and inserted into Eq. 137 and 138 we obtain

$$(\beta^2 y^2 - \nu^2)\hat{v} = ik\beta y\hat{\Phi} + i\nu\frac{\partial\hat{\Phi}}{\partial y} \quad (139)$$

$$(\nu^2 - gh_e k^2)\hat{\Phi} + i\nu gh_e \left(\frac{\partial\hat{v}}{\partial y} - \frac{k}{\nu}\beta y\hat{v} \right) = 0. \quad (140)$$

Finally, Eq. 140 is inserted into Eq. 139 to eliminate $\hat{\Phi}$, yielding a second-order differential equation in the single unknown, \hat{v}

$$\frac{\partial^2\hat{v}}{\partial y^2} + \left[\left(\frac{\nu^2}{gh_e} - k^2 - \frac{k}{\nu}\beta \right) - \frac{\beta^2 y^2}{gh_e} \right] \hat{v} = 0. \quad (141)$$

We seek solutions of this equation for the meridional distribution of \hat{v} , subject to the boundary condition that the disturbance fields vanish for $|y| \rightarrow \infty$. This boundary condition is necessary since the approximation $f \approx \beta y$ is not valid for latitudes much beyond $\pm 30^\circ$, so that solutions must be equatorially trapped if they are to be good approximations to the exact solutions on the sphere. Equation 141 differs from the classic equation for a harmonic oscillator in y because the coefficient in square brackets is not a constant but is a function of y . For sufficiently small y this coefficient is positive and solutions oscillate in y , while for large y , solutions either grow or decay in y . Only the decaying solutions, however, can satisfy the boundary conditions.

It turns out that solutions to Eq. 141 which satisfy the condition of decay far from the equator exist only when the constant part of the coefficient in square brackets satisfies the relationship (which is as well the dispersion relation!)

$$\frac{\sqrt{gh_e}}{\beta} \left(-\frac{k}{\nu}\beta - k^2 + \frac{\nu^2}{gh_e} \right) = 2n + 1; \quad n = 0, 1, 2, \dots \quad (142)$$

which is a cubic dispersion equation determining the frequencies of permitted equatorially trapped free oscillations for zonal wave number k and meridional mode number n . These solutions can be expressed most conveniently if y is replaced by the nondimensional meridional coordinate

$$\xi = \left(\frac{\beta}{\sqrt{gh_e}} \right)^{1/2} y. \quad (143)$$

With the Eqs. 142 and 143, Eq. 141 becomes

$$\frac{\partial^2 \hat{v}}{\partial \xi^2} + (2n + 1 - \xi^2) \hat{v} = 0 . \quad (144)$$

This is the differential equation for a quantum mechanical, simple harmonic oscillator. The solution has the form

$$\hat{v}(\xi) = H_n(\xi) e^{-\xi^2/2} , \quad (145)$$

where $H_n(\xi)$ designates the n th *Hermite polynomial*. The first of these polynomials have the values

$$H_0 = 1, \quad H_1(\xi) = 2\xi, \quad H_2(\xi) = 4\xi^2 - 2 . \quad (146)$$

Thus, the index n corresponds to the number of nodes in the meridional velocity profile in the domain $|y| < \infty$. Inserting the solution 145 into Eq. 144 leads to one of the defining differential equations for Hermite polynomials. In general, the three solutions of Eq. 142 can be interpreted as eastward- and westward-moving equatorially trapped gravity waves and westward-moving equatorial Rossby waves. The case $n = 0$ (for which the meridional velocity perturbation has a gaussian distribution centered at the equator) must be treated separately. In this case the *dispersion relationship* 142 (which is something like a characteristic equation that gives the $\nu(k)$ -dependence from which we may derive the phase velocities) factors as

$$\left(\frac{\nu}{\sqrt{gh_e}} - \frac{\beta}{\nu} - k \right) \left(\frac{\nu}{\sqrt{gh_e}} + k \right) = 0 . \quad (147)$$

The root $\nu/k = -\sqrt{gh_e}$, corresponding to a westward-propagating gravity wave, is not permitted since the second term in parentheses in Eq. 147 was explicitly assumed not to vanish when Eqs. 139 and 140 were combined to eliminate Φ . The roots given by the first term in parentheses in Eq. 147 are

$$\nu = k\sqrt{gh_e} \left[\frac{1}{2} \pm \frac{1}{2} \left(1 + \frac{4\beta}{k^2\sqrt{gh_e}} \right)^{1/2} \right] . \quad (148)$$

The positive root corresponds to an eastward-propagating equatorial inertio-gravity wave, while the negative root corresponds to a westward-propagating wave, which resembles an inertio-gravity wave for long zonal scale $k \rightarrow 0$ and resembles a Rossby wave for zonal scales characteristic of synoptic-scale disturbances. This mode is generally referred to as a Rossby-gravity wave.

5.2.2 Equatorial Kelvin Waves

In addition to the modes discussed in the previous section, there is another equatorial wave that is of great practical importance. For this mode, which is called the equatorial *Kelvin wave*, the meridional velocity perturbation vanishes and Eqs. 136 to 138 are reduced to the simpler set

$$-i\nu\hat{u} = -ik\hat{\Phi} \quad (149)$$

$$\beta y\hat{u} = -\frac{\partial\hat{\Phi}}{\partial y} \quad (150)$$

$$-i\nu\hat{\Phi} = -gh_e(ik\hat{u}) . \quad (151)$$

Eliminating Φ between Eq. 149 and Eq. 151, we see that the Kelvin wave dispersion equation is that of the shallow-water gravity wave

$$c^2 = \left(\frac{\nu}{k}\right)^2 = gh_e . \quad (152)$$

According to Eq. 152 the phase speed c can be either positive or negative. But, if Eq. 149 and Eq. 150 are combined to eliminate Φ we obtain a first-order equation for determining the meridional structure

$$\beta y\hat{u} = -c\frac{\partial\hat{u}}{\partial y} , \quad (153)$$

which may be integrated immediately to yield

$$\hat{u} = u_0 e^{-\beta y^2/(2c)} , \quad (154)$$

where u_0 is the amplitude of the perturbation zonal velocity at the equator. Equation 154 shows that if solutions decaying away from the equator are to exist, the phase speed must be positive ($c > 0$). Thus Kelvin waves are eastward propagating and have zonal velocity and geopotential perturbations that vary in latitude as Gaussian functions centered on the equator. The e-folding decay width is given by

$$Y_K = |2c/\beta|^{1/2} , \quad (155)$$

which for a phase speed $c = 30 \text{ m s}^{-1}$ gives $Y_K = 1600 \text{ km}$. The meridional force balance for the Kelvin mode is an exact geostrophic balance between the zonal velocity and the meridional pressure gradient. It is the change in sign of the Coriolis parameter at the equator that permits this special type of equatorial mode to exist.

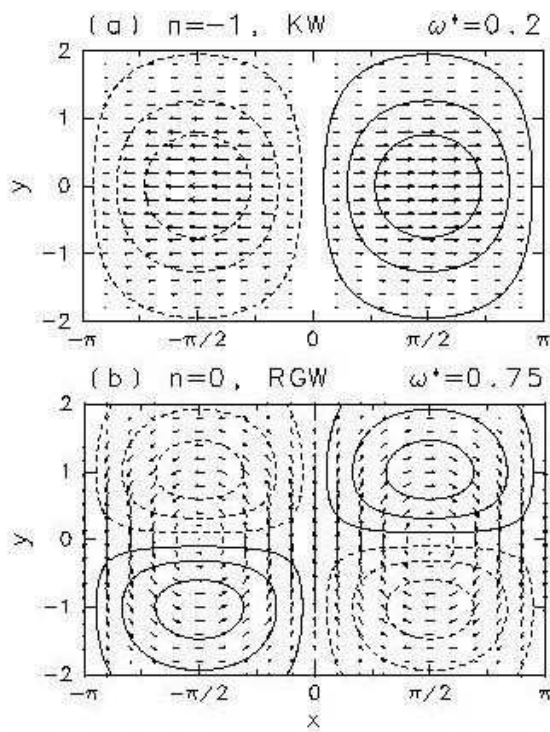


Fig.1 Horizontal structure of (a) Kelvin wave and (b) mixed-Rossby gravity wave. Contours show geopotential height component and arrows show horizontal wind components.

Figure 11: Illustration of Kelvin (upper panel) and Rossby-gravity (lower panel) waves.

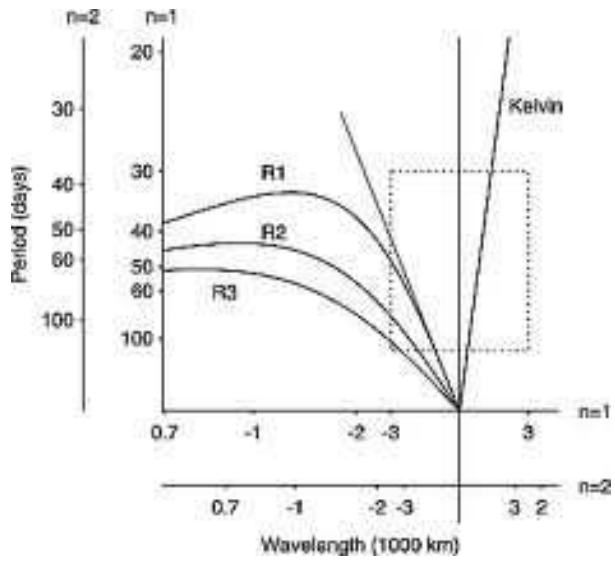


Figure 12: Dispersion diagram for equatorial Rossby-gravity and Kelvin waves.

6 ENSO atmosphere and ocean feedback mechanisms

Suggested Literature:

- a) Gill, A. E., 1980: 'Some simple solutions for heat-induced tropical circulation', *Quart. J. R. Met. Soc.*, **106**, 447-462.
- b) Reference for reduced gravity model in oceans:
'Ocean Circulation' by R. X. Huang, *University Press, Cambridge*, 791 pp.
- c) Online textbooks:
oceanworld.tamu.edu/resources/ocng_textbook/contents.html
oceanworld.tamu.edu/resources/oceanography-book/contents.htm
- d) 'El Nino, La Nina, and the Southern Oscillation' by S. G. Philander, *Academic Press, INC.*, 293 pp.
- e) For the ocean simulations presented:
Chang, P., 1994: 'A study of the seasonal cycle of sea surface temperature in the tropical Pacific Ocean using reduced gravity models', *J. Geophys. Res.*, **99**, C4, 7725-7741

6.1 Some general observations

The typical equatorial Pacific background state is shown in Fig. 13, in a vertical-zonal section. As can be seen it gets colder as we go from the surface downward (why?). And it also gets colder if we go from west to east. Looking at a map of sea surface temperature (SST), we see this equatorial asymmetry clearly (Fig. 14).

A schematic what is the situation in normal conditions (or La Nina) is given in 15. Trade winds are blowing near the equator from east to west (the reason these trade winds will be discussed later in this course, but briefly it is due to the maximum convective heating that occurs in the mean around the equator). These trade winds push the warm surface waters to the west. What is happening then in the east?

In El Nino conditions this normal situation breaks down and we get to a situation where also the eastern Pacific is flushed with warm waters (intuitively one would think that this is the 'normal' situation).

The typical sea surface temperature anomaly for an El Nino event is shown in Fig. 17. A warming of typically more than 1K is occurring in the eastern Pacific and surrounded by a cooling (so-called *Horse-shoe pattern*).

Fig. 18 shows the typical (composite) response of the atmosphere (rainfall [or heating!], and low-level winds) to the typical (composite) El Nino SST anomaly of Fig. 17.

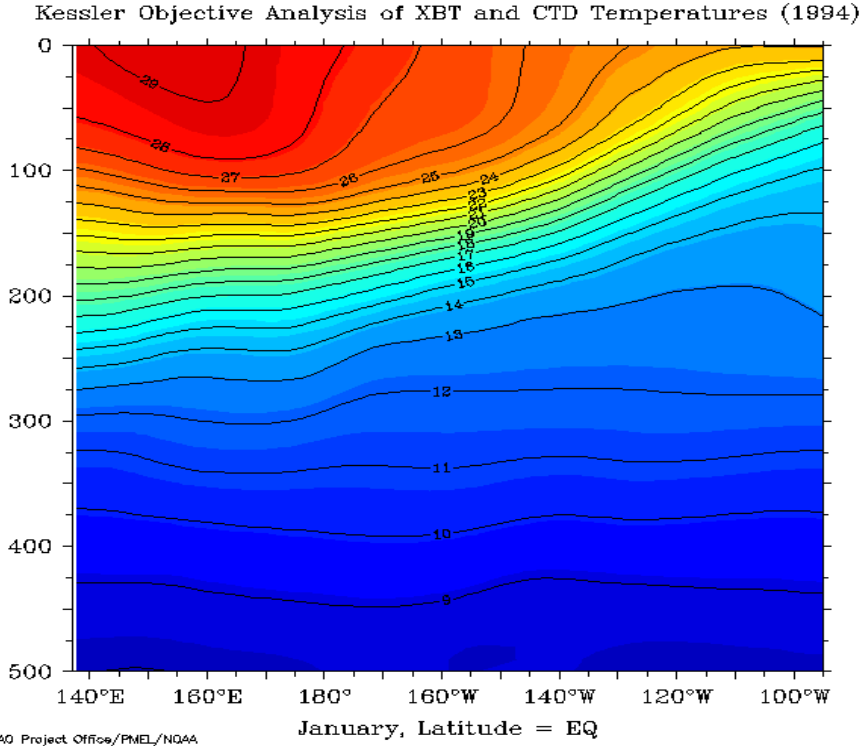


Figure 13: Average January temperature as a function of depths and longitude along the equator. Map from Pacific Marine Environmental Laboratory of NOAA, Seattle.

The response in the central equatorial Pacific is a *weakening* of the trade winds, which is the positive atmospheric feedback, because a initial warm anomaly in the eastern Pacific will cause a response that is strengthening the original SST anomaly (why?). What is the typical period of ENSO? We will try to understand this atmospheric response and the subsequent ocean response in the following subsections from a more theoretical point of view.

6.2 Atmospheric response to SST or heating anomaly

Kelvin and equatorial Rossby-gravity waves are also relevant for shaping the stationary response to an equatorial heating, so-called Gill response (Gill, 1980). In the Gill model a simple parameterization of the effect of heating on divergence, Q , is added to the continuity equation

$$\frac{\partial u'}{\partial t} = -\frac{\partial \Phi'}{\partial x} + \beta y v' \quad (156)$$

$$\frac{\partial v'}{\partial t} = -\frac{\partial \Phi'}{\partial y} - \beta y u' \quad (157)$$

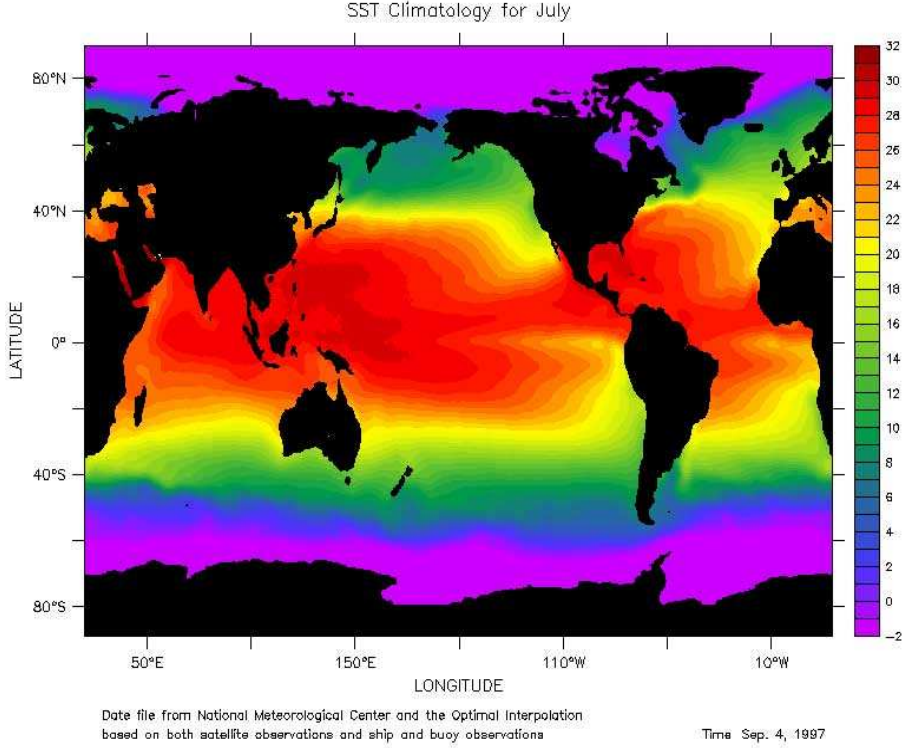


Figure 14: Mean sea-surface temperature calculated from the optimal interpolation technique (Reynolds and Smith, 1995) using ship reports and AVHRR measurements of temperature.

$$\frac{\partial \Phi'}{\partial t} = -gh_e \left(\frac{\partial u'}{\partial x} + \frac{\partial v'}{\partial y} \right) - Q, \quad (158)$$

Finally, rayleigh friction and Newtonian cooling are added to the equations by replacing the time derivatives $\partial/\partial t$ by $\partial/\partial t + \epsilon$, and the equations are solved for a stationary state. The result of the (complicated) computations are illustrated in Fig. 19. To the west of the heating, we find the Rossby-gravity wave-type response, to the east we find the Kelvin wave-type response. Note that the Gill model is used, for example, to explain the atmospheric part of the positive (Bjerknes) feedback that leads to the ENSO phenomenon. Also note that Q has to change sign to explain the upper-level response (upper-level divergence in case of a positive heating! Discuss!).

6.3 Response in the equatorial Ocean

6.3.1 Reduced gravity model

In this subsection we want to derive the equatorial ocean response to an atmospheric forcing of the gill-type. If we consider the mean stratification of the equatorial Pacific

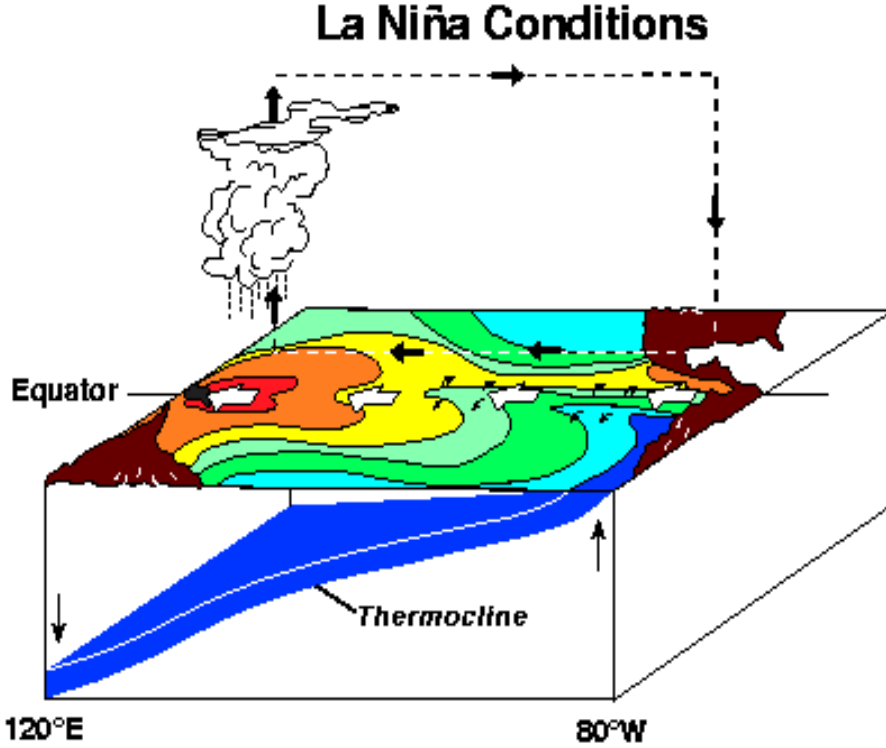


Figure 15: La Niña conditions in the Pacific with strong trade winds (black arrows) pushing surface water toward the west (white arrows) and heavy rain in the west driving the atmospheric circulation (black arrows). Colors give temperature of the ocean surface, red is hottest, blue is coldest. From: NOAA Pacific Marine Environmental Laboratory.

Ocean of Fig. 13, one sees that warm water is residing on top of colder waters, divided by the thermocline. The simplest model of the upper Pacific are assuming therefore that there are 2 layers, divided by a density jump. Let layer 2 be the lower layer of density ρ_2 and height h_2 , and the upper layer be of density ρ_1 and height h_1 . The aim here is to derive the pressure gradient force in the upper layer in this situation. We derive the pressure gradient force by integrating the hydrostatic equation 120 first in layer 2

$$\int_z^{h_2(x,y,t)} \frac{\partial p_2}{\partial z} dz = - \int_z^{h_2(x,y,t)} \rho_2 g dz, \quad \text{or} \quad (159)$$

$$p_2(h_2) - p_2(x, y, z, t) = -\rho_2 g [h_2(x, y, t) - z]. \quad (160)$$

Then we integrate further in layer 1

$$\int_{h_2(x,y,t)}^z \frac{\partial p_1}{\partial z} dz = - \int_{h_2(x,y,t)}^z \rho_1 g dz, \quad \text{or} \quad (161)$$

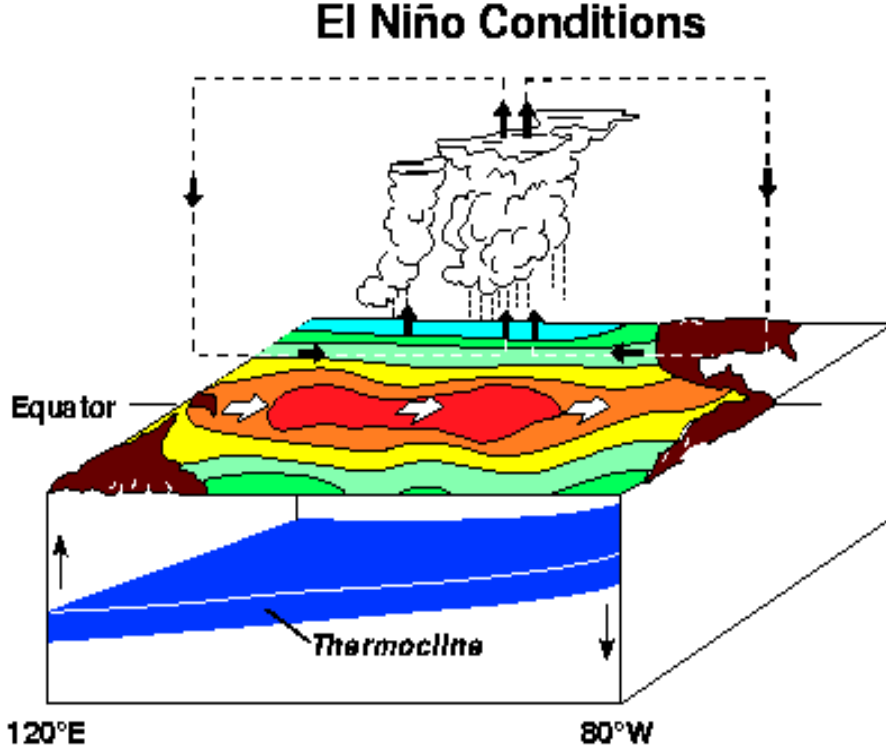


Figure 16: El Nio conditions in the Pacific with weak or reversed trade winds in the west (black arrows) allowing surface water to surge eastward (white arrows) and with heavy rain in the central equatorial Pacific driving the atmospheric circulation (black arrows). Colors give temperature of the ocean surface, red is hottest, blue is coldest. From: NOAA Pacific Marine Environmental Laboratory.

$$p_1(x, y, z, t) - p_1(h_2) = -\rho_1 g [z - h_2(x, y, t)] . \quad (162)$$

Continuity demands that $p_1(h_2) = p_2(h_2)$, therefore inserting 159 into 161 leads to:

$$p_1(x, y, z, t) = p_2(x, y, z, t) - (\rho_2 - \rho_1) g [h_2(x, y, t) - z] . \quad (163)$$

Calculating the horizontal pressure gradient of this leads to:

$$\nabla p_1(x, y, z, t) = \nabla p_2(x, y, z, t) - (\rho_2 - \rho_1) g \nabla h_2(x, y, t) . \quad (164)$$

Assuming the lower layer motionless and without pressure gradient $\nabla p_2(x, y, z, t) = 0$ and $H = h_1 + h_2 = \text{const}$ (rigid lid; an approximation here), and therefore $\nabla h_1 = -\nabla h_2$ we get

$$\nabla p_1(x, y, z, t) = (\rho_2 - \rho_1) g \nabla h_1(x, y, t) , \quad (165)$$

or

$$\frac{1}{\rho_1} \nabla p_1(x, y, z, t) = \frac{\rho_2 - \rho_1}{\rho_1} g \nabla h_1(x, y, t) . \quad (166)$$

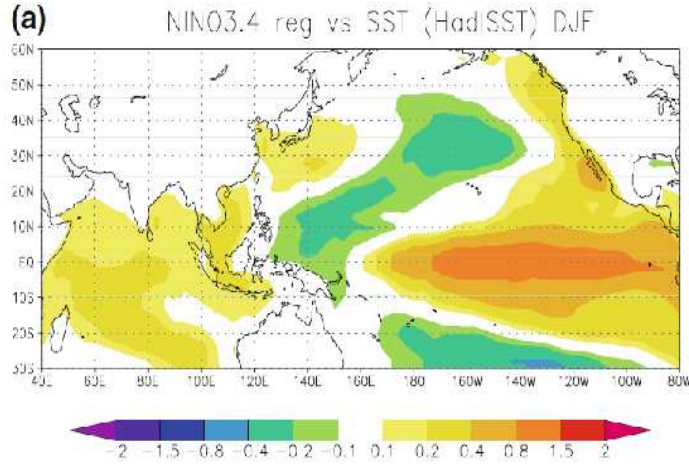


Figure 17: Composite sea surface temperature anomaly for an El Niño condition. Units are K.

The pressure gradient in the upper layer can be, to a first approximation, expressed in terms of the change in density between lower and upper layer and the gradient of the *thermocline depth* h_1 . Since with respect the standard one-layer case the factor g is replaced by $(\rho_2 - \rho_1)/\rho_1 g = g'$, this model is called *reduced gravity model*. The density change $(\rho_2 - \rho_1)/\rho_1$ is typically about 1%. The *reduced gravity model* is identical to the shallow water equations, but with the pressure gradient force 166, because of the slight change of density between the 2 layers. We add a wind-stress forcing on the rhs of the following equations to mimic the ocean forced case. These equations are similar to atmospheric Gill model, but with forcing in the momentum equations instead of in the continuity equation.

$$\frac{\partial u}{\partial t} + (\mathbf{u} \cdot \nabla)u = -g' \frac{\partial h}{\partial x} + fv + \frac{1}{\rho h} \tau_x \quad (167)$$

$$\frac{\partial v}{\partial t} + (\mathbf{u} \cdot \nabla)v = -g' \frac{\partial h}{\partial y} - fu + \frac{1}{\rho h} \tau_y \quad (168)$$

$$\frac{\partial h}{\partial t} + \mathbf{u} \cdot \nabla h = -h \nabla \cdot \mathbf{u} \quad (169)$$

We have used h instead of h_1 for simplicity as the *thermocline depth*, and ρ instead of ρ_1 as density in the upper layer. It is quite instructive to consider the motionless stationary state of such a model (even in a more complex situation this may be a

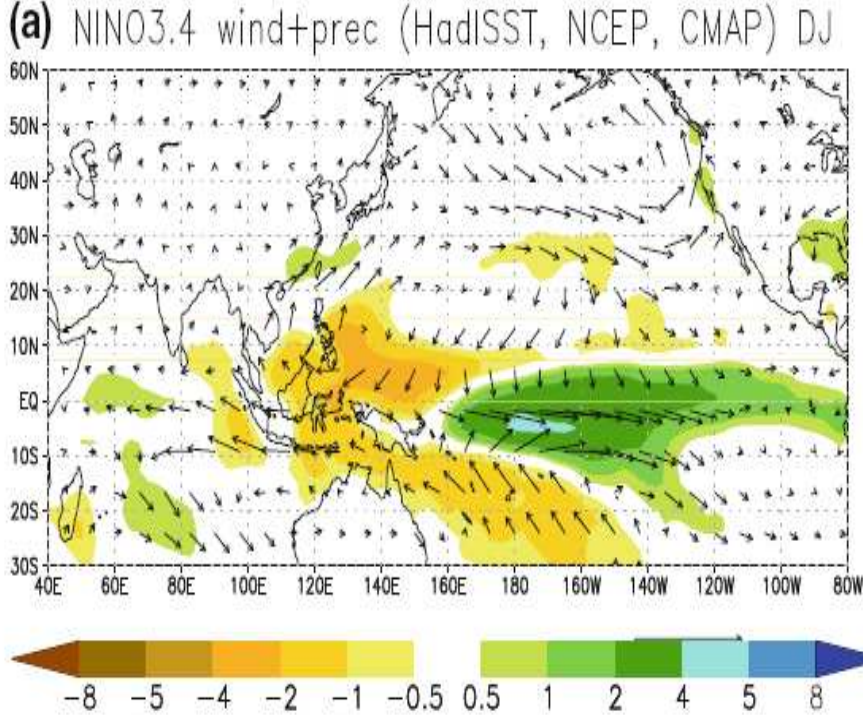


Figure 18: Composite of response to an El Niño forcing. Shading Precipitation in mm/day, vectors 925 hPa wind.

good approximation):

$$\frac{\partial h}{\partial x} = \frac{1}{\rho h g'} \tau_x \quad (170)$$

$$\frac{\partial h}{\partial y} = \frac{1}{\rho h g'} \tau_y \quad , \quad (171)$$

assuming a typical situation in the equatorial Pacific with purely easterly trade winds ($\tau_x < 0$, $\tau_y = 0$) it becomes clear why the equatorial Pacific thermocline is tilted from west to east!!!!

It is interesting to note that the (forcing) free Eq. (167) - (169) are formally identical to the shallow water equations 126, 127 and 131 that we used to derive the equatorial Rossby and Kelvin waves, if we replace g by g' , the reduced gravity. This means that the reduced gravity equations support the same solutions as the shallow water equations near the equator, if we also in all phase velocities replace g by g' . We will see these kind of waves in the following example.

In the following we present and discuss the ocean adjustment to a constant atmospheric wind-stress forcing of the ocean derived from a model similar, but slightly more complicated than Eq. 167 - 169. The addition is basically an equation for the surface temperature that is not present in Eq. 167 - 169. In a strict sense, the surface

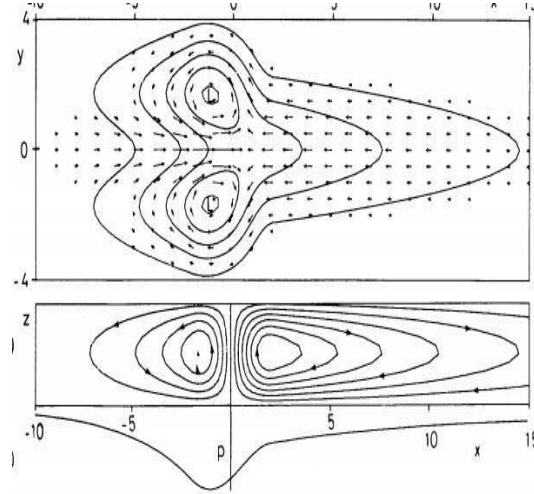


Figure 19: Illustration response to equatorial heating according to the gill model. Equatorial rossby waves shape the response to the west and Kelvin waves shape the response to the east

temperature would never be influenced by the thermocline depth as long as this is positive. However, in the real world, there is a still a gradient present in the upper-layer, meaning that if the thermocline is nearer to the surface, the temperature is lower there, just as seen in Fig. 13. Furthermore, if temperature is allowed to vary horizontally then there will also be horizontal advection of temperature.

6.4 Ocean response to a zonal wind stress anomaly

Fig. 20 shows the wind-stress forcing applied with maximum at equator at 180 E, and a Gaussian shape of with 10 degrees in east-west and 5 degrees in north south direction. The forcing is of magnitude 0.015 N/m^2 , which is a typical response of the atmosphere to a typical ENSO anomaly. This forcing is mimicing the atmospheric Gill-response on the equator to the ENSO-induced heating (SST) anomaly. We are considering the time evolution of the thermocline response to the constant forcing. Fig. 21a shows the response after the first month of forcing, and we see interestingly that the response resembles the Gill response that we discussed for the atmosphere to a diabatic heating anomaly, with an equatorial Kelvin wave to the east of the wind stress forcing and 2 Rossby waves struddeling the equator to the west. The kelvin wave signal moves to the east as time evolves and the Rossby wave signal moves to the west (as they should). The Kelvin waves reach the eastern boundary after about 4 month (Fig. 21b) and appear to transform into coastal Kelvin waves that move north- and soutward from the equator. The maximum response is reached after about 6 month, and is then decaying somewhat. The stationary response is

seen in Fig. 21f. The thermocline tilt in the steady-state solution seems to balance the wind-stress forcing, showing that Eq. 170 are a good approximation.

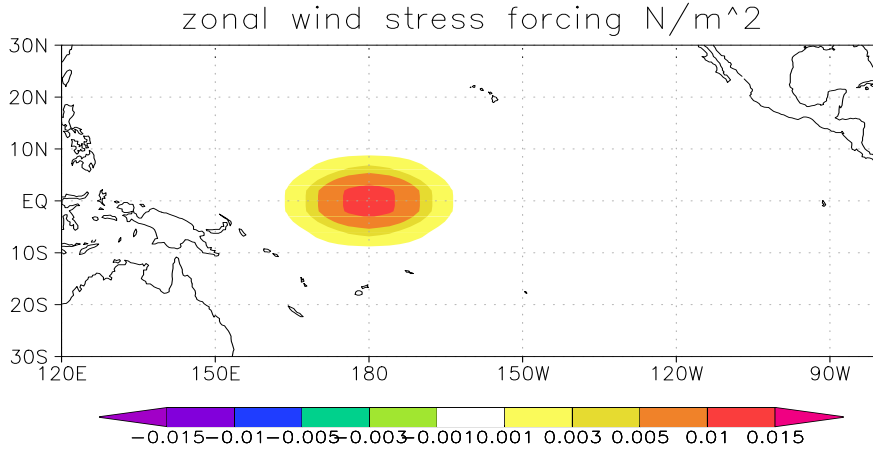


Figure 20: Zonal wind stress forcing. Units are N/m^2 .

Fig. 22 show the corresponding response in sea surface temperatures (using an additional equation not present in Eq. (167) - (169)). Remember that the atmospheric forcing was mimicing the Gill-type response to a warm SST anomaly. From Fig. 22 we clearly identify that the ocean response to the atmospheric forcing provides a positive feedback: The SST in the eastern equatorial Pacific is further increased. The SST response evolves slower than the thermocline response (because the response starts in the central/western Pacific where the thermocline is relatively deep in the mean state and its fluctuations are therefore less coupled to the surface). The maximum positive feedback seems to occur after about 6 to 12 months and it decays to reach an equilibrium. This decay could be interpreted as the delayed negative feedback provided by the ocean to the ENSO phenomenon.

Exercises

1. Assume a mean wind stress distribution along the equator:

$$\begin{aligned}
 \tau_x &= 0 & \text{for } \text{lon} \leq 170 \text{ E} \\
 \tau_x &= -0.06 \text{ N/m}^2 & \text{for } 170 \text{ E} \leq \text{lon} \leq 240 \text{ E} \\
 \tau_x &= 0 & \text{for } \text{lon} \geq 240 \text{ E}
 \end{aligned}
 \tag{172}$$

Using the approximation 170, calculate the thermocline distribution along the equator, assuming that the thermocline depth at the western edge is 150 m. What is the total change in height between 170 E and 240 E?

2. Calculate the oceanic Kelvin wave speed of (using the reduced gravity approximation) of an ocean with a mean thermocline depth of 100 m.

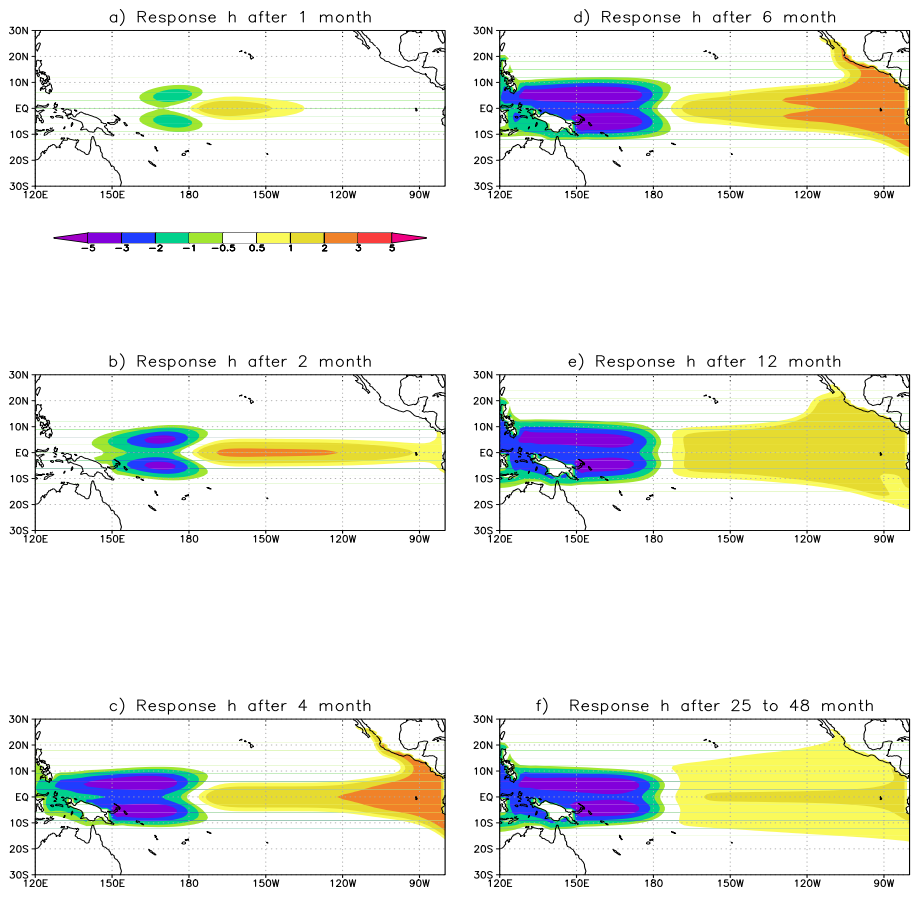


Figure 21: Thermocline response to anomalous zonal wind stress forcing of Fig. 20. a) after 1 month, b) after 2 months, c) after 4 months, d) after 6 months, e) after 12 months. f) stationary response. Units are m.

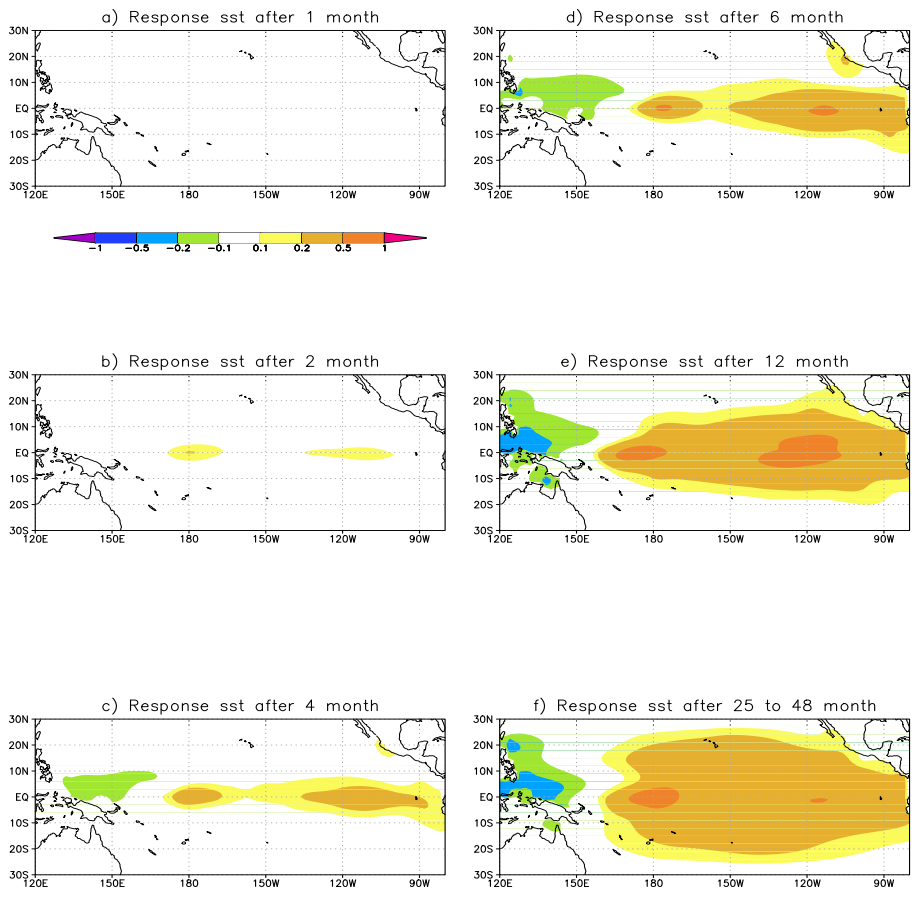


Figure 22: SST response to anomalous zonal wind stress forcing of Fig. 20. a) after 1 month, b) after 2 months, c) after 4 months, d) after 6 months, e) after 12 months. f) stationary response. Units are K.

7 (Atmospheric) Planetary Boundary Layer Processes

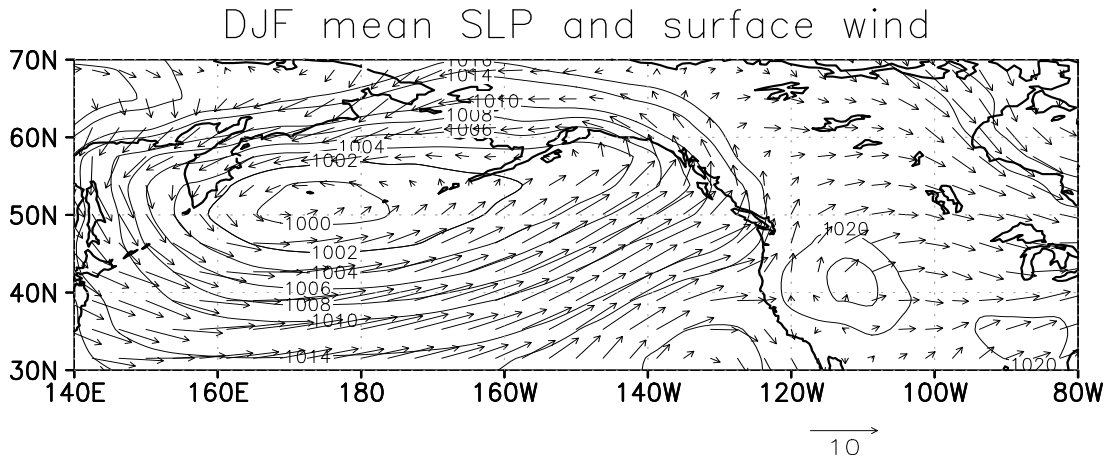


Figure 23: Mean DJF Sea Level Pressure (SLP) and surface winds in the North Pacific from observations (NCEP-NCAR re-analysis). Units are m/s for wind and hpa for SLP.

Figure 24 shows the winter mean (DJF) climatology of Sea Level Pressure (SLP) and surface winds in the North Pacific. As we expect for geostrophy, winds are mainly parallel to the isobars (lines of constant pressure). However, there seems to be a systematic tendency for a component of the winds towards the low pressure. In this section we will try to understand this systematic departure from geostrophy. Do you have a guess why this departure exists?

So far we have ignored the effect of friction on the flows. However, in order to understand climate dynamics it is important to consider the effects of friction, particularly the one provided by the *planetary boundary layer*, which covers roughly the lowest kilometer(s) of the atmosphere. The boundary layer frictional processes are ultimately induced by the molecular viscosity. However, this effect is only relevant in the few millimeters closest to the surface. In the largest part of the planetary boundary layer turbulent eddies take over the role of molecular friction. This is part of the *energy cascade*, meaning that in the large-scale flow ever smaller eddies are embedded that carry energy to ever smaller scales until finally molecular viscosity takes over. As for all sections, a whole lecture course could be devoted to this topic. Therefore we will concentrate on the features that are most relevant and essential to understand climate dynamics.

7.1 The Boussinesq Approximation

The density in the lowest part of the Atmosphere varies little (about 10 % of its mean value). The flow may be considered as essentially incompressible if only the

momentum equation is considered. Therefore, for simplicity we assume the density to be constant. Let us consider therefore horizontal momentum equations 118 and 119, in which ρ is considered to be a constant

$$\frac{du}{dt} = -\frac{1}{\rho} \frac{\partial p}{\partial x} + fv \quad (173)$$

$$\frac{dv}{dt} = -\frac{1}{\rho} \frac{\partial p}{\partial y} - fu . \quad (174)$$

and the continuity equation for incompressible flows 128

$$\frac{\partial u}{\partial x} + \frac{\partial v}{\partial y} + \frac{\partial w}{\partial z} = 0 . \quad (175)$$

This set of equations is equivalent to the barotropic shallow water equations introduced and used several times already. However, the *Boussinesq approximation* goes beyond this, because it also involves an approximation to the vertical momentum equation that is different from the hydrostatic equation and allows for buoyancy effects there. Here we do not need to consider this equation.

7.2 Reynolds Averaging

In order to simulate the effect of the smaller scale eddies on the larger scale (“resolved”) flow, is it useful to apply an averaging operator to the equations. The idea is that the total flow can be divided into a slow evolving large scale field and into small-scale eddy fluctuations

$$u = \bar{u} + u', \quad v = \bar{v} + v' . \quad (176)$$

Formally, the operator could be a temporal and/or spatial average. For the total derivative of a quantity A

$$\frac{dA}{dt} = \left(\frac{\partial}{\partial t} + u \frac{\partial}{\partial x} + v \frac{\partial}{\partial y} + w \frac{\partial}{\partial z} \right) A + A \left(\frac{\partial u}{\partial x} + \frac{\partial v}{\partial y} + \frac{\partial w}{\partial z} \right) , \quad (177)$$

where we have added a zero according to the incompressibility condition 175. Therefore we may write the total derivative (for incompressible flow!) as

$$\frac{dA}{dt} = \left(\frac{\partial A}{\partial t} + \frac{\partial Au}{\partial x} + \frac{\partial Av}{\partial y} + \frac{\partial Aw}{\partial z} \right) , \quad (178)$$

Application of the averaging operator yields

$$\frac{d\bar{A}}{dt} = \left(\frac{\partial \bar{A}}{\partial t} + \frac{\partial(\bar{A}\bar{u} + \overline{A'u'})}{\partial x} + \frac{\partial(\bar{A}\bar{v} + \overline{A'v'})}{\partial y} + \frac{\partial(\bar{A}\bar{w} + \overline{A'w'})}{\partial z} \right) , \quad (179)$$

because

$$\overline{ab} = \overline{(\bar{a} + a')(\bar{b} + b')} = \overline{\bar{a}\bar{b}} + \overline{\bar{a}b'} + \overline{a'\bar{b}} + \overline{a'b'} = \overline{\bar{a}\bar{b}} + \overline{a'b'} ,$$

and $\overline{a'} = \overline{b'} = 0$. Therefore application of the averaging operator to Eqs. 173 and 174 yields

$$\frac{\overline{du}}{dt} = -\frac{1}{\rho} \frac{\partial \overline{p}}{\partial x} + f\overline{v} - \frac{\overline{\partial u' u'}}{\partial x} - \frac{\overline{\partial u' v'}}{\partial y} - \frac{\overline{\partial u' w'}}{\partial z} \quad (180)$$

$$\frac{\overline{dv}}{dt} = -\frac{1}{\rho} \frac{\partial \overline{p}}{\partial y} - f\overline{u} - \frac{\overline{\partial v' u'}}{\partial x} - \frac{\overline{\partial v' v'}}{\partial y} - \frac{\overline{\partial v' w'}}{\partial z}, \quad (181)$$

where

$$\frac{\overline{d}}{dt} = \frac{\partial}{\partial t} + \overline{u} \frac{\partial}{\partial x} + \overline{v} \frac{\partial}{\partial y} + \overline{w} \frac{\partial}{\partial z} \quad (182)$$

is the rate of change following the large-scale (or resolved) flow. Applying the zonal average to the continuity equation leads to

$$\frac{\partial \overline{u}}{\partial x} + \frac{\partial \overline{v}}{\partial y} + \frac{\partial \overline{w}}{\partial z} = 0 \quad . \quad (183)$$

If we compare Eqs. 180 and 181 with 174 and 174 we see that extra terms emerge if we follow a particle with the average large-scale flow. These can be interpreted as the effects of the small-scale eddies on the large-scale flow, and are called *convergence of eddy momentum fluxes*. Obviously, in order to solve Eqs. 180 and 181 for the large-scale flow, the additional terms have to be *parameterized* in terms of mean flow properties. This is big topic in fluid dynamics, and is called *closure problem*. Note that a very similar problem occurs when we write down the Navier-Stokes equations for numerical models which intrinsically have a grid (and time) spacing. Turbulence theories give some clues how such parameterizations should look like. One of the simplest one is the *flux-gradient theory*, which states that the effect of small-scale eddies on the large-scale flow is similar to the effect of molecular viscosity on smaller scale flow. The effect of viscosity on the small scale flow is to bring the flow into equilibrium, that is to reduce contrasts or gradient. Also note that the geometry (horizontal surface) means that changes in the vertical direction are much larger than in the horizontal direction (horizontal homogeneity). We have parametrizations of the type:

$$\overline{u'w'} = -K_m \frac{\partial \overline{u}}{\partial z} \quad (184)$$

$$\overline{v'w'} = -K_m \frac{\partial \overline{v}}{\partial z}, \quad (185)$$

where K_m can be a function of the vertical coordinate z . All other momentum fluxes can be approximated to be close to zero in Eqs. 180 and 181.

7.3 The Ekman Layer

The Ekman layer is the layer that connects a layer very close to the surface to the free atmosphere where we have near geostrophic equilibrium. Using the geostrophic

wind (note that we can consider for the current analysis $f = f_0 = \text{const}$)

$$u_g = -\frac{1}{f\rho} \frac{\partial p}{\partial y}, v_g = \frac{1}{f\rho} \frac{\partial p}{\partial x},$$

with this and Eqs. 184-185, the stationary (equilibrium) approximation to Eqs. 180 and 181 are

$$K_m \frac{\partial^2 u}{\partial z^2} + f(v - v_g) = 0 \quad (186)$$

$$K_m \frac{\partial^2 v}{\partial z^2} - f(u - u_g) = 0, \quad (187)$$

where we have dropped the overbar for average quantities for convenience (only average quantities appear). Note that also the mean vertical advection term has been dropped because of smallness compared to the other terms. The horizontal advection terms are dropped because of the horizontal homogeneity condition. If we assume $u_g = \text{const.}$, and $v_g = \text{const.}$ with height, then we can substitute $u_* = u - u_g$ and $v_* = v - v_g$. to get a system of the type

$$K_m \frac{\partial^2}{\partial z^2} \begin{pmatrix} u_* \\ v_* \end{pmatrix} + \begin{pmatrix} 0 & f \\ -f & 0 \end{pmatrix} \begin{pmatrix} u_* \\ v_* \end{pmatrix} = 0 \quad . \quad (188)$$

We assume a solution of the type $u_* = Ae^{imz}$, $v_* = Be^{imz}$, then it follows

$$\begin{pmatrix} -K_m m^2 & f \\ -f & -K_m m^2 \end{pmatrix} \begin{pmatrix} A \\ B \end{pmatrix} = 0 \quad . \quad (189)$$

Following basic algebra, non-trivial solutions of such a linear are found by setting the determinant of the 2x2 matrix to zero

$$K_m^2 m^4 + f^2 = 0. \quad (190)$$

The four solutions are for positive f (northern hemisphere; otherwise we have to use negative f for southern hemisphere)

$$m_1 = \sqrt{i} \sqrt{\frac{f}{k_m}}, m_2 = -\sqrt{i} \sqrt{\frac{f}{k_m}}, m_3 = \sqrt{-i} \sqrt{\frac{f}{k_m}}, m_4 = -\sqrt{-i} \sqrt{\frac{f}{k_m}}. \quad (191)$$

With $\sqrt{i} = (1+i)/\sqrt{2}$, we have

$$m_1 = (1+i) \sqrt{\frac{f}{2k_m}}, m_2 = -(1+i) \sqrt{\frac{f}{2k_m}}, m_3 = (i-1) \sqrt{\frac{f}{2k_m}}, m_4 = (1-i) \sqrt{\frac{f}{2k_m}}. \quad (192)$$

The boundary conditions are geostrophy ($u = u_g$, $v = v_g$) as z goes to infinity, therefore $u_* = v_* = 0$ and $u = v = 0$ or $v_* = -v_g$, $u_* = -u_g$ at $z=0$. The boundary condition as z goes to infinity excludes solutions that grow, therefore the solutions

with negative i (m_2 and m_4) are excluded. If we insert the solutions m_1 and m_3 back into the original system 189, we can determine the two eigenvectors, which are

$$\mathbf{x}_1 = \begin{pmatrix} 1 \\ i \end{pmatrix}$$

and

$$\mathbf{x}_3 = \begin{pmatrix} 1 \\ -i \end{pmatrix}$$

The two eigenvectors are complex conjugate and therefore not independent. Therefore the solution simply given by m_1 ,

$$u_* = ae^{im_1 z} = a[\cos(\gamma z) + i \sin(\gamma z)]e^{-\gamma z} \quad (193)$$

$$v_* = iae^{im_1 z} = ia[\cos(\gamma z) + i \sin(\gamma z)]e^{-\gamma z}, \quad (194)$$

where we have used $\gamma = \sqrt{f/(2K_m)}$. Let $a = b + ic$, then the real part of the solution is

$$u_* = b \cos(\gamma z)e^{-\gamma z} - c \sin(\gamma z)e^{-\gamma z} \quad (195)$$

$$v_* = -b \sin(\gamma z)e^{-\gamma z} - c \cos(\gamma z)e^{-\gamma z} \quad (196)$$

and with $z = 0$: $u_*(z = 0) = -u_g = b$, $v_*(z = 0) = -v_g = -c$ or

$$u = u_g - [u_g \cos(\gamma z) + v_g \sin(\gamma z)]e^{-\gamma z} \quad (197)$$

$$v = v_g + [u_g \sin(\gamma z) - v_g \cos(\gamma z)]e^{-\gamma z}, \quad (198)$$

The height of the boundary layer may be defined where the wind is for the first time parallel to the geostrophic wind, which is at $De = \pi/\gamma = \pi\sqrt{2K_m/f}$. We can use this formula to estimate the value of the eddy viscosity K_m . Observations of the mean boundary layer height in mid-latitudes give $De \approx 1$ km, therefore $K_m = 1/2f(De/\pi)^2 \approx 5 \text{ m}^2 \text{ s}^{-1}$. An important application of the Ekman solutions 197 and 198 is that we can calculate the vertical velocity at the top of the Ekman Layer induced by the action of turbulent eddies.

Let us calculate the divergence of the of the winds in the Ekman Layer

$$\begin{aligned} \frac{\partial u}{\partial x} + \frac{\partial v}{\partial y} &= \left(\frac{\partial u_g}{\partial x} + \frac{\partial v_g}{\partial y} \right) (1 - \cos(\gamma z)e^{-\gamma z}) \\ &\quad - \left(\frac{\partial v_g}{\partial x} - \frac{\partial u_g}{\partial y} \right) \sin(\gamma z)e^{-\gamma z} \\ &= -\xi_g \sin(\gamma z)e^{-\gamma z}. \end{aligned} \quad (199)$$

This equation states that the divergence in the Ekman layer is proportional to the negative geostrophic vorticity, a very important effect of the boundary layer. Positive

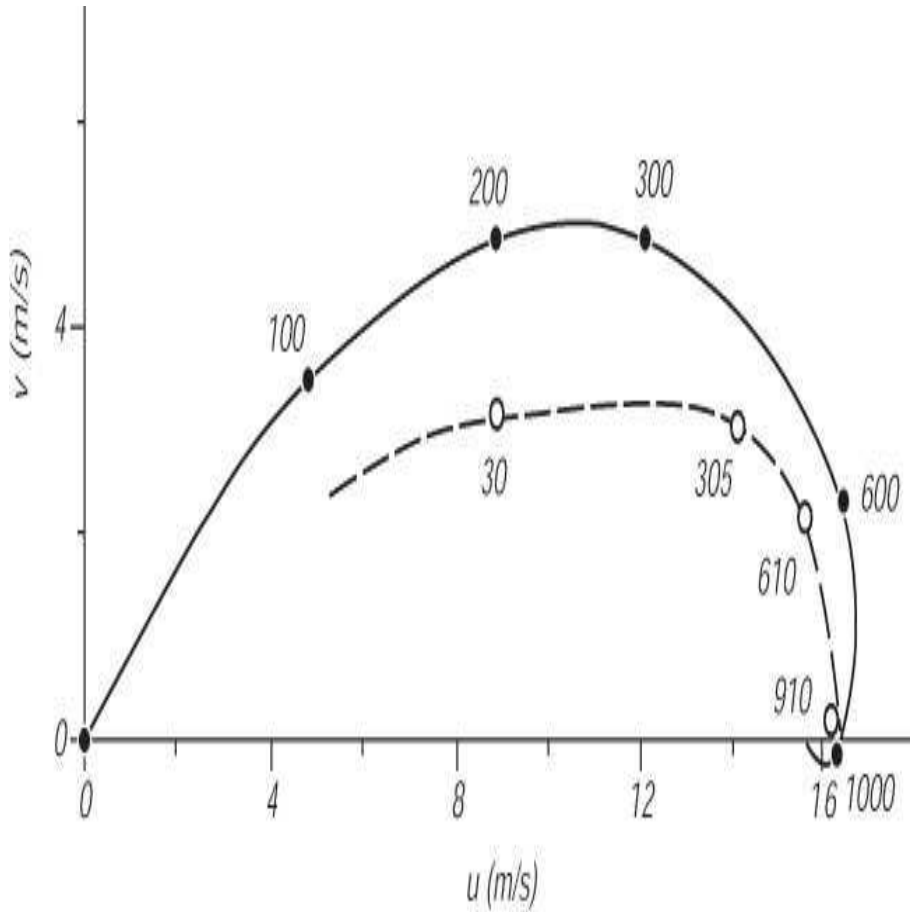


Figure 24: Idealized and observed Ekman Layer velocities Source: http://oceanworld.tamu.edu/resources/ocng_textbook/chapter09/chapter09_02.htm.

(cyclonic vorticity) leads to convergence! According to the continuity equation 175, this will lead to vertical motion, which is on top of the Ekman Layer

$$\begin{aligned}
 w(De) &= - \int_0^{De} \left(\frac{\partial u}{\partial x} + \frac{\partial v}{\partial y} \right) dz & (200) \\
 &= \xi_g \frac{e^{-\gamma z}}{2\gamma} [\sin(\gamma z) - \cos(\gamma z)] \Big|_0^{De} \\
 &= \frac{\xi_g}{2\gamma} (1 + e^{-\pi}) \\
 &\approx \frac{\xi_g}{2\gamma} = \xi_g \sqrt{\frac{K_m}{2f}},
 \end{aligned}$$

where we have assumed that the geostrophic wind is independent of height within the Ekman Layer. This is again an important result, a positive vorticity leads

to upward motion through Ekman effects on top of the boundary layer. This is called *boundary layer pumping* or *Ekman pumping*. It may be used to explain vertical motions and therefore rainfall anomalies induced by the Gill responses in tropical regions as derived in Section 6.2. It states that whenever we calculate a flow response that has (geostrophic) vorticity, this will lead to vertical motion and therefore a rainfall response. Given that geostrophy is valid from approximately 10 degrees away from the equator, this rule can be used for many flow responses. Remember that we have shown in chapter 5 that even the zonal winds in the close equatorial Kelvin waves are in exact geostrophic equilibrium. We can estimate the typical magnitude of the vertical velocity 200 by inserting $\xi_g = 10^{-5} \text{s}^{-1}$, $De = 1 \text{km}$ or $\gamma = 3 \times 10^{-3} \text{m}^{-1}$ to be $w(De) \approx 10^{-5}/(2 \times 3 \times 10^{-3}) \text{m s}^{-1}$ or $2 \times 10^{-3} \text{m s}^{-1}$. This a substantial vertical velocity, comparable to the one induced by a heating anomaly of about Q/c_p 1 k/day in the tropical regions, if we use equation 37 and $S_p \approx 5 \times 10^{-4} \text{K Pa}^{-1}$ to estimate the vertical velocity:

$$-S_p \omega \approx S_p \rho g w \approx \frac{Q}{c_p}$$

or

$$w \approx \frac{Q}{c_p} \frac{1}{S_p \rho g} .$$

Also in the Ocean Ekman Layers exist (have you discussed them?). Clearly at the bottom of the ocean very similar processes take place as discussed here. Even at the top of the oceans we have an Ekman Layer (have you discussed this?). However, the main change is the boundary condition at the surface, which is given by the atmospheric winds that drive the ocean, in the interior the boundary condition can be assumed to be geostrophic again. Otherwise we can use the above derived methodology also to derive the ocean surface Ekman Layer.

Exercises

1. Verify that the Ekman solution 197 and 198 is indeed a solution of the original system of equations 186 and 186.
2. Calculate the scalar product between the pressure gradient and the wind within the Ekman layer given by Eqs. 197 and 198. Is the wind directed into or out of a low pressure system?
3. Write a fortran code that uses the Eqs. 197 and 198 and plot the solution as a phase space diagram (u,v) as in Fig 24. Also, solve the original equations 186 and 187 numerically by keeping the local time derivative in the Ekman equations:

$$\frac{\partial u}{\partial t} = K_m \frac{\partial^2 u}{\partial z^2} + f(v - v_g) \quad (201)$$

$$\frac{\partial v}{\partial t} = K_m \frac{\partial^2 v}{\partial z^2} - f(u - u_g) . \quad (202)$$

For both analytical and numerical solutions use $K_m = 5 \text{ m}^2 \text{ s}^{-1}$, the coriolis parameter at $45^\circ N$, $u_g = 10 \text{ m s}^{-1}$, $v_g = 0$. The vertical domain should be $[0 \text{ m}, 3000 \text{ m}]$. Use as initial condition $u = u_g, v = 0$. Compare the numerical stationary with the analytical solution. How long does it take for the solution to become approximately stationary?

8 The general circulation

The *general circulation* of the atmosphere is usually considered to include the totality of motions that characterize the global-scale atmospheric flow. Climate dynamics is one of the main topics of the study of the general circulation. Here we are interested in the temporally (i.e. monthly) averaged fields of wind, temperature, humidity, precipitation, and other meteorological variables and their long-term variations (also called *low-frequency variability*). For example, monsoon systems are a very important feature of the general circulation. For example, on the web-page http://users.ictp.it/~kucharsk/speedy8_clim.html we find some features relevant to the general circulation.

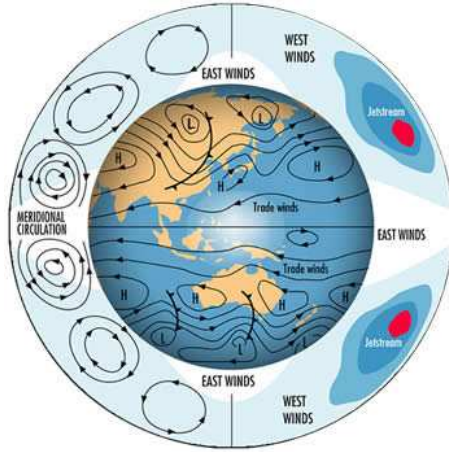


Figure 25: Schematic of some features of the general circulation.

8.1 Zonally averaged circulation

The aim of this section is to analyse the zonal mean circulation. The basis for the following analysis are the thermo-hydrodynamic equations in pressure coordinates Eqs. (26, 27, 34 and 37)

We apply in the following an averaging operator to these equations

$$\bar{A} \equiv \frac{1}{2\pi r \cos\phi} \int_0^{2\pi} A r \cos\phi d\lambda \quad . \quad (203)$$

All quantities are then expressed as the zonal mean plus a deviation from the zonal mean $A = \bar{A} + A'$ (see Figure 6).

For the total derivative of a quantity A

$$\frac{dA}{dt} = \left(\frac{\partial}{\partial t} + u \frac{\partial}{\partial x} + v \frac{\partial}{\partial y} + \omega \frac{\partial}{\partial p} \right) A + A \left(\frac{\partial u}{\partial x} + \frac{\partial v}{\partial y} + \frac{\partial \omega}{\partial p} \right) , \quad (204)$$

where we added zero on the rhs according to the continuity equation. Therefore we may write the total derivative (in pressure coordinates!) as

$$\frac{dA}{dt} = \left(\frac{\partial A}{\partial t} + \frac{\partial Au}{\partial x} + \frac{\partial Av}{\partial y} + \frac{\partial A\omega}{\partial p} \right), \quad (205)$$

Application of the zonal operator (203) yields (as in section 7)

$$\frac{\overline{dA}}{dt} = \left(\frac{\partial \overline{A}}{\partial t} + \frac{\partial(\overline{A}\overline{v} + \overline{A'v'})}{\partial y} + \frac{\partial(\overline{A}\overline{\omega} + \overline{A'\omega'})}{\partial p} \right), \quad (206)$$

because $\overline{\partial(\cdot)\partial x} = 0$ and

$$\overline{ab} = \overline{(\overline{a} + a')(\overline{b} + b')} = \overline{a\overline{b}} + \overline{a'b'} + \overline{a'\overline{b}} + \overline{a\overline{b}'} = \overline{a\overline{b}} + \overline{a'b'} ,$$

because the quantities $\overline{(\cdot)}$ are independent of x and $\overline{a'} = \overline{b'} = 0$. Applying the zonal average to the continuity equation leads to

$$\frac{\partial \overline{v}}{\partial y} + \frac{\partial \overline{\omega}}{\partial p} = 0 \quad . \quad (207)$$

Note that with Eq. 207 we can define a streamfunction:

$$\Psi = \int_0^p \overline{v} dp \quad , \quad (208)$$

so that

$$\overline{v} = \frac{\partial \Psi}{\partial p} \quad ; \quad \overline{\omega} = -\frac{\partial \Psi}{\partial y} \quad . \quad (209)$$

To show 209 will be an Exercise! From Eq. (206) we can also derive

$$\frac{\overline{dA}}{dt} = \frac{\overline{d}}{dt} \overline{A} + \frac{\partial \overline{A'v'}}{\partial y} + \frac{\partial \overline{A'\omega'}}{\partial p}, \quad (210)$$

where

$$\frac{\overline{d}}{dt} = \frac{\partial}{\partial t} + \overline{v} \frac{\partial}{\partial y} + \overline{\omega} \frac{\partial}{\partial p} \quad (211)$$

is the rate of change following the mean motion. Averaging the zonal component of the momentum equation 26 and the thermodynamic equation 37 leads to

$$\frac{\partial \overline{u}}{\partial t} - f_0 \overline{v} = -\frac{\partial \overline{u'v'}}{\partial y} \quad (212)$$

$$\frac{\partial \overline{T}}{\partial t} - S_p \overline{\omega} = -\frac{\partial \overline{v'T'}}{\partial y} + \frac{\overline{Q}}{c_p} \quad (213)$$

Here several further approximations have been introduced which are all consistent with quasi-geostrophic scaling. A similar scaling shows that the meridional momentum equation is in quasi-geostrophic balance. For the zonal averaged meridional momentum equation, the first order geostrophic approximated balance is

$$f_0 \bar{u} = -\frac{\partial \bar{\Phi}}{\partial y} \quad . \quad (214)$$

Together with the zonal average of the hydrostatic equation 27 this leads to the thermal wind equation for zonal averaged motion

$$\frac{\partial \bar{u}}{\partial p} = \frac{R}{f_0 p} \frac{\partial \bar{T}}{\partial y} \quad . \quad (215)$$

This equation is similar to equation (41), but for zonal averages. Equations (212) and (213) tell us that in order to get a steady-state meridional, vertical circulation cell $(\bar{v}, \bar{\omega})$ we must have the balances

Coriolis force $f_0 \bar{v} \approx$ divergence of eddy momentum fluxes

Adiabatic cooling \approx diabatic heating plus convergence of eddy heat fluxes

Also note that any \bar{v} and $\bar{\omega}$ separately induces the other due to continuity 207.

Analysis of observations shows that outside the tropics these balances appear to be approximately true above the boundary layer. Close to the equator we have that the heating is mainly balanced by mean vertical motion, driving the *Hadley Cell*, whereas in the extratropics the meridional, vertical circulations are mainly driven by the convergence of eddy momentum and eddy heat fluxes. These cells are called *Ferrell Cells*.

Exercises

1. Show that with the streamfunction definition Eq. 208, the relationships 209 are fulfilled.

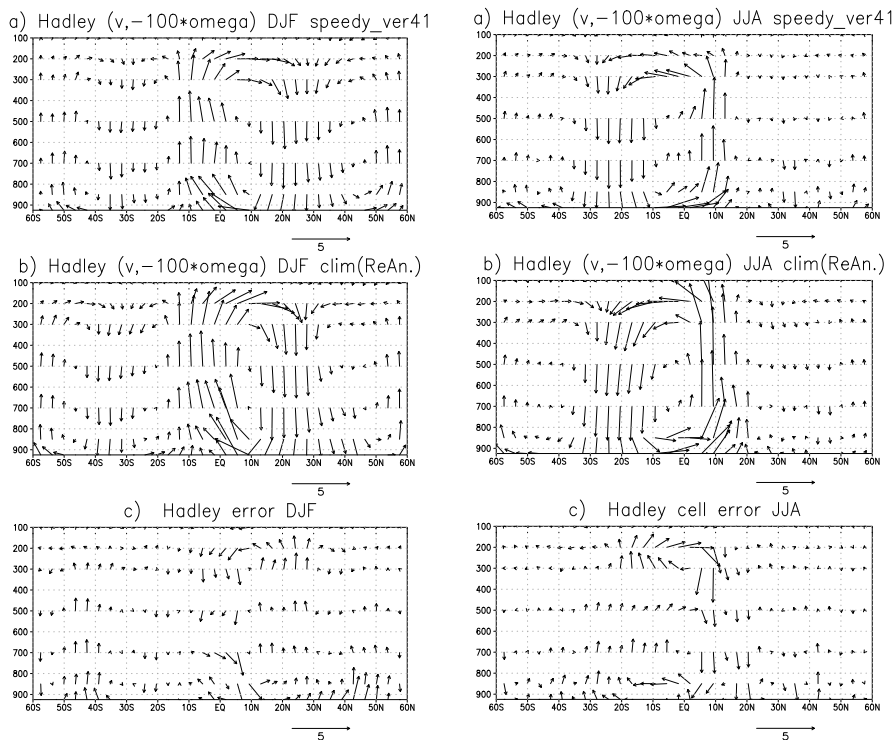


Figure 26: Illustration of the Hadley cell by a $(\bar{v}, -\omega)$ vector plot. left panel: Boreal winter, right panel: boreal summer.

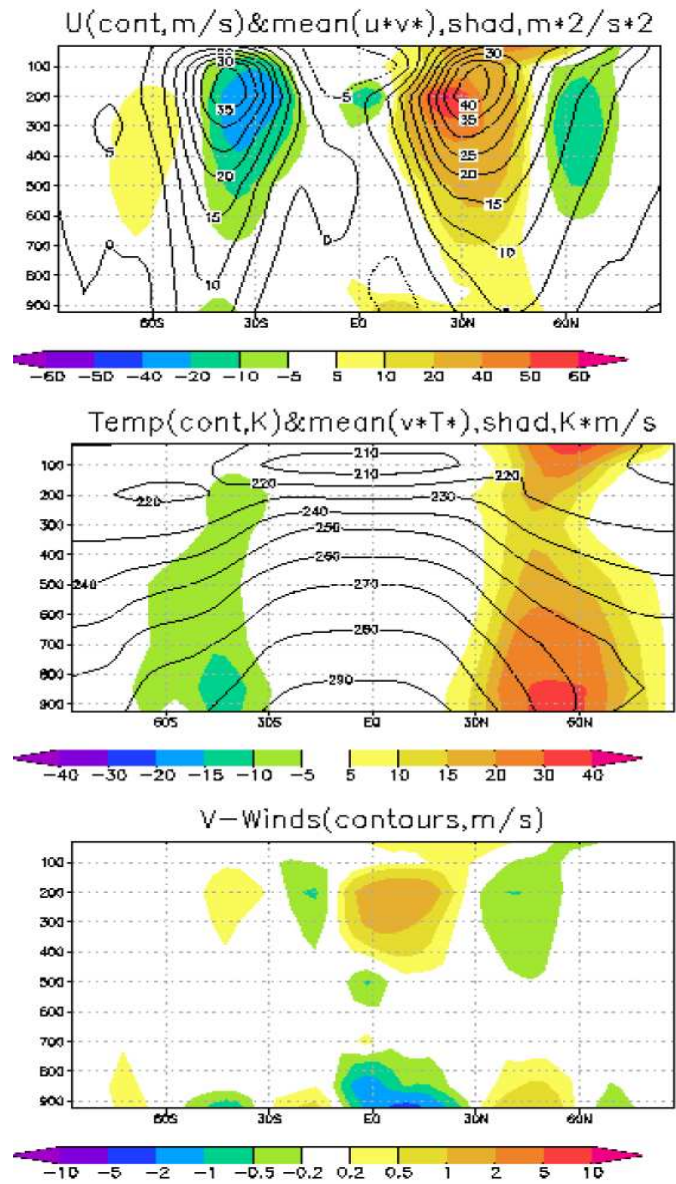


Figure 27: Upper panel: \bar{u} (contours), and $\overline{u'v'}$, middle panel: \bar{T} (contour) and $\overline{v'T'}$, lower panel $\overline{v'v'}$.

9 Tropical zonal and meridional circulations

More reading:

1. Rodwell MJ, Hoskins BJ (2001) Subtropical Anticyclones and Summer Monsoons. *J Clim*, **14**, 31923211
2. Chao WC, Chen B (2001) The origin of Monsoons. *J Atmos Sci*, **58**, 3497350
3. Kucharski, F, Bracco, A, Barimalala, R, Yoo, J-H (2011) Contribution of the eastwest thermal heating contrast to the South Asian Monsoon and consequences for its variability, *Clim Dyn*, **37**, 721735, DOI 10.1007/s00382-010-0858-3

Let's have a look at the global June-to-September rainfall distribution in Fig. 28. We can clearly identify the Intertropical Convergence Zone (ITCZ), identified by the rainfall maximum north of the equator that can reach 30°N in some land region. We also see that this strip of large rainfall is not zonally homogeneous, but is stronger in some locations than in others. Some of the features may be explained by the distributions of sea surface temperatures (SSTs) in 29.

The western Pacific rainfall maximum is related to high SSTs in that region, as we have already discussed several times. Also, the land-sea contrast are likely important due to different heat capacities. As we have already discussed regarding the ENSO phenomenon, the distribution of SSTs, rainfall and atmospheric circulations in the tropical Pacific provide positive feedbacks between them, so that it's difficult to say what is cause and what is effect (chicken-egg problem). The mean zonal circulation in the tropical regions is called *Walker circulation* (see also Fig. 15). Note that this circulation is not a strict closed circulation cell as we could derive for the zonal mean circulation (Hadley Cell). A good measure of this zonal tropical circulation is the upper-level *velocity potential*, χ , for which we have the relation to the divergent wind

$$\mathbf{v}_\chi = \nabla\chi \quad (216)$$

The distribution of the 200 hpa velocity potential χ is shown in Fig. 30a (which height is this, approximately). According to the definition 216, a minimum means divergent wind. The centre of upper-level divergence (rising motion, why?) is in the western Pacific region, and the centers of upper-level convergence (sinking motion, why?) are located in the eastern Pacific (that is the classical Walker circulation) and in the tropical South Atlantic region.

Fig. 30 b) shows the *streamfunction*, ψ , which is related to the rotational flow in the following way (see, e.g. Eq. 16)

$$\mathbf{v}_\psi = \mathbf{k} \times \nabla\psi \quad . \quad (217)$$

It is clear that there is a systematic relationship between upper-level velocity potential and upper-level streamfunction, they are in 'quadrature', that is the extreme values of one lie in the gradient regions of the other. Can we propose an explanation

for this behaviour? The solution is an approximate version of the vorticity equation 55 for the tropics

$$\frac{d_g \xi_g}{dt} = -f_0 \left(\frac{\partial u_a}{\partial x} + \frac{\partial v_a}{\partial y} \right) - \beta v_g \quad . \quad (218)$$

It turns out that in the tropical regions relative vorticity changes and advections are relatively small, mainly because of approximate geostrophy and small pressure gradients. We may estimate it to be one order of magnitude smaller than in the extratropics. Therefore, the left hand side of Eq. 218 may be set to zero. This leaves us with the approximation

$$\beta v_\psi = -f_0 \left(\frac{\partial u_\chi}{\partial x} + \frac{\partial v_\chi}{\partial y} \right) \quad , \quad (219)$$

where we have used that the geostrophic wind is the rotational wind defined in Eq. 217, and the ageostrophic wind is the divergent wind defined in Eq. 216. Eq. 219 is called *Sverdrup balance*. If we take a divergence field as given (e.g. the field that corresponds to Fig. 30a; we can imagine it has been caused by the dominance of the west Pacific heating), then according to the Sverdrup balance, this will cause rotational winds. An upper level divergence maximum will lead to southward rotational motion in the northern hemisphere, an upper-level convergence maximum will lead to northward rotational motion. This is consistent with the streamfunction distribution in Fig. 30b, and explains why velocity potential and streamfunction are in quadrature (exercise!). Note that the interpretation of the Asian monsoon high to be partially forced by Sverdrup balance from the heating differences between the western Pacific and the Atlantic Ocean is a relatively new one. The conventional point of view is that the Asian monsoon high (*Tibetan high*) is forced exclusively by the land sea contrast between the Asian land mass (including importance of Himalayas) and the Indian Ocean. We also note that all the structures that we have considered for upper levels should be reversed for low levels, thus a part of the low-level monsoon trough can be attributed to the western Pacific/Atlantic heating differences. Keep in mind that secondary vertical motions can be induced then by surface friction, because the streamfunction centres that we can derive are fields with vorticity, which according to equation 200 induces vertical motion. Positive (negative) vertical motion, in turn, leads to increased (decreased) rainfall (why?). These effects have been analysed with idealized numerical experiments in the paper cited in the beginning of the section (see also Figs. 31, 32, 33).

Exercises

1. Let the velocity potential distribution in zonal direction at latitude 30°N be

$$\chi = A \cos(\lambda) \quad ,$$

where λ is longitude. Calculate using the Sverdrup balance 219 to derive the zonal distribution of the streamfunction at the same latitude.

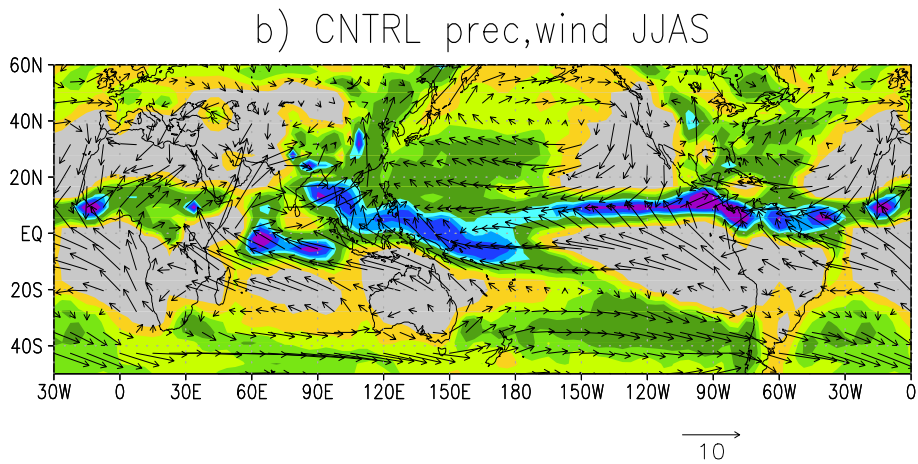
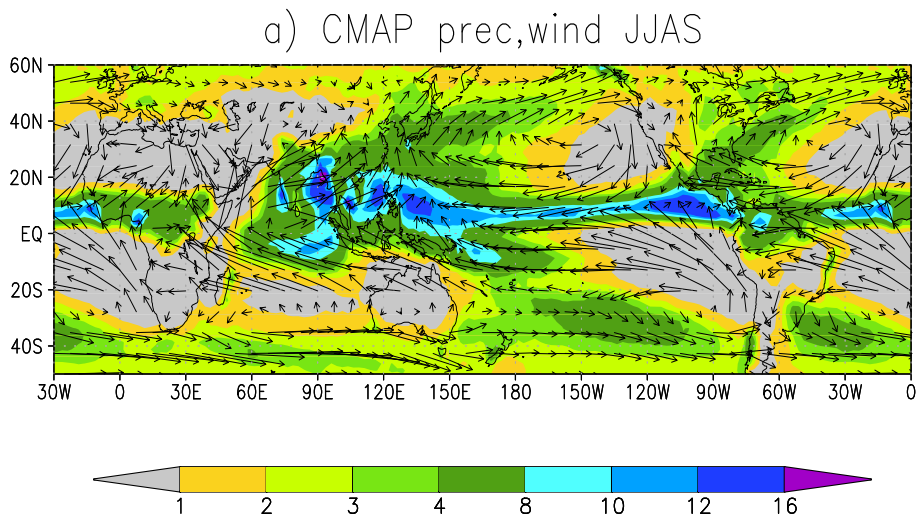


Figure 28: Mean JJAS rainfall and surface winds a) from observations (CMAP,NCEP-NCAR re-analysis), b) from the ICTPAGCM. Units are mm/day for rainfall and m/s for wind.

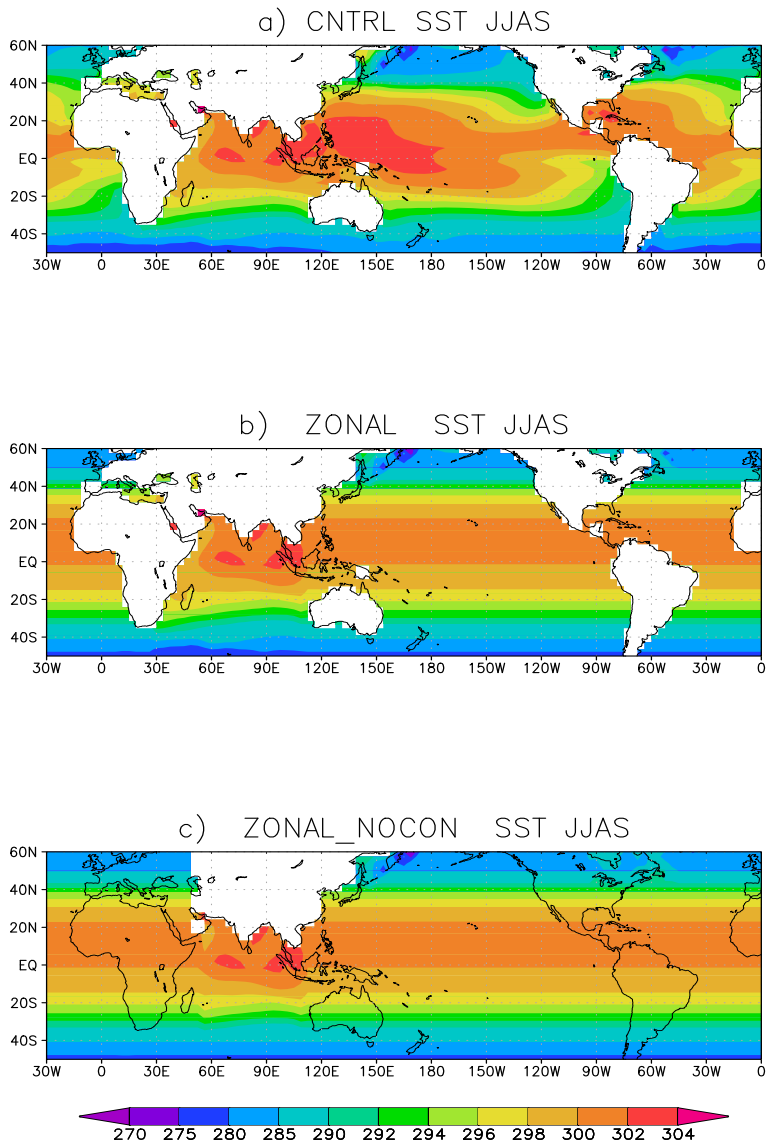


Figure 29: Mean JJAS sea surface temperature distribution a) observed, b) and c) idealized distribution for numerical experimentation.

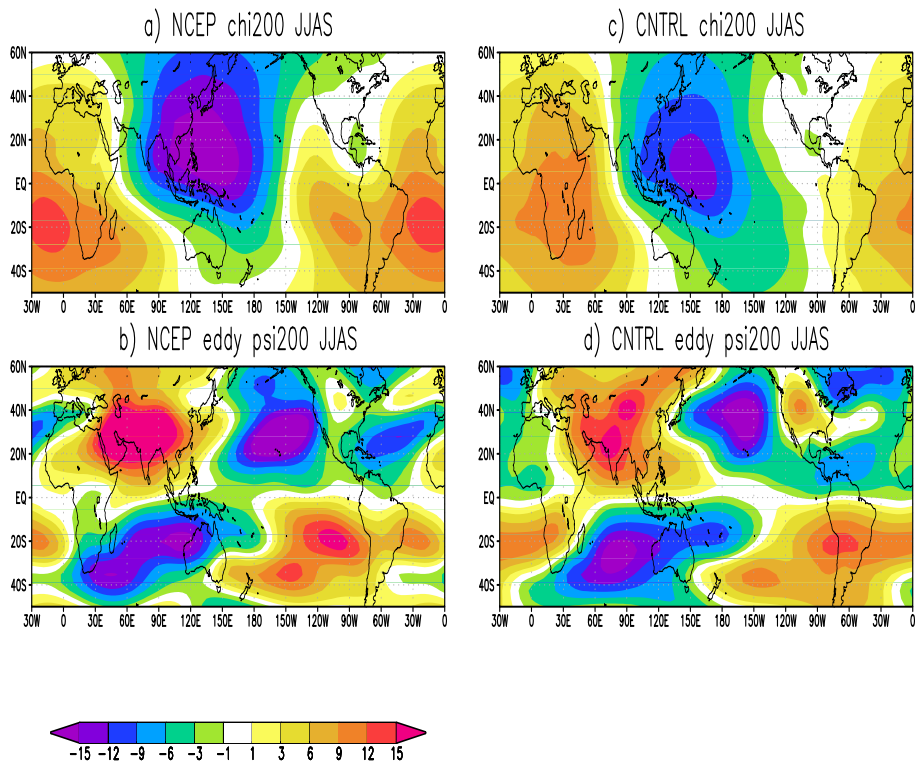


Figure 30: Mean JJAS distributions at 200 hPa of a) observed velocity potential χ , c) modeled observed velocity potential χ , b) observed streamfunction ψ , d) modeled streamfunction ψ . Units are $10^6 \text{ m}^2 \text{ s}^{-2}$.

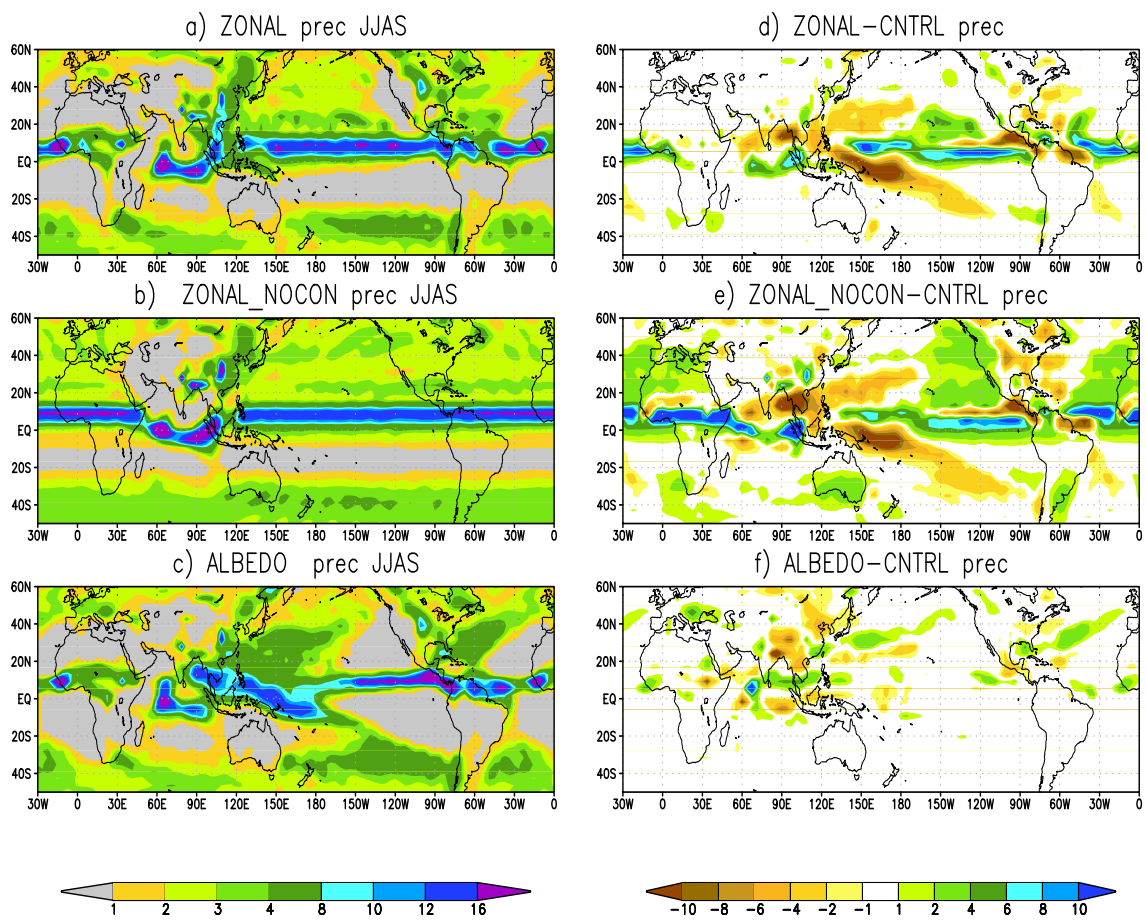


Figure 31: Response in rainfall to zonal (a, d) and zonal with removed African and American continents (b, e). Units are mm/day.

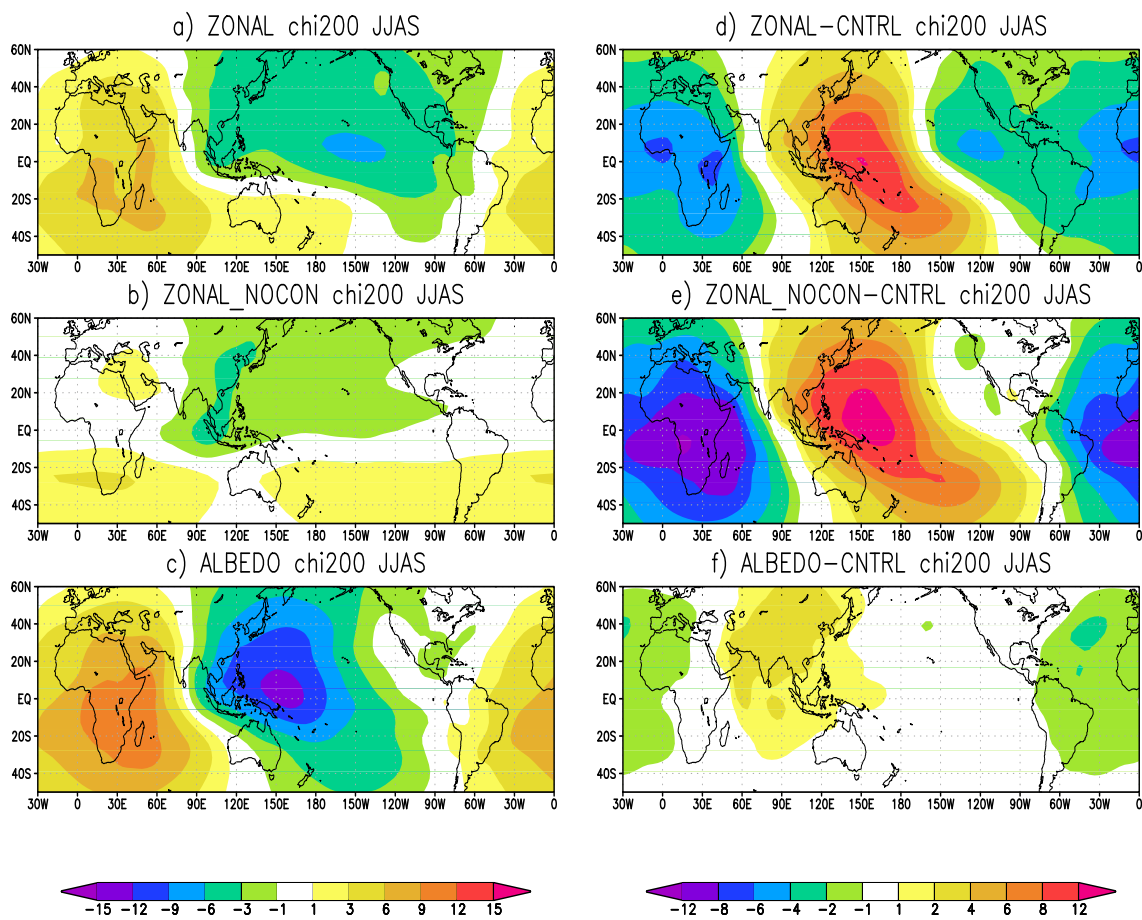


Figure 32: Response in velocity potential χ to zonal (a, d)) and zonal with removed African and American continents (b, e). Units are $10^6 \text{ m}^2 \text{ s}^{-2}$.

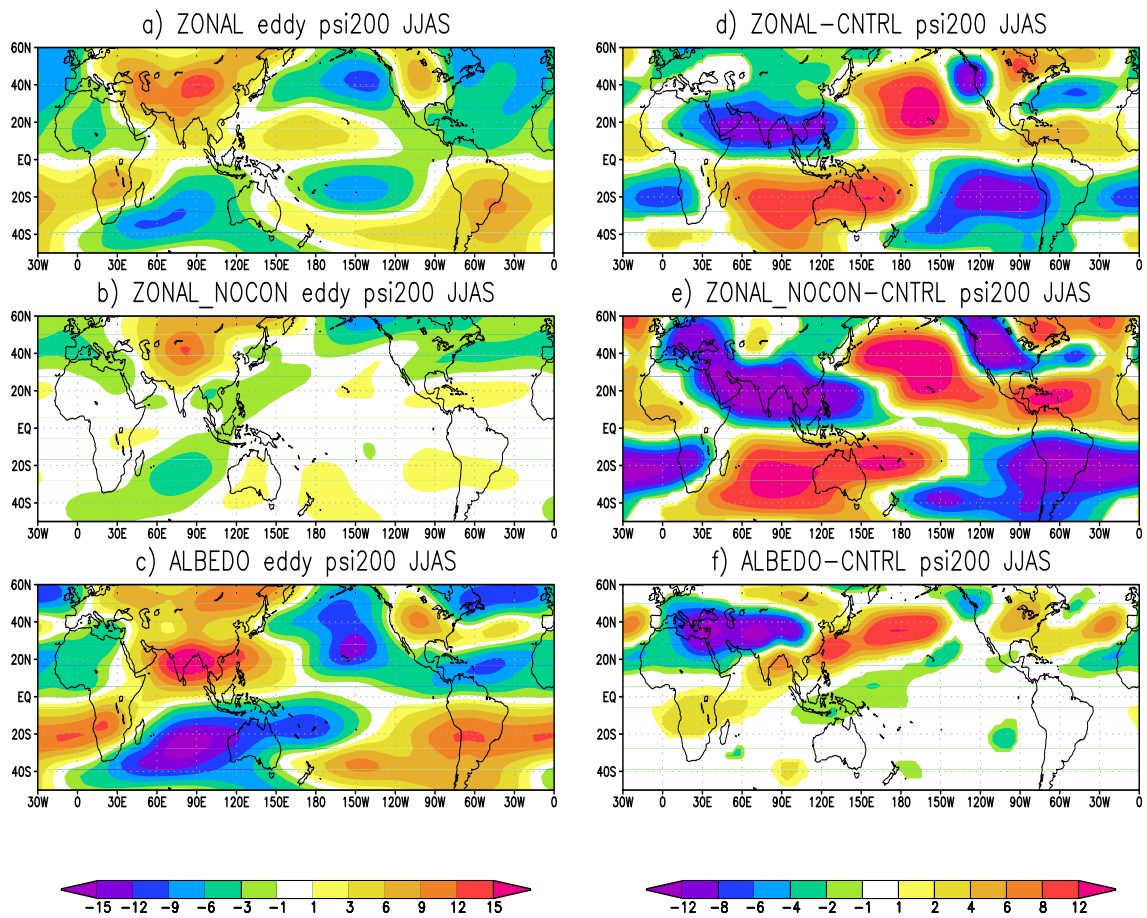


Figure 33: Response in eddy streamfunction ψ to zonal (a, d)) and zonal with removed African and Americal continents (b, e). Units are $10^6 \text{ m}^2 \text{ s}^{-2}$.

10 Energetics of the general circulation

Suggested textbooks, reading:

- a) *James R. Holton*: Dynamic Meteorology, Third edition, Academic Press.
- b) *Joseph Pedlosky*: Geophysical Fluid Dynamics, Springer-Verlag.
- c) Lorenz, E. N.; 1955: Available Potential Energy and the maintenance of the General Circulation. *Tellus*, **7**, 157-167
- d) *Peixoto, J. P. and Oort A. H.*: Physics of Climate, Springer-Verlag.
- e) Tailleux, R.; 2013: Available Energy and Exergy in Stratified Fluids. *Annual Review of Fluid Mechanics*, **45**, 35-58, doi: 10.1146/annurev-fluid-011212-14620
- f) Marquet, M.; 1991: On the concept of Exergy and available enthalpy: application to atmospheric energetics. *Q. J. R. Meteorolog. Soc.*, **117**, 449-475
- g) Kucharski, F.; 1997: On the concept of exergy and available potential energy. *Q. J. R. Meteorolog. Soc.*, **123**, 2141-2156
- h) Kucharski, F. and Thorpe, A. J.; 2000: Local Energetics of an Idealized Baroclinic Wave Using Extended Exergy. *Journal of the Atmospheric Sciences*, **57**, 3272-3284

We go back to the full (unapproximated) momentum equation

$$\rho \frac{d\mathbf{v}}{dt} = -\nabla p - 2\rho\boldsymbol{\Omega} \times \mathbf{v} - \rho\nabla\phi - \nabla \cdot \mathbf{F} \quad , \quad (220)$$

where \mathbf{F} is the frictional tensor. Multiplying with the velocity gives

$$\rho \frac{dk}{dt} = -\nabla \cdot (p\mathbf{v} + \mathbf{F} \cdot \mathbf{v}) + p\nabla \cdot \mathbf{v} - \rho\mathbf{v} \cdot \nabla\phi + \mathbf{F} : \nabla\mathbf{v} \quad , \quad (221)$$

where $k = 1/2(\mathbf{v} \cdot \mathbf{v})$ is the kinetic energy. We can reformulate equation 221 as equation

$$\rho \frac{d(k + \phi)}{dt} = -\nabla \cdot (p\mathbf{v} + \mathbf{F} \cdot \mathbf{v}) + p\nabla \cdot \mathbf{v} + \mathbf{F} : \nabla\mathbf{v} \quad . \quad (222)$$

The equation for internal energy is

$$\rho \frac{du}{dt} = -\nabla \cdot \mathbf{J} - p\nabla \cdot \mathbf{v} - \mathbf{F} : \nabla\mathbf{v} \quad . \quad (223)$$

\mathbf{J} is the radiative flux vector and the only heating term for a one-component system in which no phase transitions are possible. The addition of condensational heating

is an approximation to a one-component system and strictly possible only if more components are considered (dry air, water vapo and liquid water). The pressure work term $p\nabla \cdot \mathbf{v}$ may therefore be interpreted as reversible conversion term between kinetic plus potential and internal energy. The dissipational heating, $\mathbf{F} : \nabla \mathbf{v}$, is just transferring energy into the internal energy reservoir. The other terms are energy fluxes into the climate system. If we for the time being assume a closed system, then these terms vanish after an integration over the this system. In this case, we may assume that reservoirs of internal, potential and kinetic energy can only change by exchanging energy between them. Imagine an initial situation with a given temperature distribution, but without motion (this is, for example, the typical initial condition of ICTP AGCM). How much kinetic energy could the climate 'gain' in such a situation? A naive estimation would be $u = c_v T \approx 2 \cdot 10^5$ J/kg as typical local value. However, experience tells us that typical values of specific kinetic energy are about 10^2 J/kg, so that there is an overestimation of a factor of about 1000 in this simple (an naive) approach. Clearly, only a small portition of the large internal energy reservoir can be released into kinetic energy. It is obvious that we have to consider *differences* with respect to some reference state in order to define the proper amout of internal energy that is available for conversion into kinetic energy. An approach like $\Delta u = c_v \Delta T$, where $\Delta T = T - T_r$, with T_r some reference temperature, leads still to overestimations, but has the even more severe problem of not being positively definite. Note that the above arguments also apply to the potential energy, because of the proportionality of their total amounts in the atmopsphere ($P = R/c_v U$; Exercise!). The problem of identifying the energy available for conversion into kinetic energy is a classical one. For the atmosphere, Lorenz (1955) has developed a new energy concept, called *Available Potential Energy*. We can re-write the equations in a more suitable form:

$$\rho \frac{dk}{dt} = -\nabla \cdot (\mathbf{F} \cdot \mathbf{v}) - \mathbf{v} \cdot (\nabla p + \rho \nabla \phi) + \mathbf{F} : \nabla \mathbf{v} \quad . \quad (224)$$

$$\rho \frac{d(u + \phi)}{dt} = -\nabla \cdot (p\mathbf{v}) + \mathbf{v} \cdot (\nabla p + \rho \nabla \phi) + T\rho \frac{ds}{dt} \quad . \quad (225)$$

s is the specific entropy, governing all irreversible processes (for an ideal gas we have $s = c_p \ln \theta$). From these equations we see that in a hydrostatic atmosphere ($\nabla p = -\rho \nabla \phi$), there is no reversible conversion from the internal plus potential to kinetic energy. If in Eq. 225 we define a function that just depends on entropy, $T_0(s)$, then it is possible to remove from the internal plus potential energy a part that merely depends on entropy:

$$\rho \frac{d(u + \phi - q_0(s))}{dt} = -\nabla \cdot (p\mathbf{v}) + \mathbf{v} \cdot (\nabla p + \rho \nabla \phi) + (T - T_0(s))\rho \frac{ds}{dt} \quad , \quad (226)$$

where $q_0(s) = \int_{s_B}^s T_0(s') ds'$. Note that for isothermal processes, $T_0(s) = T$, then $q_0(s) = Ts + const.$ and $u + \phi - q_0(s) = u - Ts + \phi$, and $(u - Ts)$ is the *Free Energy* (a famous quantity for available energy for isothermal processes). The interpretation is that we can remove from the internal plus potential energy amounts a portion

that is not available for conversion into kinetic energy. However, the problem of the positive definiteness of the *useful* energy $u + \phi - q_0(s)$ remains. We have to use a transformation of thermodynamic variables that guarantees positive definiteness in the end.

10.1 Exergy transformation

The exergy transformation is usually applied to the internal energy u to provide a positive quantity with properties of a thermodynamic potential (see Figure 34).

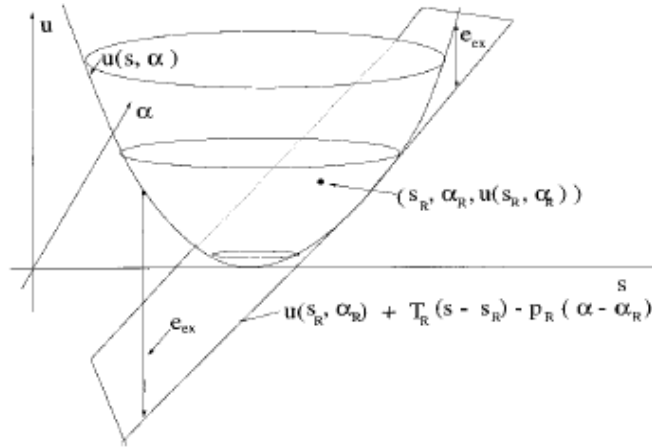


Figure 34: The convex internal energy, u , as a function of specific entropy, s , and specific volume, α , in phase space. The exergy transformation is just the (always positive) difference between u the tangente at the reference point.

Application of this transformation to the energy $u + \phi - q_0$ results in

$$e_{APE} = \Delta u - \Delta q_0 + p_R \Delta \alpha \quad , \quad (227)$$

where $\Delta \psi = \psi - \psi_R$, where the subscript R indicates the reference state. The quantity e_{APE} is the available potetial energy first introduced by Lorenz (1955) in a globally integrated form. It is a positive quantity the for a closed volume the only *reversible* production/destruction term is the conversion to/from kinetic energy. This quantity therefore has all the required properties. The reference state is arbitrary at this point, but following our idea of e_{APE} being the available energy, it should be derived from a variational principle, minimizing the volume integral of e_{APE} . However, for practical purposes, determination of the reference state by, for example, horizontal averaging of temperature is sufficient. All other reference state variables can be determined by vertically integrating the hydrostatic equation for an ideal gas. Note that e_{APE} according to Eq. 227 becomes the classical exergy in case of an isothermal reference temperature $T_0(s) = const. = T_R$. Finally, for an

ideal gas, the lowest order approximation of e_{APE} is

$$e_{APE} \approx \frac{1}{2} \left[\frac{g^2}{N_R^2} \left(\frac{\Delta\theta}{\theta_R} \right)^2 + RT_R \frac{c_v}{c_p} \left(\frac{\Delta p}{p_R} \right)^2 \right] , \quad (228)$$

where

$$N_R^2 := \frac{g}{c_p} \frac{ds_R}{dz} = \frac{g^2}{c_p^2} \left[\frac{T_R}{c_p} - \frac{dT_R}{dz} \left(\frac{ds_R}{dz} \right)^{-1} \right]^{-1} . \quad (229)$$

From Eq. 229 follows that e_{APE} is positive if the stratification of the reference state is statically stable ($N_R^2 > 0$). For application of this concept to the general circulation of the atmosphere this condition is certainly fulfilled (just look at a potential temperature cross section in meridional and height direction, e.g. Fig. 1). However, to a system where the stratification is unstable even in the horizontal average, the available potential energy concept cannot be applied, and we have to return to other methods of identifying useful energy. The balance equation for e_{APE} can be derived by noting that

$$\frac{de_{APE}}{dt} = (T - T_0(s)) \frac{ds}{dt} - \Delta p \frac{d\alpha}{dt} + \Delta\alpha \frac{dp_R}{dt} \quad (230)$$

The energy equations 224 and 225 can be reformulated in the following form

$$\rho \frac{dk}{dt} = -\nabla \cdot (\Delta p + \mathbf{F} \cdot \mathbf{v}) + \Delta p \nabla \cdot \mathbf{v} + \rho \frac{\Delta\alpha}{\alpha_R} \mathbf{v} \cdot \nabla\phi + \mathbf{F} : \nabla\mathbf{v} \quad (231)$$

$$\rho \frac{de_{ape}}{dt} = -\Delta p \nabla \cdot \mathbf{v} - \rho \frac{\Delta\alpha}{\alpha_R} \mathbf{v} \cdot \nabla\phi + \rho \frac{T - T_0(s)}{T} q , \quad (232)$$

where the abbreviation for diabatic processes $Tds/dt = q$ has been used. The factor $(T - T_0(s))/T = \eta$ may be interpreted as *Carnot factor* controlling the efficiency of the energy gain for a given heating. It can be approximated to the first order as (exercise!)

$$\eta \approx \left(\frac{g^2}{c_p N_R^2} \frac{\Delta\theta}{\theta_R} + T_R \frac{R}{c_p} \frac{\Delta p}{p_R} \right) \frac{1}{T} . \quad (233)$$

The interpretation is then that the volume integrated generation of e_{APE} is dependent of the correlation of η and q . It's not the heating per se that is important, but the differential heating has to be correlated with potential temperature perturbations (dominant part in Eq. 233). On the other hand, frictional dissipation is the main process that destroys kinetic energy. A few remarks are appropriate here. If we forget for the time being about the approximative expressions given for an ideal gas, e_{APE} , and its evolution equation are really very general for a stably stratified one-component system. For example consider a simple solid body. We know from experience that even if a differential heating is applied, the only process that may result is heat diffusion (diabatic process), but certainly no kinetic energy can be

gained. Indeed, in case of a solid body the function $q_0(s)$ can be chosen as the internal energy u plus the constant potential energy, because $T = T(s)$, therefore we can define $T_0(s) = T$. In case of a simple incompressible fluid, we can also identify $T_0(s) = T$ and $q_0(s)$ can be chosen to equal to the internal energy, but the potential energy may not be constant, because of fluctuations of surface height, and could therefore provide the available potential energy.

To derive a slightly different formulation that has been derived by Lorenz (1955), equation has to be integrated over the systems volume

$$\int_{\tau} \frac{de_{ape}}{dt} d\tau = \int_{\tau} \left\{ -p \frac{d\alpha}{dt} + p_R \alpha \nabla \cdot \mathbf{v} - \frac{\alpha}{\alpha_R} \mathbf{v} \cdot \nabla \phi + \frac{d\phi}{dt} + \frac{T - T_o(s)}{T} q \right\} d\tau \quad , \quad (234)$$

where $d\tau = \rho dx dy dz$ is a mass element. Using

$$p \frac{d\alpha}{dt} = \frac{d}{dt}(p\alpha) - \alpha \frac{dp}{dt}$$

and $P = R/c_v U$ (see exercise 1!), it follows

$$\int_{\tau} \frac{de_{ape}}{dt} d\tau = \int_{\tau} \left\{ \frac{RT}{p} \omega + \frac{T - T_o(s)}{T} q \right\} d\tau \quad , \quad (235)$$

where the orographic term from the exercise has been ignored. This is the integral available potential energy balance for a hydrosatic atmosphere that was first derived by Lorenz (1955). Apart from the diabatic production term, which can be reformulated for an idealized gas to get a formulation identical to Lorenz, this form is highlighting the conversion term to kinetic energy $-\omega RT/p$, which states that energy is converted into kinetic energy by *rising of warm air and sinking of cold air*. This makes the conversion term positive on average. This process is lowering the *centre of mass* of the atmosphere, thus releasing kinetic energy. In baroclinic waves, warm air is typically moving northward, and cold air southward. This together with the tendency for motions to be adiabatic, thus following lines of constant potential temperature (see Fig. 1), means that the warm air moving to the north tends to rise and the cold air moving to the south tends to sink, thus providing the conditions for conversion of available potential energy into kinetic energy.

It is further possible to decompose the kinetic and available potential energy in their zonal mean and eddy components (see Section 8.1), and to derive their evolution equations. If we identify the global volume averages of k and e_{APE} and their mean and eddy components as E_K , E'_K and E_P , E'_P then the resulting global energy cycle according to Peixoto and Oort (1983) is shown in Fig. 37. As can be seen most production goes into E_P , but also a considerable part into E'_P . These are related to heating in equatorial regions and cooling in polar regions for E_P , and diabatic heat release in cyclones in case of E'_P . The energy is then transformed into eddy kinetic energy, E'_K , from where most of the dissipation occurs. A smaller part is transferred into mean kinetic energy E_K , and eventually dissipated and also transformed back into E_P .

For the ocean we have a much simpler picture, mainly driven by atmospheric winds and friction:

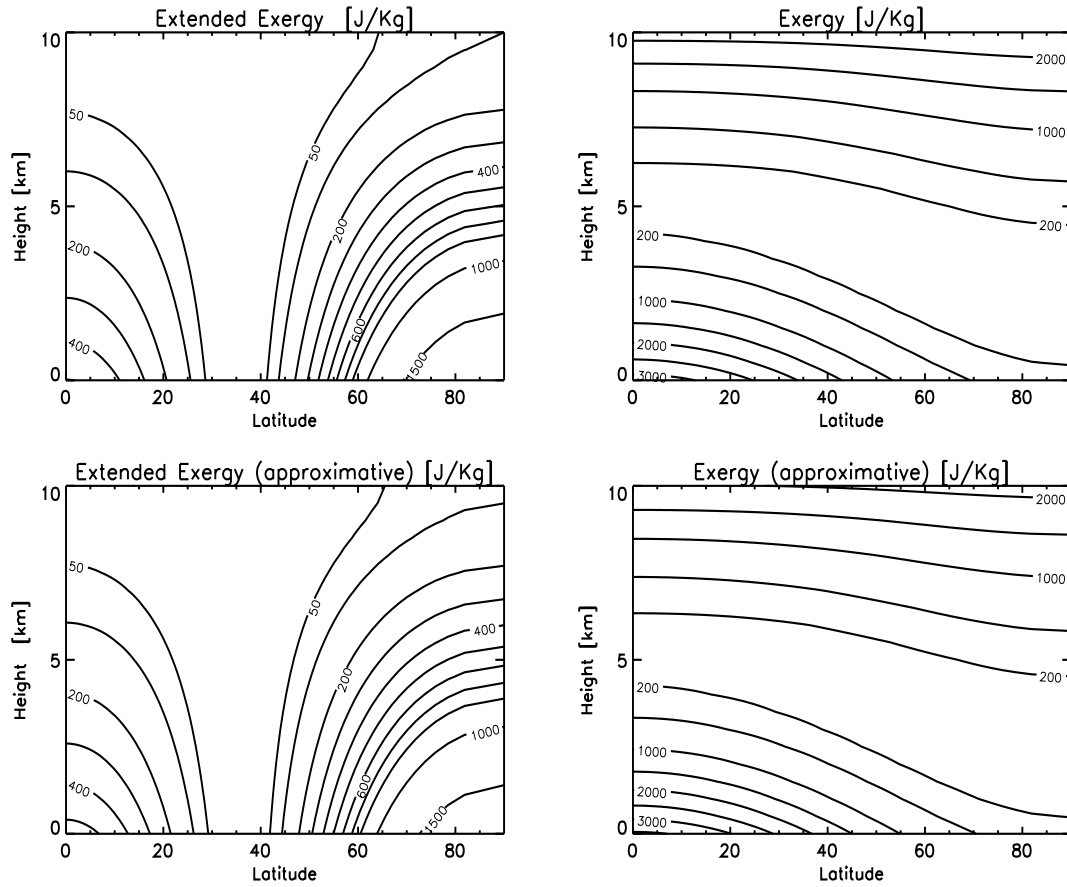


Figure 35: Distribution of classical Exergy and extended Exergy (local available potential energy). Units are J/kg.

Exercises

1. Show that for a hydrostatic atmosphere the volume integral of potential energy is proportional to the volume integral of internal energy, i.e. $P = R/c_v U$. (Hint: Use a partial integration!)

$$P = \int \int_A \int_{Z_s}^{\infty} \rho g z dz dx dy = \frac{R}{g} \int \int_A \int_0^{p_s} T dp dx dy + \int \int_A \frac{\Phi_s p_s}{g} dx dy$$

2. Show that

$$T - T_0(s) \approx \left(\frac{g^2}{c_p N_R^2} \frac{\Delta \theta}{\theta_R} + T_R \frac{R}{c_p} \frac{\Delta p}{p_R} \right)$$

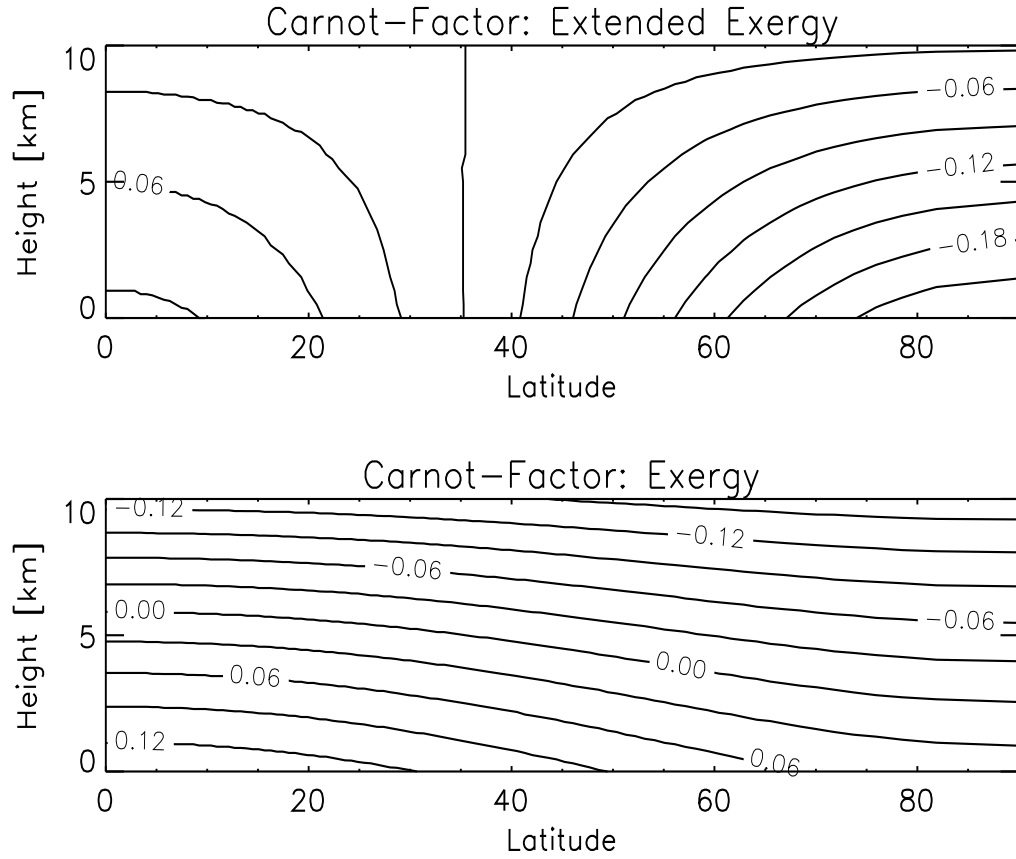


Figure 36: Distribution of Carnot factors of Exergy and extended Exergy (local available potential energy).

in first order by developing $T(s, p)$ and $T_0(s)$ in taylor series around a reference state s_R, α_R . Hint: Note that $\partial T / \partial s = T / c_p$, $\partial T / \partial p = \alpha / c_p$ and

$$\frac{dT_0}{ds}(s_R) = \frac{dT_R}{dz} \left(\frac{ds_R}{dz} \right)^{-1}$$

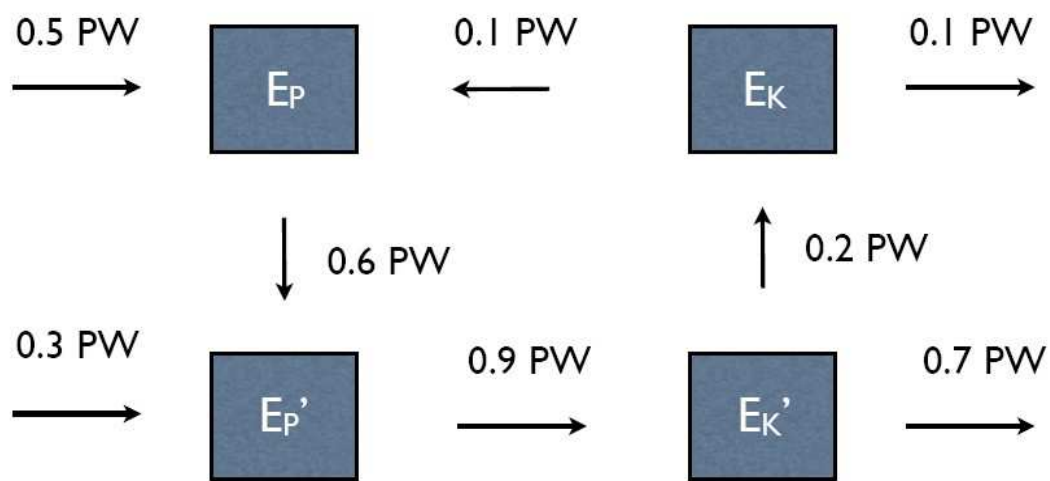


Figure 37: The global atmospheric energy cycle for the global integrals of mean and eddy available potential and kinetic energies (E_P , E_P' , E_K , E_K'), respectively.

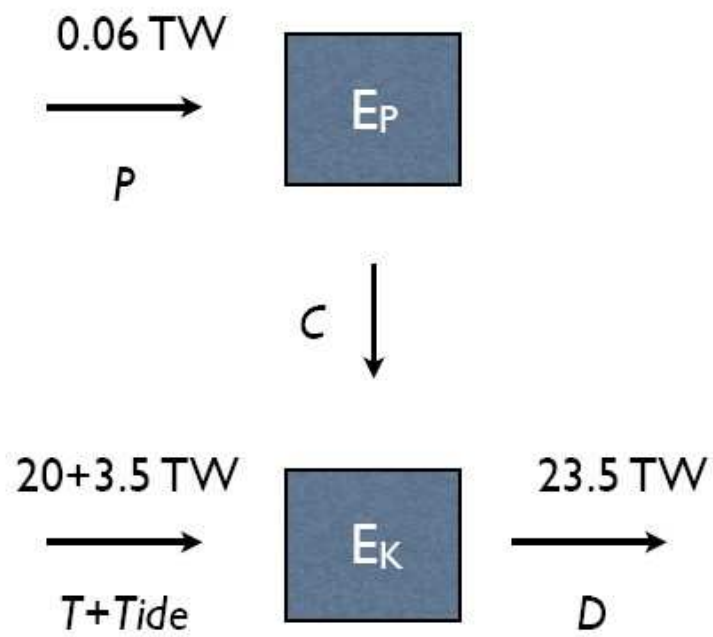


Figure 38: The global oceanic energy cycle therefore the global integrals of available potential and kinetic energies.

11 Analysis of Climate Variability: EOF/PCA Analysis

Suggested textbooks:

- a) Statistical Methods in the Atmospheric Sciences. D. S. Wilks, Second Edition, International Geophysics Series, Academic Press, 2006
- b) Statistical Analysis in Climate Research. H. von Storch and F. W. Zwiers, Cambridge University Press, 1999
- c) Analysis of Climate Variability. H. von Storch, A. Navarra (Eds.), Springer, 1995.
- d) Or simply look things up on Wikipedia.....

11.1 Motivation

The problem and necessity of the *analysis of climate variability* becomes clear if we consider the series of 500 hPa winter mean anomaly fields shown in Fig. 39. Lacking a precise theory of what we are seeing (apart from the fact that we know that what we see are solutions of the complex Navier-Stokes equations), how can we try to find some order in the *chaos* that we are confronted with? One way to tackle this problem is the *Empirical Orthogonal Function (EOF)* analysis (guess who introduced this in climate analysis?) or *Principle Component Analysis (PCA)*.

11.2 What does the EOF analysis do?

The EOF analysis solves our problem (how, see below) by finding orthogonal functions (EOFs) to represent a time series of horizontal fields in the following way:

$$Z'(x, y, t) = \sum_{l=1}^L PC_l(t) EOF_l(x, y) \quad . \quad (236)$$

$Z'(x, y, t)$ is the original (anomaly) time series as a function of time (t) and (horizontal) space (x,y), for example the fields that are displayed in Fig. 39. $EOF_l(y, x)$ show the spatial structures of the major factors that can account for the temporal variations of Z' . $PC_l(t)$ are the principal components that tell you how the amplitude of each EOF varies with time. In practice, time and space dimensions are discretized (as in the Numerical Methods Course!). Therefore, dealing with $Z'(x, y, t)$ and $EOF_l(y, x)$ means to deal with matrices.

11.3 Some useful specific definitions and notations

In the following, matrices will be denoted by capital bodyface roman letters (**A**, **B**, **Y**, etc.). Vectors will be denoted by a lowercase boldface letters. Let's consider the

data matrix:

$$\mathbf{Z} = \begin{bmatrix} z_{11} & z_{12} & \dots & z_{1k} \\ z_{21} & z_{22} & \dots & z_{2k} \\ \vdots & \vdots & & \vdots \\ z_{n1} & z_{n2} & \dots & z_{nk} \end{bmatrix} \quad (237)$$

In the following we assume that time and space are discretized and time is represented by the columns of this matrix, whereas space is represented by the rows (space (x,y) is just discretized a one vector, i.e. order $f(i, j)$ as one long vector $f(i, 1), f(i, 2), \dots, f(i, M), i = 1, N$, with $N \times M = k$). EOF analysis is based on anomalies, therefore anomaly data has to be defined. In order to define anomalies, a mean has to be defined. This is done in time, meaning a k-dimensional vector of means can be defined by averaging along the columns of the matrix of Eq. 237 (i.e. the time mean at every grid point). This mean has to be subtracted at every time and gridpoint in order to define the anomaly matrix. The mean subtracted is in general different at different gridpoints, but must be the same at a fixed gridpoint. An elegant way to write this is:

$$\mathbf{Z}' = \mathbf{Z} - \frac{1}{n} \mathbf{1} \mathbf{Z} \quad , \quad (238)$$

where $\mathbf{1}$ is a $n \times k$ matrix that contains 1 everywhere which is multiplied with \mathbf{Z} (to confirm, simply try this procedure with a 2x2 matrix!).

With these notations Equation 236 may be re-written in (discretized) matrix notation as

$$\mathbf{Z}' = \sum_{l=1}^k \mathbf{p} \mathbf{c}_l \mathbf{e}_l^T \quad , \quad (239)$$

where $\mathbf{p} \mathbf{c}_l$ is a $n \times 1$ vector and \mathbf{e}_l is a $k \times 1$ vector, therefore the transpose \mathbf{e}_l^T is a $1 \times k$ vector. Note that the product of an arbitrary $n \times 1$ vector \mathbf{a} and a $1 \times k$ vector \mathbf{b}^T results in

$$\mathbf{a} \mathbf{b}^T \equiv \begin{bmatrix} a_1 \\ a_2 \\ \vdots \\ a_n \end{bmatrix} \begin{bmatrix} b_1 & b_2 & \dots & b_k \end{bmatrix} \equiv \begin{bmatrix} a_1 b_1 & a_1 b_2 & \dots & a_1 b_k \\ a_2 b_1 & a_2 b_2 & \dots & a_2 b_k \\ \vdots & \vdots & & \vdots \\ a_n b_1 & a_n b_2 & \dots & a_n b_k \end{bmatrix} \quad (240)$$

If we demand the vectors \mathbf{e}_l to be orthogonal unit vectors, such that $\mathbf{e}_i^T \mathbf{e}_j = 0$ for $j \neq i$, and $\mathbf{e}_l^T \mathbf{e}_l = 1$, then we have

$$\mathbf{Z}' \mathbf{e}_m = \sum_{l=1}^k \mathbf{p} \mathbf{c}_l \mathbf{e}_l^T \mathbf{e}_m = \sum_{l=1}^k \mathbf{p} \mathbf{c}_l \delta_{lm} = \mathbf{p} \mathbf{c}_m \quad , \quad (241)$$

where $\delta_{lm} = 1$ if $l=m$ and zero otherwise. We call $\mathbf{Z}' \mathbf{e}_m$ the *projection* (or in climate analysis sometimes called *regression*) of the data matrix onto the subspace defined by the EOF \mathbf{e}_m . Thus the principle components corresponding the m th EOF can simply be derived by projection of the data matrix \mathbf{Z}' onto the m th EOF. The vector $\mathbf{p} \mathbf{c}_m$ has therefore n components.

11.4 Minimum criterium leading to EOF definition

EOF analysis can be interpreted as a recursive process, we start to determine the first EOF (\mathbf{e}_1), then the second, and so on. The criterion to determine the first EOF is the minimization of the residual

$$\epsilon_1 = \| \mathbf{Z}' - \mathbf{Z}'\mathbf{e}_1\mathbf{e}_1^T \|^2 , \quad (242)$$

with respect to the k dimensional vector \mathbf{e}_1 designing the first EOF in our notation. Here, if \mathbf{Y} is any matrix,

$$\| \mathbf{Y} \|^2 = \frac{1}{(nk)} \mathbf{Y}^T : \mathbf{Y} \equiv \text{tr} \left(\frac{1}{(nk)} \mathbf{Y}^T \mathbf{Y} \right) = \frac{1}{(nk)} \sum_{i=1}^n \sum_{j=1}^k y_{ij}^2 . \quad (243)$$

This means first the matrix product of \mathbf{Y}^T and \mathbf{Y} , then the trace of the resulting matrix by summing up the diagonal elements and this is the total variance of \mathbf{Y} . The normalization by (nk) is arbitrary, but represents the *natural* definition of the total variance. In some cases you may find that the normalization is just done by n , meaning in time. The final results is however independent of this. The meaning of Eq. 242 is that we are searching for a k - dimensional subspace \mathbf{e}_1 to represent the data such that the residual (242) is minimal.

Note that $\mathbf{Z}'\mathbf{e}_1$ is a n -dimensional vector to be matrix multiplied by the k -dimensional vector \mathbf{e}_1^T to give a $k \times n$ matrix according to Eq. 240. Also note that $\mathbf{Z}'\mathbf{e}_1$ is just the definition of the vector of (discretized) Principle Components corresponding to the first EOF in Eq. 239. Some further manipulation leads to:

$$\epsilon_1 = \| \mathbf{Z}' \|^2 - \| \mathbf{Z}'\mathbf{e}_1 \|^2 , \quad (244)$$

which means that minimizing ϵ_1 according to Eq. 242 with respect to \mathbf{e}_1 is equivalent to maximizing the principle component projections

$$\epsilon_{proj} = \| \mathbf{Z}'\mathbf{e}_1 \|^2 \quad (245)$$

with respect to \mathbf{e}_1 (see, e.g. Wikipedia). This leads to the often used 2-dimensional example of the *geometrical* interpretation of EOFs shown in Fig. 40, where samples of 2-dimensional data vectors are considered and we search for the unit vector (EOF) that maximizes the variance of the projection of the data on this vector (straight line).

The minimization (a lot of matrix calculus) leads to the eigenvalue problem

$$\mathbf{S}\mathbf{e}_1 = \lambda\mathbf{e}_1 , \quad (246)$$

where λ is the largest eigenvalue and $\mathbf{S} = \frac{1}{nk}\mathbf{Z}'^T\mathbf{Z}'$ is the $k \times k$ variance-covariance matrix of the anomalies. Therefore the first EOF \mathbf{e}_1 becomes the eigenvector of the matrix \mathbf{S} corresponding to the largest eigenvalue. The other EOFs are found by simply iteratively minimizing the reduced residual

$$\epsilon_2 = \| \mathbf{Z}' - \mathbf{Z}'\mathbf{e}_1\mathbf{e}_1^T - \mathbf{Z}'\mathbf{e}_2\mathbf{e}_2^T \|^2 ' \quad (247)$$

and

$$\epsilon_l = \| \mathbf{Z}' - \mathbf{Z}'\mathbf{e}_1\mathbf{e}_1^T - \mathbf{Z}'\mathbf{e}_2\mathbf{e}_2^T - \dots - \mathbf{e}_l\mathbf{e}_l^T \|^2 , \quad (248)$$

and the results is that \mathbf{e}_2 is the eigenvector of \mathbf{S} that corresponds to the second largest eigenvalue, and \mathbf{e}_l is the eigenvector of \mathbf{S} that corresponds to the l th largest eigenvalue. Since \mathbf{S} has k eigenvectors we can continue this until $l=k$.

11.5 Some further properties

Note that also the principal components are orthogonal, that is $\mathbf{pc}_i \cdot \mathbf{pc}_j^T = 0$ for $j \neq i$. For practice purposes, we hope that a good approximation for the data matrix is given by

$$\mathbf{Z}' \approx \sum_{l=1}^N \mathbf{pc}_l \mathbf{e}_l^T , \quad (249)$$

with $N \ll k$.

A further property is

$$\sum_{l=1}^k \lambda_l = \frac{1}{(nk)} \mathbf{Z}'^T : \mathbf{Z}' = \frac{1}{(nk)} \sum_{i=1}^n \sum_{j=1}^k z'_{ij}^2 , \quad (250)$$

which means that the sum of all eigenvalues gives the trace of the variance-covariance matrix \mathbf{S} which is the total variance of \mathbf{Z}' . To evaluate the importance of EOFs it is useful to consider the portion of variance explained by it:

$$\text{expl var of } \lambda_i = \frac{\lambda_i}{\sum_{l=1}^k \lambda_l} \quad (251)$$

A further property of eigenvalues of a matrix is of importance for the practical implementation of the EOF analysis, and is indeed used in the fortran program that you will use in the exercises of this section: If λ is an eigenvalue of the variance-covariance matrix $\mathbf{Z}'^T \mathbf{Z}'$ (we drop the scaling $1/(nk)$ for here because it is just a factor), then it is also an eigenvalue of the $n \times n$ matrix $\mathbf{Z}' \mathbf{Z}'^T$. In this case the variance-covariance matrix is defined as by the spatial variances and covariances. Thus if $n \ll k$, then we may prefer to find the eigenvalues of $\mathbf{Z}' \mathbf{Z}'^T$. If there are m independent eigenvectors $(\mathbf{e}_1, \mathbf{e}_2, \dots, \mathbf{e}_s)$ of $\mathbf{Z}'^T \mathbf{Z}'$ the eigenvectors of $\mathbf{Z}' \mathbf{Z}'^T$ are $\mathbf{Z}'\mathbf{e}_1, \mathbf{Z}'\mathbf{e}_2, \dots, \mathbf{Z}'\mathbf{e}_s$, which are the projections of the data matrix on the EOFs \mathbf{e}_s which are therefore the (normalized) principal components of the original problem. This means that EOFs and principal components are exchangeable. Instead of calculating the eigenvectors of $\mathbf{Z}'^T \mathbf{Z}'$, we may calculate the eigenvectors of $\mathbf{Z}' \mathbf{Z}'^T$, interpret the eigenvectors as the principal components and calculate the EOFs as projections of the transpose data matrix \mathbf{Z}'^T onto the eigenvectors: $\mathbf{e}_1 = \mathbf{Z}'^T \mathbf{pc}_1$. In this case the principal components are normalized (that is standard deviation = 1), whereas the EOFs are not. In the approximation 249 it does not matter if the principle component or the EOF is normalized, because they are multiplied with each other.

As stated above EOFs are found by determining the eigenvalues and eigenvectors of the variance-covariance matrix. Do you remember how to find these? You have to demand that the *determinant* of the variance-covariance matrix vanishes, this leads to an equation, the *characteristic equation* that contains k th-order polynomials and has at most k roots. There are standard techniques to find eigenvalues and eigenvectors, you may have learned some in your Numerical Methods course?

11.6 Geometric interpretation of PCs and EOFs

The geometric interpretation of the principle components mentioned before is as follows: The eigenvectors empirical orthogonal function (EOF) define a new coordinate system in which to view the data. This coordinate system is oriented such that each new axis is aligned along the direction of the maximum joint variability of the data, consistent with that axis being orthogonal to the preceding one.

The goal is to account for the variation in a sample in as few variables as possible. In the example here, the data is essentially 1-dimensional in the new coordinate system defined by the EOFs.

11.7 Interpretation of EOFs

As we have learned by now, EOFs may be useful to compress the information contained in complex data sets and to structure the data (according to the largest variances). As for the physical interpretation of EOFs, it is tempting to try to give physical explanations to the first few EOFs of a complex data set. Indeed, we expect that if the variability of our fields are governed by a strong low-dimensional physical mechanism (e.g. ENSO in the Pacific region), then one of the first EOFs will reflect this mechanism (indeed in case of EOFs of the interannual variability in the tropical Pacific, we find that the first EOF reflects the canonical ENSO pattern). Unfortunately, the opposite is not true: Not every first (or second or third, ...) is related to a simple and unique physical mechanism! Furthermore it is often even misleading to try to provide a physical mechanism for higher EOFs (e.g. EOF4, EOF5, etc.), because of the orthogonality of the EOFs. This constraint may make higher EOFs less 'physical' than the first or second EOF! The EOF analysis applied to the fields in Fig. 39 gives as first 2 EOFs the maps displayed in Fig. 42. Do you have ideas about possible 'physical' explanations of these EOFs? They are at least well know patterns, do you know their names?

11.8 Related Methods of Climate Analysis

The EOF analysis is probably the most basic of all analysis methods of climatic fields. For example a different question could arise considering 500 hPa geopotential height fields and sea surface temperature fields together. We may ask the question are the 500 hPa fields and the sea surface temperature (SST) fields we see related? This could be due to the fact that one is *forcing* the other. We may get some idea performing an EOF analysis on both fields separately and then try to connect the

emerging EOFs by a physical interpretation (e.g. similar to what we will do in the exercise in this section). We could go one step further and compare (e.g. correlate) the principle components (pcs) of the first EOFs, etc. If we are lucky and the pcs are highly correlated, then there is likely some physical connection between the two first EOFs. However, it could also be that the first pc in geopotential height is a little correlated with the first pc in SSTs and also a little with the second, and so on. This means our interpretation of the connections between 500 hPa geopotential height and SST fields are not much easier after the EOF analysis. There are methods to address this question systematically. For example, the Canonical Correlation Analysis (CCA) or Maximum Covariance Analysis (MCA) provide tools to address the question stated above in a systematic way.

Exercises

1. Using the fortran programme provided, calculate the (winter-mean: DJF) EOFs of a) surface temperature and b) 200 hPa geopotential height in the tropical Pacific. Display the covariance of the resulting principal components related to the first EOF with the global surface temperature and 200 hPa geopotential height fields and interpret the results. How much variance does the first EOF explain in each case? Are the first EOFs of surface temperature and 200 hPa geopotential height related? If yes, what could be the physical mechanism?

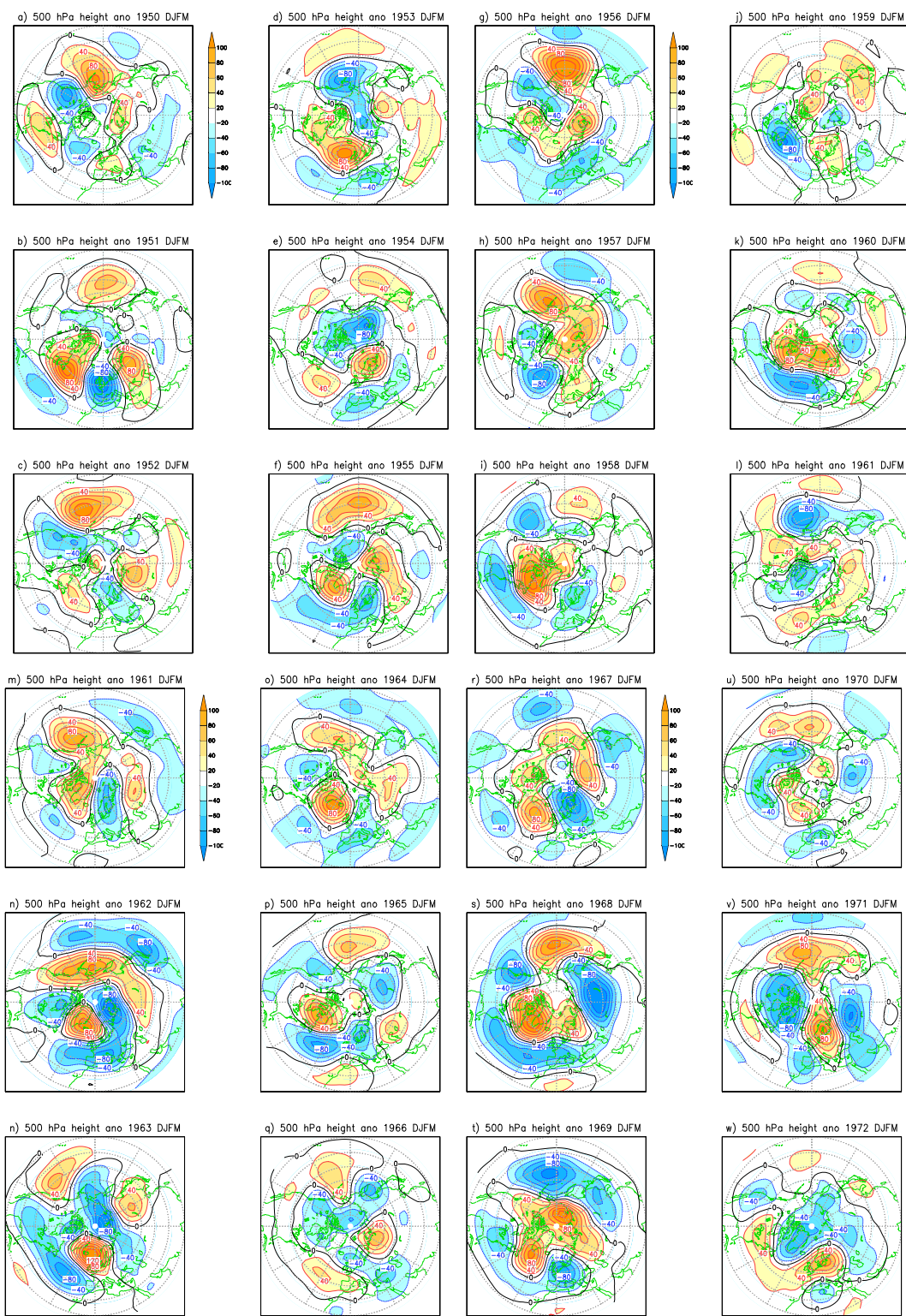


Figure 39: Anomalies of winter 500 hPa height fields for several years. Units are m.

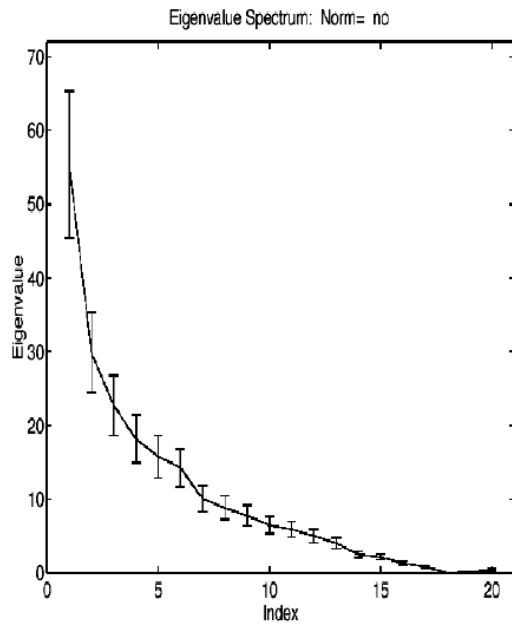


Figure 40: A typical example of the distribution of eigenvalues.

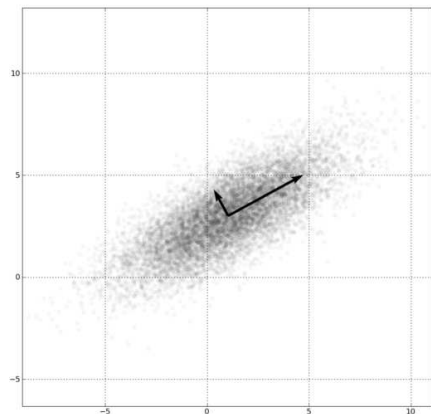


Figure 41: A sample of n observations in the 2-D space $x = (x_1, x_2)$.

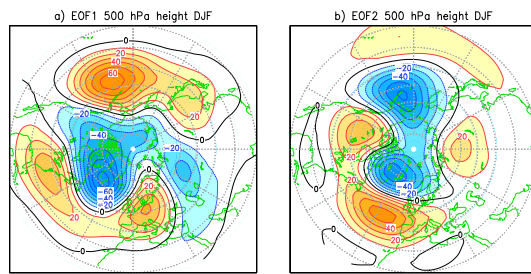


Figure 42: EOFs of the 500 hPa fields presented in Fig . 39